Applications of Padé Approximation Theory in Fluid Dynamics

This page is intentionally left blank

Series on Advances in Mathematics for Applied Sciences – Vol. 14

Applications of Padé Approximation Theory in Fluid Dynamics

Amilcare Pozzi
Istituto di Gasdinamica
Facoltà di Ingegneria
Università di Napoli
Italia

World Scientific
Singapore • New Jersey • London • Hong Kong

Published by

World Scientific Publishing Co. Pte. Ltd.

P O Box 128, Farrer Road, Singapore 9128

USA office: Suite 1B, 1060 Main Street, River Edge, NJ 07661

UK office: 73 Lynton Mead, Totteridge, London N20 8DH

Library of Congress Cataloging-in-Publication Data

Pozzi, Amilcare.

Applications of Padé approximation theory in fluid dynamics / Amilcare Pozzi.

p. cm. -- (Series on advances in mathematics for applied sciences ; vol. 14)

Includes bibliographical references and indexes.

ISBN 9810214146

1. Fluid dynamics--Mathematics. 2. Padé approximant. I. Title. II. Series.

QC151.P65 1993

532'.05'0151142--dc20 93-37547

CIP

Printed in Singapore by Utopia Press.

Preface

Although Padé presented his fundamental paper at the end of the past century while he was working with Hermite at the Ecole Normale Superieure de France, the studies on Padé approximants only became significant in the second part of this century. A systematic analysis of this subjet was made by G.A. Baker and J.L. Gammel in 1960; G.A. Baker, J.L. Gammel and J. Willis in 1961 presented an invariance theorem, the unitarity theorem was published by J.L. Gammel and F.A. Mc Donald in 1966 and in 1972 W.B. Gragg studied the connection between Padé approximants and some algorithms of numerical analysis. In 1973 (with the Institute of Physics London and Bristol) P.R. Graves-Morris edited some lectures delivered at a summer school held at the University of Kent in July 1972 on theoretical and applied aspects of the Padé approximants.

Padé's procedure is related to the theory of continued fractions, born in the seventeenth century, and some convergence theorems can be expressed only in terms of continued fractions, but Padé approximants have some advantages of practical applicability with respect to the continued- fraction theory. Moreover, as Chisholm notes, a given power series determines a set of approximants which are usually unique, whereas there are many ways of writing an associated continued fraction.

The principal advantage of Padé approximants with respect to the generating Taylor series is that they provide an extension beyond the interval of convergence of the series.

This procedure has been used as a standard technique by many applied math-

ematicians, theoretical physicists, theoretical chemists and electrical engineers. In the fluid-dynamics field there is also interest for Padé methods: in a recent congress Padé approximants were defined "magic". In fact the possibility of extracting information from a diverging series and constructing a powerful sequence of approximants of a function seems too good to be real.

Padé approximants can be applied in many parts of fluid-dynamics, both in steady and in nonsteady flows, both in incompressible and in compressible regimes.

The exposition is divided into four parts. The first one deals with the properties of the Padé approximants that are useful for the applications and illustrates, with the aid of diagrams and tables, effectiveness of this technique in the field of applied mathematics. The second part recalls the basic equations of fluid-dynamics (those associated with the names of Navier-Stokes, Euler and Prandtl) and gives a quick derivation of them from the general balance equation.

The third, the longest, shows eight examples of application of the Padé approximants to steady flows, taking also into account the influence of the coupling of heat conduction in the body along which a fluid flows with the conduction and convection in the fluid itself.

The fourth part considers two examples of application of the Padé approximants to unsteady flows.

The purpose of this work is to show that the Padé approximants constitute an useful tool for solving fluid-dynamics problems.

No specialized topic either in mathematics or in fluid-dynamics is presumed to be known by readers of this book.

Only a basic knowledge is required of calculus: properties of series (convergence of power series, Cauchy product), etc.

In particular the determination of the Padé approximants, starting from the MacLaurin series, is obtained by the solution of a system of linear algebraic equations, the coefficients of which are given in the first part.

The derivation of the basic equations of Fluid Dynamics, contained in the second part, is obtained in a non standard way following a microscopic approach. This point of view, which uses the Dirac δ function to describe the microscopic discontinuity of the medium, has two advantages: it enables us to easily understand the physical meaning of the terms in the general balance equation and represents a compact and fast procedure to obtain the Navier-Stokes equations. Thus no previous knowledge of the equation of fluid-dynamics, and in particular of the energy equation, is required.

The main part of this work is the third, in which eight problems of steady fluid-dynamics are chosen to show how the Padé approximants enable us to obtain the full determination of the fluid-dynamics field even in those regions in which the Taylor series is inadequate to describe the field.

The exposition is self-contained because it presents the physical problem, its mathematical model, the solution and the analysis of the results. Of course a particular emphasis is given to the application of the Padé approximants technique.

The last part shows that even in unsteady flows such a procedure is useful.

These ten examples, which refer to situations very different from each other, allow us to conclude that in many fields of fluid-dynamics it is possible to successfully apply the Padé approximants technique.

This page is intentionally left blank

Contents

Chapter 1

ELEMENTS OF PADE' APPROXIMANTS THEORY

1.1 Introduction

In many problems of applied mathematics one needs to represent a function in an approximate way either in proximity of a point or in a given interval.

The basic approach for finding such representations is the Taylor series in the first case and the expansion in a series of orthogonal functions in the second: in general the Taylor series does not allow us to approximate a function in a given interval. In fact if one writes

$$f(x) = \sum_{n=0}^{\infty} a_n (x - x_0)^n \tag{1}$$

where x_0 is the initial point of the series (when $x_0 = 0$ the series (1) is called MacLaurin series) and

$$a_n = \frac{1}{n!} \left(\frac{\partial^n f}{\partial x^n} \right)_{x=x_0}$$

such equality holds only for $x_0 - r < x < x_0 + r$ where r is the radius of convergence of the series.

r is infinity only in particular cases, i.e., the expansion holds for any value of x. This situation occurs, for example, for exponential, sine and cosine functions.

In order to obtain the advantages of the Taylor expansion for small value of $| x - x_0 |$ and to extend such representation of a function to high values of $| x - x_0 |$ the Padé approximant technique can be used.

This procedure requires the knowledge of a certain number of coefficients a_n of Eq.(1): in this way it is still possible to approximate the function $f(x)$ near the initial point x_0. The second step allows us to determine a rational function $Q(x)/D(x)$, where $Q(x)$ and $D(x)$ are polynomials, that approximates $f(x)$ far from x_0 as well. The coefficients of $Q(x)$ and $D(x)$ can be obtained from a system of linear equations.

Moreover it is possible to gain an approximate evaluation of the radius of convergence r of the series in Eq.(1), by finding the roots of $D(x)$: if $r_1, r_2, \ldots, r_M$ are the moduli of such roots, the smallest of r_i gives an approximation of r. (In fact, this would be the exact radius of convergence of the Taylor series of a rational function).

2.1 MacLaurin series and Padé approximants

A regular function $f = f(x)$ can be represented by means of a power series (MacLaurin series) in the form

$$f(x) = \sum_{n=0}^{\infty} a_n x^n \tag{1'}$$

within the convergence interval (-r, r), where r is the radius of convergence of the series and $a_n = f^{(n)}(o)/n!$. Among the available formulas for calculating r we may quote the following

$$r = \lim_{n\to\infty} \mid a_n/a_{n-1} \mid . \tag{2}$$

This representation is very useful when x is small because it is possible to consider only a few terms of the series and thus obtain a good accuracy. The knowledge of r is important in order to correctly handle Eq.(1') that does not hold when $\mid x \mid > r$.

A technique that extends the range of the MacLaurin expansion is the one suggested by Padé through its approximants. This method, that uses the coefficients a_n of Eq. (1'), allows us to calculate r and to obtain a representation of $f(x)$ which is valid even when $\mid x \mid > r$. Padé approximants are defined in the following manner

$$P_M^N(x) = \frac{Q_N(x)}{D_M(x)}, \tag{3}$$

where

$$Q_N = \sum_{n=0}^{N} A_n x^n ; \quad D_M = \sum_{n=0}^{M} B_n x^n . \tag{4}$$

The $M+N+1$ unknown coefficients (we can assume $B_0 = 1$ because P_M^N is defined as the ratio of two polynomials) are obtained by the condition that the equation

$$f(x) \simeq P_M^N \tag{5}$$

holds up to terms of order x^{N+M}.

In particular the sequence $P_N = P_N^N$ is called ***diagonal sequence***.

When $f(x)$ is represented by Eq.(1'), then Eq.(5) can be written as

$$Q_N \;=\; D_M \sum_{n=0}^{\infty} a_n x^n \;. \tag{6}$$

From this equation, by using Cauchy's rule for the product of series, we have

$$\sum_{n=0}^{N} A_n x^n \;=\; \sum_{n=0}^{\infty} c_n x^n \;, \tag{7}$$

where

$$c_n \;=\; \sum_{i=0}^{n} B_i a_{n-i} \;. \tag{8}$$

Therefore the equations that determine the coefficients A_n and B_n are

$$A_n \;=\; \sum_{i=0}^{n} a_{n-i} B_i \;, \tag{9}$$

where $n = 0, 1, ..., N + M$.

We notice in these equations that $A_n = 0$ for $n > N$. Therefore Eq.(9) for $N < n < N + M$ may be written in the following form

$$\sum_{i=1}^{n} a_{n-i} B_i = -B_0 a_n \ , \tag{10}$$

whereas for $0 \leq n \leq N$ the equations are in the general form (9).

If $n > M$ coefficients B_i with $i > M$ appear in Eq.(10): these coefficients are zero.

We put $B_0 = 1$ as suggested by Baker (this choice is not trivial as we shall show in Chap. 2). Then the system defined in Eq.(10) determines the coefficients B_i. Once the coefficients B_i are known Eq.(9), written for $0 \leq n \leq N$, gives the coefficients A_i in terms of the B_i's.

For any P_M^N the knowledge of the polynomial D_M allow us to obtain an approximant of the radius of convergence r of the series (1'). If $r_1, r_2, ..., r_M$ are the moduli of the roots of D_M, the smallest of r_i gives an approximation of r.

For $M = 2, r$ is the smaller of the two numbers $\mid B_1/2B_2 \pm (B_1^2/4B_2^2 - 1/B_2)^{1/2} \mid$.

3.1 The case of the diagonal sequence

When $N = M$, diagonal sequence, the N coefficients B_i are determined by the equations

$$\sum_{i=1}^{n} a_{n-i} B_i = -a_n \quad (N < n \leq 2N) \tag{11}$$

and the $N+1$ coefficients A_i are given by the equation

$$A_n = \sum_{i=0}^{n} a_{n-i} B_i \qquad (0 \leq n \leq N)\,. \tag{12}$$

The Cramer rule enables us to write the coefficients B_i in the form

$$B_i = -d_i/d, \tag{13}$$

where d is the determinant of the system (11) and d_i is the determinant obtained by replacing the i-th column of d by $a_{N+1}, ..., a_{2N}$. For $N = 2$ one has $d = a_2^2 - a_1 a_3, d_1 = a_3 a_2 - a_1 a_4, d_2 = a_2 a_4 - a_3^2$. For $N = 3$ one has

$$\begin{aligned}
d &= a_1(a_4^2 - a_3 a_5) - a_2(a_3 a_4 - a_2 a_5) + a_3(a_3^2 - a_2 a_4),\\
d_1 &= a_1(a_5 a_4 - a_3 a_6) - a_2(a_5 a_3 - a_2 a_6) + a_4(a_3^2 - a_2 a_4),\\
d_2 &= a_1(a_4 a_6 - a_5^2) - a_4(a_4 a_3 - a_5 a_2) + a_3(a_5 a_3 - a_2 a_6),\\
d_3 &= a_3(a_3 a_6 - a_4 a_5) - a_2(a_4 a_6 - a_5^2) + a_4(a_4^2 - a_3 a_5).
\end{aligned}$$

4.1 Padé approximants for functions whose Taylor series has an infinite radius of convergence

When the radius of convergence of a power series of a given function $f(x)$ is infinite

one can obtain an accurate approximation of $f(x)$ by the first n terms of the series with a high value of n. In this case the application of the Padé approximants is not very useful because the approximation given by the series expansion is comparable with that given by the Padé approximants (calculated with the same number of coefficients).

As examples we consider two functions: $exp(x)$ and $1/\Gamma(x)$, where $\Gamma(x)$ is the gamma function.

For the first function the MacLaurin expansion has $a_n = 1/n!$. At $x = 1, exp(x) = 2.7183$. The Padé approximant for $N = 2$ (which has $B_2 = 1/12, B_1 = -1/2, A_2 = 1/12, A_1 = 1/2, A_0 = 1$) gives 2.7142, whereas the first five terms of the MacLaurin expansion give 2.7083. At $x = 2, exp(x) = 7.3891$ and both P_2 and the first five terms of the MacLaurin expansion give 7. The radius of convergence obtained from P_2 is 3.5 and that obtained from P_8 is 11.3.

An idea of the convergence of Padé approximants is given by the sequence of P_N for $exp(x)$. At $x = 1$ the exact value with six figures is 2.71828, whereas the Padé approximants give: $P_1 = 3, P_2 = 2.71429, P_3 = 2.71831, P_4 = 2.71828$. At $x = 5$ the exact value with six figures is 148.413, whereas the Padé approximants give: $P_4 = 128.619, P_5 = 149.697, P_6 = 148.362, P_7 = 148.415, P_8 = 148.413$.

In Bender and Orsag [1] it is shown that for this function the Padé approximants reduce the error after N terms by a factor proportional to 2^N.

The diagram of $exp(x)$ is displayed in Fig.1, together with its expansion in series (five and seven terms) and with the Padé representation (for N=2 and 3), for $0 \leq x \leq 4$. One can see that the Padé approximants give, with the same number of coefficients, the same accuracy, and that the approximation that one can reach increases with the number of coefficients.

A second example is given by the function $1/\Gamma(x)$, the coefficients of whose MacLaurin expansion are given in Abramowitz and Stegun [2]. The first seven coefficients are $a_0 = 0$, $a_1 = 1$, $a_2 = 0.577216$, $a_3 = -0.655878$, $a_4 = -0.042002$, $a_5 = 0.166539$, $a_6 = -0.042198$. At $x = 1$, $\Gamma(x) = 1$; the first five terms of the MacLaurin series gives 0.87934 and Padé approximant with $N = 2$ gives 0.83052. The diagram of $1/\Gamma(x)$ is displayed in Fig.2, together with its expansion in series (five and seven terms) and the Padé representation (for N=2 and 3) for $0 \leq x \leq 1.5$.

This figure shows the same qualitative behaviour as Fig.1. Small value of N gives accurate results for small x, both for the MacLaurin expansion and for Padé approximants: the accuracy obtained depends, of course, on the particular function considered.

As N increases any degree of approximation can be reached.

5.1 Padé approximants for functions whose Taylor series has a finite radius of convergence

In order to give an idea of the convergence of Padé approximants when the corresponding MacLaurin series does not converge let us consider two series, whose radius of convergence is 1, obtained by the binomial series. If $f(x) = 1/(1+x)^{1/2}$ the a_n coefficients of Eq.(1') are $a_n = (-1)^n d_{2n-1}/p_n$, where $d_m = 1 \cdot 3 ... m$, $(d_{-1} = 1)$ and $p_{2n} = 2 \cdot 4 \cdot ... 2n$ $(p_0 = 1)$. One has $a_0 = 1$, $a_1 = -1/2$, $a_2 = 3/8$, $a_3 = -5/16$, $a_4 = 35/128$ and so on.

For $N = 2$ one finds $B_2 = 5/16$, $B_1 = 5/4$; $A_2 = -1/16$; $A_1 = 3/4$; $A_0 = 1$. At

$x = 1$, $1/(1+x)^{1/2} = 0.7071$, the Padé approximant with $N = 2$ gives 0.6585 and the first 5 terms of MacLaurin expansion gives 0.8359. At $x = 2$, $1/(1+x)^{1/2} = 0.5773$, the Padé approximant with $N = 2$ gives 0.4737 and the first 5 terms of MacLaurin expansion gives 2.625. Padé approximant gives for the radius of convergence the value 0.8944.

The diagram of $1/(1+x)^{1/2}$ is displayed in Fig.3 together with its expansion in series (five and seven terms) and the Padé representation (for N=2 and 3) for $0 \leq x \leq 10$. This figure shows the strong difference between the Padé approximants and the expansion in series of a given function $f(x)$. When x belongs to the interval of convergence both representations hold, but even when x is external to such interval Padé approximants represent the function well: in this case P_3 is accurate up to $x = 10$.

A second example is given by $f(x) = log(1+x)$; in this case the expansion in series can be obtained by integrating a binomial series. The a_n coefficients of Eq.(1') are $a_n = (-1)^{n-1}$ for $n > 0$ and $a_0 = 0$. At $x = 1$, $log(1+x) = 0.6931$. The Padé approximant with $N = 2$ ($B_2 = 1/6, B_1 = 1, A_2 = 1/2, A_1 = 1, A_0 = 0, r = 1.27$) gives 0.6923 and the first five terms of MacLaurin expansion gives 0.0833. At $x = 2$, $log(1+x) = 1.0986, P_2$ gives 1.0909 and the first five terms of MacLaurin expansion gives -1.3333.

The diagram of $log(1+x)$ is displayed in Fig.4 together with its expansion in series (five and seven terms) and the Padé representation (for N=2 and 3) for

$0 \leq x \leq 10$. In this case we find again similar behaviours as those shown in Fig.3.

6.1 Two-point Padé approximants

The procedure of determining the Padé approximants for a given $f(x)$ described above can be generalized by calculating its $N + M + 1$ coefficients in a different way.

If $f(x)$ has the expansion

$$f(x) = \sum a_n (x - x_0)^n \tag{14}$$

where the initial point is x_0 and has the expansion

$$f(x) = \sum b_n (x - x_1)^n \tag{15}$$

when the initial point is x_1, one can determine p coefficients of P_M^N by requiring that the first p terms of the expansion of P_M^N agree with the first p terms of the expansion (14) of f and the remaining $M + N + 1 - p$ coefficients by requiring that the first $M + N + 1 - p$ terms of the Taylor series expansion of P_M^N agree with the first $M + N + 1 - p$ terms of the expansion (15).

This procedure has been used with success, for instance, in the approximate evaluation of inverse Laplace transform, as it allows the substitution of a rational

function, where inverse Laplace transform is easily calculated, for a general function whose Laplace transform may not be available in closed form.

References to Chapter 1

[1] C.M. Bender and S.A. Orsag, Advanced mathematical methods for scientists and engineers, Mc Graw-Hill (1978).

[2] M. Abramovitz and I.A. Stegun, Handbook of mathematical functions, Dover (1969).

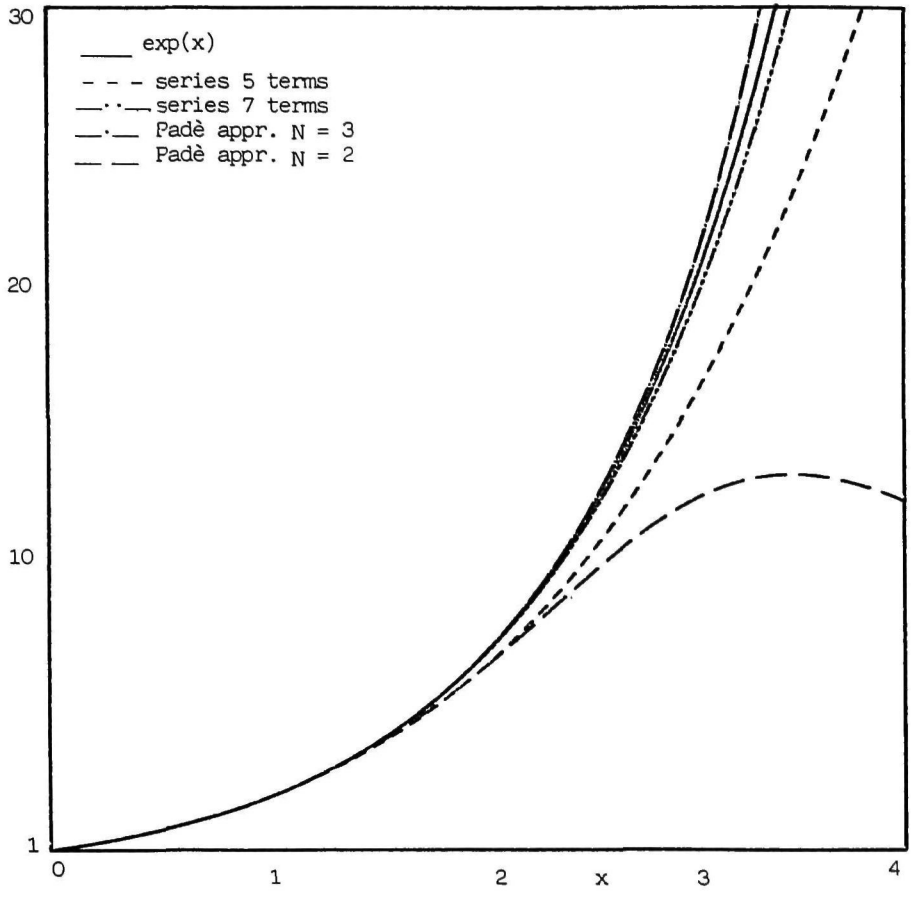

Fig.1 Comparison between Padé approximants and MacLaurin expansion for the exponential.

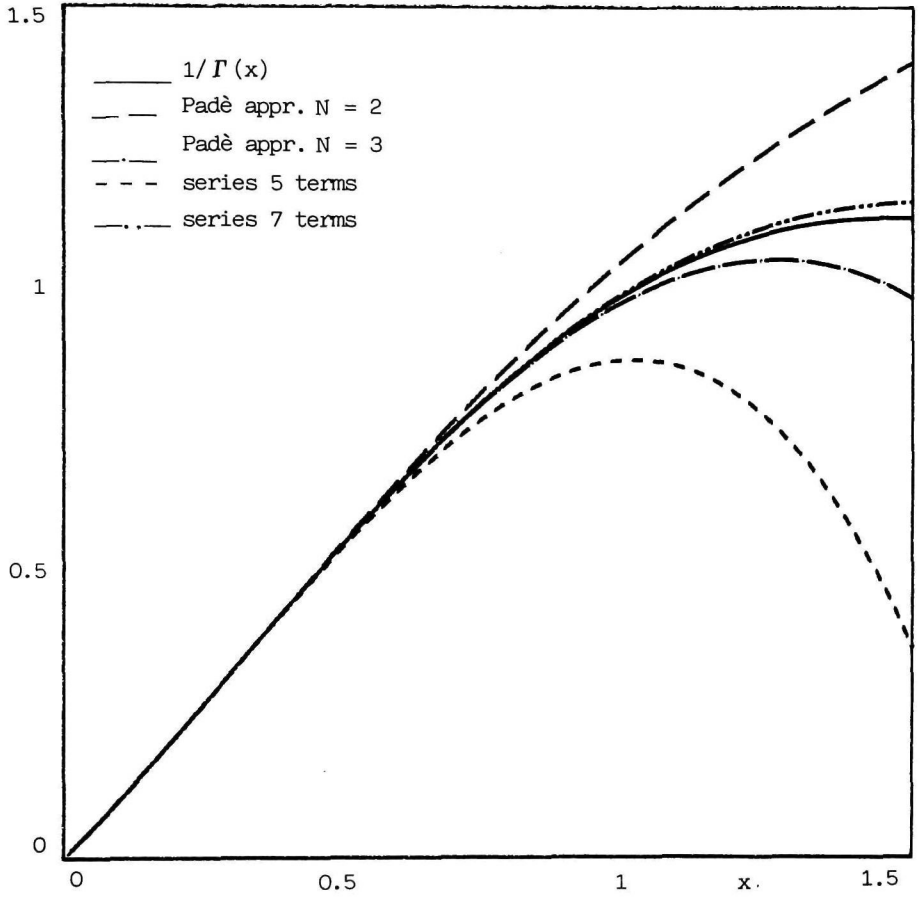

Fig.2 Comparison between Padé approximants and MacLaurin expansion for the inverse of the gamma function.

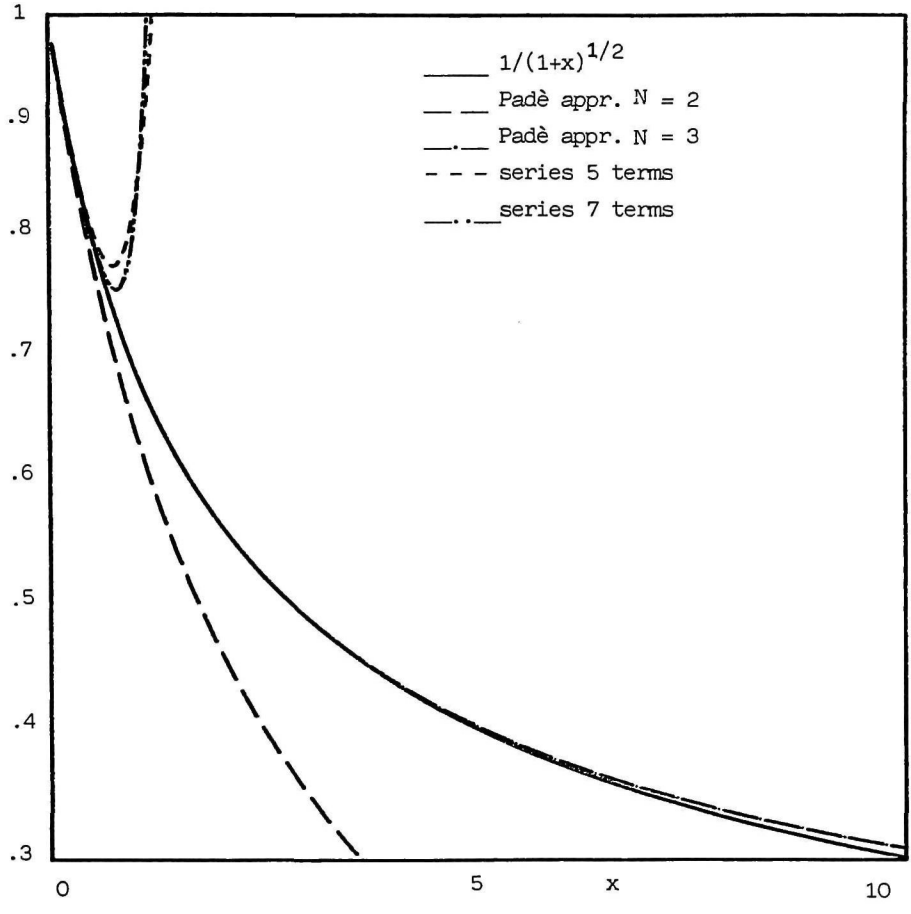

Fig.3 Comparison between Padé approximants and MacLaurin expansion for $1/(1+x)^{1/2}$.

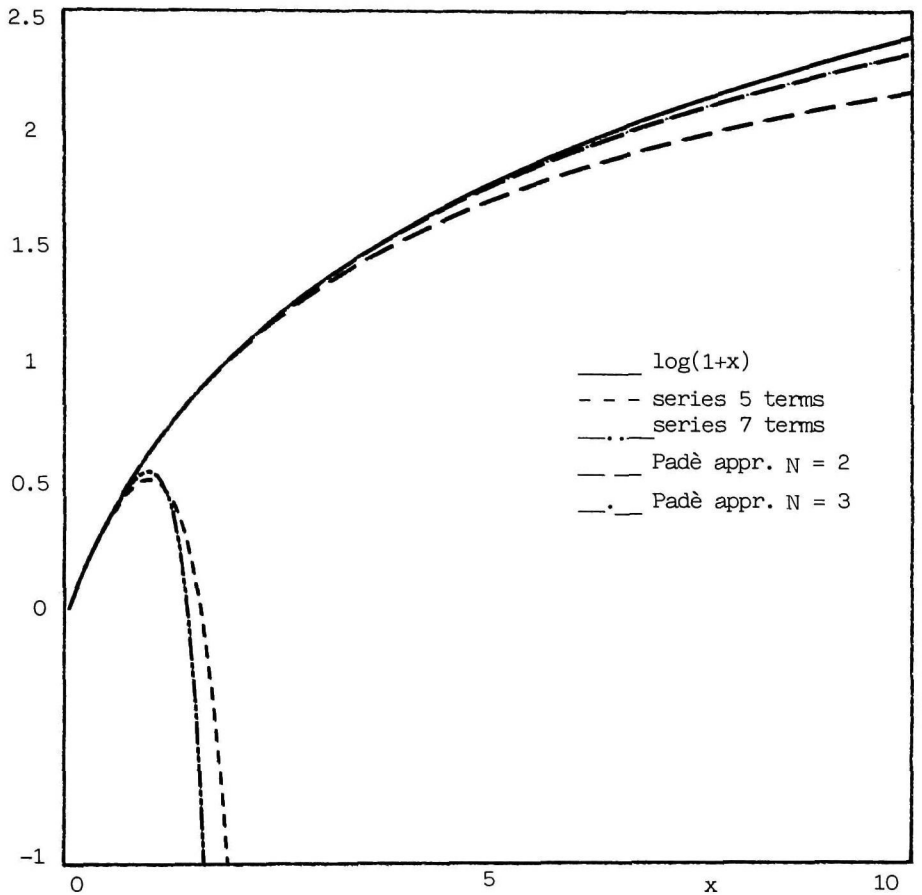

Fig.4 Comparison between Padé approximants and MacLaurin expansion for the logarithm.

Chapter 2

SOME THEORETICAL ASPECTS OF PADÉ APPROXIMANTS

1.2 Uniqueness of Padé approximants

Padé approximants, presented by Padé in 1882, have been introduced in different ways as analytically continuing a Taylor series (Wall 1948), or through moments theory, (Wall 1948, Yndurain 1973), or through Hilbert's method of minimal iterations (Garibotti and Villani 1969, Chisholm 1963) or through the theory of orthogonal polynomials (Szego 1949), or by using variational theory.

Padé approximants can be considered more general than continued fractions (that constitute a particular set of rational functions), a technique that is much older (it was used by Wallis, Gauss and Euler) but was only studied in a systematic way by Markov and Stieltjes at the end of the past century.

Bessis (1973) proved some invariance properties in a non commuting algebra.

In order to discuss the uniqueness of the sequence of Padé approximants we write them again in the form

$$P_M^N = \frac{Q_N}{D_M} \tag{1}$$

where

$$Q_N = \sum_{n=0}^{N} A_n x^n; \qquad D_M = \sum_{n=0}^{M} B_n x^N. \tag{2}$$

The rational form (1) implies that one coefficient of the polynomials (2) can be chosen arbitrarily.

Baker suggests to put $B_0 = 1$. This choice is important because if $B_0 = 0$ is allowed an ambiguity can arise. A classical example was discussed by Wallin (1972) and by Baker (1973). Let us consider a function $f(x)$ whose expansion in MacLaurin series, gives the following two-term approximation:

$$f(x) = 1 + x^2. \tag{3}$$

The four coefficients of P_1 given by

$$P_1 = \frac{A_0 + A_1 x}{B_0 + B_1 x} \tag{4}$$

must satisfy Eqs. (9.1) that for $N = 1$ become

$$\begin{aligned} A_0 &= a_0 B_0 \,, \\ A_1 &= a_1 B_0 + a_0 B_1 \,, \\ A_2 &= a_2 B_0 + a_1 B_1 + a_0 B_2 \,, \end{aligned} \tag{5}$$

where $A_2 = B_2 = 0$ and $a_0 = 1$, $a_1 = 0$, $a_2 = 1$. These three equations present four unknowns because there is a free parameter.

If we assume $B_0 = 0$ we have $A_0 = 0$ and $A_1 = B_1$; it turns out that

$$P_1 = \frac{x}{x} .$$

This approximation is correct because it satisfies Eq.(5,1) up to terms of order x^2: in fact it leads to the equation

$$x(1 + x^2) = x .$$

But if we write P_1 in the form $P_1 = 1$ we have

$$1 + x^2 = 1$$

and this equation is not satisfied up to terms of order x^2.

The choice $B_0 = 1$ avoids this inconvenience.

Another ambiguity in defining P_M^N arises when the solution of the system (10.1) is not unique, i.e. when the rank of the matrix of coefficients of such system is less than M. In this case there is a common polynomial factor in Q_N and D_M (Chisholm 1973).

In order to analyse the uniqueness of Padé approximants let us consider two rational functions

$$\frac{Q_{N,1}}{D_{M,1}} \quad \text{and} \quad \frac{Q_{N,2}}{D_{M,2}}$$

both approximating a given function f up to term x^{M+N}. One may write the following approximate equations

$$\begin{aligned} Q_{N,1} &= fD_{M,1} \\ Q_{N,2} &= fD_{M,2} \, . \end{aligned}$$

Multiplying the first equation by $Q_{N,2}$ and the second one by $Q_{N,1}$ and subtracting one has (always up to terms of order x^{M+N})

$$D_{M,1}Q_{N,2} - D_{M,2}Q_{N,1} = 0 \, .$$

This equation proves that

$$\frac{Q_{N,1}}{D_{M,1}} = \frac{Q_{N,2}}{D_{M,2}}$$

and that there is a unique P_M^N of minimum order in numerator and denominator.

2.2 Padé approximants and inverse series

Let us consider two functions $f(x)$ and $F(x)$, with $f(0) \neq 0$, satisfying the identity

$$F(x)f(x) = 1 . \tag{6}$$

Let the expansions in series of f and F be

$$f(x) = \sum_{i=0}^{\infty} c_i x^i \tag{7}$$

$$F(x) = \sum_{i=0}^{\infty} C_i x^i . \tag{8}$$

Then the series (8) is said "inverse" of series (7).

The coefficients C_i may be calculated in terms of c_i by using Cauchy's rule for the product of two series.

It results that

$$c_0 C_0 = 1 \tag{9}$$

$$\sum_{i=0}^{n} c_i C_{n-i} = 0 \qquad (n = 1, 2) . \tag{10}$$

It is easy to check that the polynomial

$$F_N(x) = \sum_{i=0}^{N} C_i x^i \tag{11}$$

is the P_N^O Padé approximant to $f(x)$. More generally Baker and Gammel (1961) proved that the P_M^N approximant to $F(x)$ is equal to the inverse of the P_N^M approximant to $f(x)$.

In fact the Padé approximant to the function $f(x)$,

$$f_{P_M^N} = \frac{f_{Q_N}}{f_{D_M}},$$

(always up to terms of order x^{M+N}) obeys the equation

$$\left(\sum_{i=0}^{\infty} c_i x^i\right) f_{D_M} = f_{Q_N} \tag{12}$$

whereas the Padé approximant to $F(x)$,

$$F_{P_N^M} = \frac{F_{Q_M}}{F_{D_N}},$$

obeys the equation

$$\left(\sum_{i=0}^{\infty} C_i x^i\right) F_{D_N} = F_{Q_M} . \tag{13}$$

Now multiplying Eq.(12) by series (8) one finds

$$\left(\sum_{i=0}^{\infty} C_i x^i\right) \sum_{i=0}^{\infty} c_i x^i f_{D_M} = \left(\sum_{i=0}^{\infty} C_i x^i\right) f_{Q_N} . \tag{14}$$

Taking into account Eq.(6) one has

$$f_{D_M} = f_{Q_N} \sum_{i=0}^{\infty} C_i x^i \tag{15}$$

Eqs.(13) and (15) give

$$\frac{F_{Q_M}}{F_{D_N}} = \frac{f_{D_M}}{f_{Q_N}} . \tag{16}$$

3.2 Padé approximants and continued fractions

Series (7) may be approximated by means of continued-fraction theory, symbolically defined as

$$F_n = \cfrac{a_0}{1 - \cfrac{a_1 x}{1 - \cfrac{a_2 x}{1 - \ldots \cfrac{a_{n-1} x}{1 - a_n x}}}} . \tag{17}$$

The approximants to the series (7) are

$$a_0, \quad \frac{a_0}{1 - a_1 x}, \quad \cfrac{a_0}{1 - \cfrac{a_1 x}{1 - a_2 x}}, \quad \cfrac{a_0}{1 - \cfrac{a_1 x}{1 - \cfrac{a_2 x}{1 - a_3 x}}}, \cdots . \tag{18}$$

In particular when n is even F_n is the ratio of two polynomials of degree

$$\frac{n}{2}$$

and when n is odd F_n is the ratio of a polynomial of degree

$$\frac{n-1}{2}$$

and a polynomial of degree

$$\frac{n+1}{2}.$$

This sequence is determined by approximating the series (7) up to terms of the maximum possible order.

Let us consider for example the sequence of coefficients of the representation (17) for $\exp x$. It results that

$$a_0 = 1; \quad a_1 = 1$$

and for $n \geq 1$

$$a_{2n} = -\frac{1}{(4n-2)}; \quad a_{2n+1} = \frac{1}{(4n+2)}.$$

In Fig.1 we have plotted the continued-fraction approximation for $n = 4$ and $n = 5$ for such function.

The continued-fraction representation (18) is equal to the Padé approximants

$$P_0^0, \quad P_1^0, \quad P_1^1, \quad P_2^1, \ldots \tag{19}$$

when every member of this sequence exists and no two members are equal (under these conditions the sequence (19) is said to be normal).

4.2 Convergence theorems

There are several theorems on Padé approximants: the most significant differences among them deal with the way in which M and N go to infinity.

de Montessus de Ballore (1902) considered the convergence of P_M^N with M fixed; he proved that if a function $f(z)$, with z complex variable, is regular at all the points of a circle of radius R except for a finite number of poles, of total multiplicity M, then P_M^N converges, for $N \to \infty$, to $f(z)$ in the circle except at the poles of $f(z)$.

Some informations about the convergence of particular sequences P_M^N can be obtained from continued-fraction theory. The *diagonal sequence* P_N^N and the *para-diagonal* one P_N^{N+h}, with h fixed, have greater interest in the applications, have an invariance property (Bessis 1973), but they do not have general convergence theorems. There exists a conjecture of Baker and Gammel's (1961), neither proved nor disproved, stating that if $f(z)$ is regular in the circle $\mid z \mid \leq 1$, except for m poles inside the circle and at $z = 1$, then a subsequence of P_N^N converges uniformly to $f(z)$ inside the circle except around the poles.

The main difficulty in obtaining these results resides in the knowledge of the

poles and zeros of P_M^N.

References to Chapter 2

[1] M.H. Padé, Sur la Representation Approcheé d'une Fonction par des Fractions Rationelles, *Ann. de l'Ecole Normale Superieure 9 suppl* (1892)

[2] P.R. Graves-Morris, Padé Approximants, The Institute of Physics London and Bristol, (1973)

[3] R. de Montessus de Ballore, *Bull. Soc. Math. Fr., 30, (1902), 28*

[4] H.S. Wall, Continued Fractions - Van Nostrand, (1978) New York

[5] F.J. Yndurain Institue of Physics - Bristol (1973)

[6] C.R. Garibotti, M. Villani, *Nuovo Cimento* 61 A, (1969), 747

[7] J.S.R. Chisholm, *J. Math. Physics*, 4, (1963), 1506

[8] J.S.R. Chisholm, Mathematical Theory of Padé approximants (Padé Approximants, Editor Graves-Morris, The Institute of Physics London and Bristol) (1973)

[9] G. Szego, Orthogonal Polynomials, *American Mathematical Society*, (1959), 54

[10] D. Bessis, Padé Approximants, P.R. Graves-Morris The Institute of Physics London and Bristol, (1973)

[11] G.A. Baker, J.L. Gammel, *J. Math. Anal. Appl.*, 2, (1961), 405

[12] H. Wallin, University of Umica, Preprint S, (1973), 109-87

[13] G.A. Baker, Cornell University and BNL, Preprint, (1973)

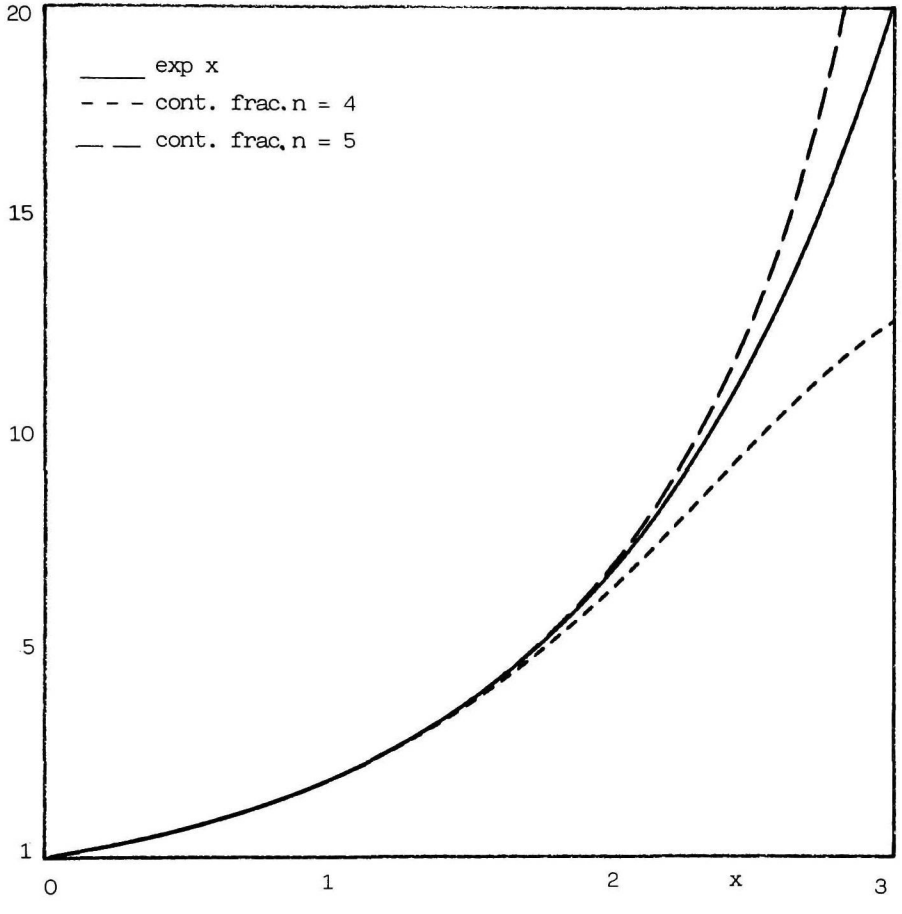

Fig.1 Continued-fraction approximation for the exponential

Chapter 1

BALANCE EQUATIONS

1.1 The general balance equation

Let Q be a point in a domain D in which there are N particles the i-th of which, at time t, is at point Q_i, has velocity $\underline{c}_i$ and the extensive property Π_i.
Denoting by the symbol $< f >$ the statistical mean value of a function $f(x_1, x_2, \ldots, x_n)$, we define density of the property Π, at a point Q of D, the function $P_\Pi(Q,t)$ such that its integral, extended to D, is equal to the sum of property Π_i over the particles that are in D.

In order to express the density in terms of Π_i, Q and Q_i we introduce the Dirac delta function $\delta(Q)$: this function is always zero except at the origin where it goes to infinity in such a way that its integral extended to any domain enclosing the origin is equal to 1. Thus the density is defined as follows

$$P_\Pi = < \sum_{i=1}^{N} \Pi_i \delta(Q - Q_i) > \ . \tag{1}$$

By integrating this equation we have

$$\int_D P_\Pi dD = < \sum \Pi_i \int_D \delta(Q - Q_i) dD > = < \sum \Pi_i > . \tag{2}$$

It is now possible to write the general balance equation by differentiating Eq.(1). It results that

$$\frac{\partial}{\partial t} P_\Pi = < \sum \dot{\Pi}_i \delta(Q - Q_i) + \Pi_i \frac{\partial}{\partial t} \delta(Q - Q_i) > \tag{3}$$

where $\dot{\Pi}$ denoted the derivative of Π with respect to t.

For any function $f[Q - Q_i(t)]$, $f_t = -\underline{c}_i(t) \cdot grad_Q f$, where $\underline{c}_i = \dot{Q}_i$, and $\underline{c}_i \cdot gradf = div(f\underline{c}_i)$, because $\underline{c}_i$ does not depend on Q. Therefore we have

$$\frac{\partial}{\partial t} \delta(Q - Q_i) = -div[\underline{c}_i \delta(Q - Q_i)] . \tag{4}$$

Then Eq.(3) becomes

$$\frac{\partial}{\partial t} P_\Pi + div J_p = P^+ \tag{5}$$

where

$$P^+ = < \sum \dot{\Pi}_i \delta(Q - Q_i) >; \quad J_P = < \sum \Pi_i \underline{c}_i \delta(Q - Q_i) > \tag{6}$$

Eq.(6) is the general balance equation for the property Π. P^+ and J are the density of production and the density of flux of Π.

2.1 The continuity equation

When we consider as property Π_i associated with the i-th particle its mass m_i Eq.(5) gives the following continuity equation

$$\rho_t + div \rho \underline{V} = 0 \tag{7}$$

where $\rho = P_m$ is the mass density. The mean mass velocity $\underline{V}$ is defined through the equation

$$\underline{J_m} = \rho \underline{V} . \tag{8}$$

The mass production P^+ is vanishing.

3.1 The momentum equation

When we consider as property Π_i the momentum $m_i \underline{c_i}$ of the i-th particle Eq.(5) gives the following momentum equation

$$(\rho \underline{V})_t + div J_{mom} = \underline{F} \tag{9}$$

where, denoting by $\underline{f}_i$ the force acting "at a distance" on the i-th particle and by $\underline{F}$ the density of production of momentum, it is

$$J_{mom} = < \sum m_i \underline{c}_i \underline{c}_i \delta(Q - Q_i) > \tag{10}$$

$$\underline{F} = < \sum \underline{f}_i \delta(Q - Q_i) > \tag{11}$$

J_{mom} is the momentum flux and $\underline{F}$, called "volume force", represents the mean force, per unit volume, acting on the volume D (the earth's field exerts a volume force $= \underline{g}\rho$, where $\underline{g}$ is the gravity acceleration).

Equation (10) can be written in a different form by putting the velocity $\underline{c}_i$ of a particle as sum of the mean velocity $\underline{V}$ and of a velocity of diffusion $\underline{C}_i$ as follows

$$\underline{c}_i = \underline{V} + \underline{C}_i \, . \tag{12}$$

In this way, taking into account that from Eq.(8) one has

$$< \sum m_i \underline{C}_i \delta(Q - Q_i) > = 0 \tag{13}$$

Eq.(10) can be written in the form

$$J_{mom} = \rho \underline{V}\,\underline{V} + I_{mom} \tag{14}$$

where the stress tensor I_{mom} is

$$I_{mom} = < \sum m_i \underline{C}_i \underline{C}_i \delta(Q - Q_i) > \ . \tag{15}$$

Then Eq.(9) becomes

$$(\rho \underline{V})_t + div \rho \underline{V}\,\underline{V} + div I_{mom} = \underline{F} \tag{16}$$

or

$$\rho \frac{D\underline{V}}{Dt} + div I_{mom} = \underline{F} \tag{17}$$

where

$$\frac{D}{Dt} = \frac{\partial}{\partial t} + \underline{V} \cdot grad \, .$$

4.1 The energy equation

When we consider as property Π_i the energy e_i of the i-th particle and we put

$$E = < \sum e_i \delta(Q - Q_i) > \tag{18}$$

$$\underline{J}_e = < \sum e_i \underline{c}_i \delta(Q - Q_i) > \tag{19}$$

$$P_e^+ = < \sum \dot{e}_i \delta(Q - Q_i) > \tag{20}$$

where $\dot{e}_i$ is the time derivative of e_i, Eq.(5) gives the following energy equation

$$E_t + div \underline{J}_e = P_e^+ \tag{21}$$

Eq.(21) holds for any form of energy which we can associate with the i-th particle of the volume D, and it is possible to write the energy equation according to the definition of e_i.

A first form of energy is the kinetic one $e_{k,i}$, which can be written as

$$e_{k,i} = m_i c_i^2/2 + e_{r,i} + e_{v,i} \, . \tag{22}$$

The three terms on the r.h.s. of this equation respectively represent the translational, rotational and vibrational energy of the particle.

The gravitational form of energy of the particle m_i due to the presence of a particle of mass m_j is given by

$$e_{gij} = -Gm_i m_j / d_{ij} \tag{23}$$

where $G = 6.67 \times 10^{-8} cm^3/gsec^2$ is the Newton's gravitational constant and d_{ij} is the distance between the i-th and the j-th particle. Therefore the gravitational energy e_{gi} of the i-th particle is given by

$$e_{gi} = \sum_j e_{g,j} \, . \tag{24}$$

Another form of energy is that due to other interactions between particles, different from the gravitational one. Moreover there are forms of energy that can be considered belonging to the particle, i.e. not arising from the presence of other bodies or fields, such as those present during chemical or nuclear reactions: these forms are constant if the associated reaction does not take place.

Let us consider as energy associated with the i-th particle the following

$$e_i = e_{k,i} + e_{gi} \, . \tag{25}$$

Then we have

$$E = \rho(U + U_g + V^2/2) \tag{26}$$

where

$$\rho U = < \sum (m_i C_i^2/2 + e_{r,i} + e_{v,i}) \delta(Q - Q_i) > \tag{27}$$

$$\rho U_g = < \sum e_{gi} \delta(Q - Q_i) > \tag{28}$$

U and U_g are called internal energy and gravitational energy respectively.

For this type of energy $\underline{J}_e$ is given by

$$\underline{J}_e = (U + U_g + V^2/2)\rho \underline{V} + \underline{J}_{ther} + \underline{V} \cdot I_{mom} \tag{29}$$

where

$$\underline{J}_{ther} = \sum (m_i C_i^2/2 + e_{r,i} + e_{v,i}) \underline{C}_i \delta(Q - Q_i) \tag{30}$$

is called heat flux density.

Then the energy equation, when e_i is given by Eq.(25), is

$$\rho \frac{D}{Dt}(U + U_g + V^2/2) + div(\underline{J}_{ther} + \underline{V} \cdot I_{mom}) = P_e^+ . \tag{31}$$

This equation can be written in a different form, in which the gravitational term appears on the r.h.s. In fact, as

$$\frac{D}{Dt} U_g = \frac{\partial}{\partial t} U_g + \underline{V} \cdot grad U_g = \underline{V} \cdot \underline{g}$$

we have

$$\rho \frac{D}{Dt}(U + V^2/2) + div(\underline{J}_{ther} + \underline{V} \cdot I_{mom}) = P_1 \tag{32}$$

where $P_1 = P_e^+ - \rho \underline{V} \cdot \underline{g}$.

The internal energy U is related to the absolute temperature T through the equation

$$dU = c_v dT \tag{33}$$

where c_v is the constant-volume heat-transfer coefficient.

5.1 The Navier-Stokes equations

For Newtonian fluids the stress tensor can be expressed as follows

$$I_{mom} = pU_n + I_d \tag{34}$$

where p is the pressure, U_n is the unit tensor and I_d, the dissipative part of the stress tensor, is given by

$$I_d = -\mu(grad\underline{V} + grad^+\underline{V}) + \frac{2}{3}\mu div\underline{V}\, U_n \tag{35}$$

where μ is the viscosity coefficient and the symbol + denotes a transposed tensor.

The heat flux density vector $\underline{J_{ther}}$ is given by the following Fourier law

$$\underline{J_{ther}} = -\lambda grad T \tag{36}$$

where λ is the coefficient of thermal conductivity.

In this way the continuity, momentum and energy equations are written in terms of the macroscopic unknowns p, ρ, T and $\underline{V}$.

It can be useful to write the energy equation in terms of the enthalpy h, defined as

$$h = U + p/\rho \tag{37}$$

and the total enthalpy H, defined as

$$H = h + V^2/2\,. \tag{38}$$

In particular, taking into account the continuity equation, yields

$$\rho \frac{d(U + V^2/2)}{Dt} = \rho \frac{DH}{Dt} - \frac{Dp}{Dt} - p div \underline{V}\,.$$

Therefore the continuity, momentum and energy equations can be written as follows

$$\rho_t + div \rho \underline{V} = 0 \tag{39}$$

$$\rho \frac{D\underline{V}}{Dt} + gradp = \underline{F} - divI_d \tag{40}$$

$$\rho \frac{DH}{Dt} = P_1 + p_t - div(\underline{V} \cdot I_d + \underline{J}_{ther}) \tag{41}$$

Eqs.(39)-(41) are called Navier-Stokes equations which, when ρ, μ and λ are constant, assume the following simplified form

$$div\underline{V} = 0 \tag{42}$$

$$\rho \frac{D\underline{V}}{Dt} + gradp = \underline{F} + \mu \Delta_2 \underline{V} \tag{43}$$

$$\rho \frac{DH}{Dt} = P_1 + p_t + \lambda \Delta_2 T - \mu div[\underline{V} \cdot (grad\underline{V} + grad^+ \underline{V})] . \tag{44}$$

The fourth equation that completes the system of equations for the four unknowns $p, \rho, T(or H)$ and $\underline{V}$ is the equation of state. The most commonly used forms of this equation are

$$\rho = const. \qquad (incompressible\ fluids)$$

$$p = \rho RT \qquad (perfect\ gases)$$

where the gas constant R is related to the universal constant R_0 by the equation $R = R_0/m$, where m is the molecular weight of the gas.

6.1 Non-dimensional form of the Navier-Stokes equations

In order to write the Navier-Stokes equations in a non-dimensional form reference quantities must be chosen.

For velocity, density, length and for the coefficients of viscosity, thermal conductivity and specific heats, at constant pressure and volume, we assume typical quantities representative of mean conditions of the flow denoted by V_0, ρ_0, L, μ_0, λ_0, $c_{p,0}$ and $c_{v,0}$ respectively. The reference time t_0 and pressure p_0 can be chosen as L/V_0 and $\rho_0 V_0^2$, but in some cases this choice is not suitable and the reference time and pressure must be denoted explicitly by t_0 and p_0. The reference quantities for F and P_1 will be denoted by F_0 and P_{10}.

A reference temperature T_0 or enthalpy (h_0 or H_0) must also be chosen.

By denoting non-dimensional quantities without any labels Eqs.(39)-(41) can be written as follows

$$\frac{L}{V_0 t_0}\rho_t + div\rho\underline{V} = 0 \tag{45}$$

$$\frac{L\rho}{V_0 t_0}\underline{V}_t + \rho\underline{V}\cdot grad\underline{V} + \frac{p_0}{\rho_0 V_0^2}gradp = \frac{LF_0}{\rho_0 V_0^2}\underline{F} - \frac{1}{Re}divI_d \tag{46}$$

$$\frac{L\rho}{V_0 t_0} H_t + \rho \underline{V} \cdot grad H = \frac{L P_{10}}{\rho_0 H_0 V_0} P_1 + \frac{p_0 L}{\rho_0 H_0 V_0 t_0} p_t$$
$$- \frac{1}{Re}\left[\frac{c_p T_0}{H_0}\frac{1}{Pr} div \underline{J}_{ther} + \frac{V_0^2}{H_0} div(\underline{V} \cdot I_d)\right] \tag{47}$$

where

$$Re = \frac{\rho_0 V_0 L}{\mu_0} \qquad (Reynolds\ number)$$

$$Pr = \frac{c_{p0}\mu_0}{\lambda_0} \qquad (Prandtl\ number)$$

when the fluid is perfect $p = \rho RT$: by introducing the velocity of sound $a = (\gamma RT)^{1/2}$, where $\gamma = c_p/c_v$, it results that

$$\frac{p_0}{\rho_0 V_0^2} = \frac{1}{\gamma M^2}$$

where the Mach number is defined as follows

$$M = \frac{V_0}{a_0} \qquad (Mach\ number)\ .$$

In the incompressible case, on assuming the transport coefficients to be constant and putting $p_0 = \rho_0 V_0^2$ and $t_0 = L/V_0$, Eqs.(42)-(44) become

$$div \underline{V} = 0 \tag{48}$$

$$\underline{V}_t + \underline{V} \cdot grad\underline{V} + gradp = \frac{LF_0}{\rho_0 V_0^2}\underline{F} + \frac{1}{Re}\Delta_2\underline{V} \tag{49}$$

$$H_t + \underline{V} \cdot gradH = \frac{LP_{10}}{\rho_0 V_0 H_0}P_1 + \frac{V_0^2}{H_0}p_t$$

$$+ \frac{1}{Re}\left[\frac{c_{p0}T_0}{H_0}\frac{1}{Pr}\Delta_2 T - \frac{V_0^2}{H_0}div(\underline{V} \cdot I_d)\right] . \tag{50}$$

Chapter 2

INNER-OUTER EXPANSIONS

1.2 Outer expansion

For large values of the Reynolds number of the flow it is possible to expand the four basic unknowns, p, ρ, T (or H) and $\underline{V}$ in terms of $\epsilon = 1/Re^{1/2}$ by writing for each of these functions an expansion of the following type (outer expansion)

$$f(x,y,z,t,\epsilon) = \sum f_i(x,y,z,t)\epsilon^i \tag{1}$$

where we used a cartesian system of reference (x,y,z). The leading terms of these expansions lead to the following Euler equations

$$\rho_t + div\rho\underline{V} = 0 \tag{2}$$

$$\rho\frac{D\underline{V}}{Dt} + gradp = \underline{F} \tag{3}$$

$$\rho\frac{DH}{Dt} = P_1 + p_t\,. \tag{4}$$

2.2 Inner expansion

The expansion (1) involves the loss of the second order derivatives of the unknowns in the systems of equations that determine the successive approximations. Thus not all the boundary conditions can be satisfied: for instance it is not possible to assure the adherence of the fluid to the body over which it flows.

This problem is solved by means of a second, different expansion, the inner expansion, that holds in a narrow region (typically near the body over which the fluid flows) while the expansion (1) holds in the region complementary with respect to this: the inner and the outer expansions are matched along a line belonging to both regions.

In order to write this second expansion we assume that the component of velocity along the x axis is the main part of velocity and that the y axis is nearly normal to the body over which the fluid flows.

Then we introduce a new variable as follows

$$y \qquad \epsilon Y \tag{5}$$

and we expand in the inner region any function f in this way

$$f(x, Y, z, t, \epsilon) \quad = \sum F_i(x, Y, z, t)\epsilon^i \,. \tag{6}$$

The leading terms of these expansions lead to the boundary layer Prandtl equations which in a non-dimensional form, assuming $t_0 = L/V_0$ and $p_0 = \rho_0 V_0^2$, can be written as

$$\rho_{ot} + (\rho_0 u_0)_x + (\rho_0 v_1)_Y + (\rho_0 w_0)_z = 0 \tag{7}$$

$$\rho_0(u_{ot} + u_0 u_{ox} + v_1 u_{oY} + w_0 u_{oz}) + p_x = \xi_0 + (\mu u_{oY})_Y \tag{8}$$

$$p_Y = \eta_0 \tag{9}$$

$$\rho_0(w_{ot} + u_0 w_{ox} + v_1 w_{oY} + w_0 w_{oz}) + p_z = \zeta_0 + (\mu w_{0Y})_Y \tag{10}$$

$$\rho_0(H_{ot} + u_0 H_{ox} + v_1 H_{0Y} + w_0 H_{0z}) = \frac{LP_{10}}{\rho_0 V_0 H_0} P_1 + \frac{V_0^2}{H_0} p_{ot}$$

$$+ \frac{1}{Pr} \frac{c_{p0} T_0}{H_0} (\lambda T_{0Y})_Y + V_0^2 (\mu u_0 u_{oY})_Y \tag{11}$$

where the components along the axes x, y and z of $\underline{V}$ and $LF_0\underline{F}/\rho_0 V_0^2$ are denoted by u, v, w and ξ, η, ζ respectively.

Notice that all the unknowns (p, ρ, u, w, T) appearing in Eqs.(7)-(11) are

represented by their "zero-order" term except v which is represented by the "first-order" term of its expansion.

3.2 Matching of the inner and outer solutions

In order to match the outer expansion (1) with the inner expansion (6) we need a new expansion for any function f_i of the outer expansion (1) in terms of the y variable. Then we can write

$$f_i(x,y,z,t) = \sum_j f_{ij}(x,z,t)y^j \tag{12}$$

where

$$f_{ij}(x,z,t) = \frac{1}{j!}\frac{\partial^j f_i}{\partial y^j}(x,0,z,t)\,. \tag{13}$$

This equation taking into account Eq.(5) can also be written as

$$f_i(x,y,z,t) = \sum_j f_{ij}(x,z,t)Y^j\epsilon^j\,. \tag{14}$$

Then by imposing that the inner and the outer solutions give the same values on a suitable surface, we can write for the Eqs.(6) and (12), on such surface $Y^+ = Y^+(x,z,t)$,

$$\sum_i F_i(x,Y^+,z,t)\epsilon^i = \sum_i \sum_j f_{ij}(x,z,t)Y^{+j}\epsilon^{j+i} \tag{15}$$

where the l.h.s. refers to the inner solution and the r.h.s. to the outer one.

Equation (15) must be satisfied for any ϵ; therefore by equating the coefficients of same powers of ϵ one has

$$F_0(x, Y^+, z, t) = f_{00}(x, z, t) \tag{16}$$

$$F_1(x, Y^+, z, t) = f_{10}(x, z, t) + f_{01}(x, z, t)Y^+ \tag{17}$$

and so on.

The surface $Y^+ = Y^+(x, z, t)$ does not coincide with $y = 0$; therefore when ϵ tends to zero, for Eq.(5) Y^+ tends to infinity. In this case Eqs. (16) and (17) become

$$\lim_{Y \to \infty} F_0(x, Y, z, t) = f_{00}(x, z, t) \tag{18}$$

$$\lim_{Y \to \infty} [F_1(x, Y, z, t) - Y f_{01}(x, z, t)] = f_{10}(x, z, t)\,. \tag{19}$$

4.2 The Euler and Prandtl equations in a two-dimensional flow and their boundary conditions

The Euler equations, which can be obtained from the Navier-Stokes ones by considering that the dissipative coefficients are vanishing, are

$$\rho_t + div(\rho \underline{V}) = 0 \tag{20}$$

$$\rho(\underline{V}_t + \underline{V} \cdot grad\underline{V}) + gradp = \underline{F} \tag{21}$$

$$\rho(H_t + \underline{V} \cdot gradH) = p_t \tag{22}$$

when we assume $P_1 = 0$.

The boundary conditions associated with this system can be written as follows.

A $t = 0$ the four unknowns must be given as functions of the spatial variables.

When we consider the flow of a fluid along a body, very far from the body the fluid assumes a given asymptotic velocity, density, pressure and enthalpy; moreover the body is a streamline, i.e. if $\underline{n}$ denotes the normal to the body $\underline{V} \cdot \underline{n} = 0$ along the body.

The boundary layer equations (7)-(11) when $P_1 = \eta_0 = \zeta_0 = 0$, for two-dimensional flows can be written as follows (the labels of the variables are missing)

$$\rho_t + (\rho u)_x + (\rho v)_Y = 0 \tag{23}$$

$$\rho(u_t + uu_x + vu_Y) + p_x = \xi_0 + (\mu u_Y)_Y \tag{24}$$

$$p_Y = 0 \tag{25}$$

$$\rho(H_t + uH_x + vH_Y) = \frac{V_0^2}{H_0} p_t + \frac{1}{Pr} \frac{c_{p0} T_0}{H_0} (\lambda T_Y)_Y + \frac{V_0^2}{H_0} (\mu u u_Y)_Y . \qquad (26)$$

From Eq.(25) one has $p(x, Y) = p(x, \infty)$; moreover Eq.(16), applied to the pressure, shows that the pressure in the inner region equals that obtained from the Euler equations at the body. If the label "e" denotes value of functions of the outer region calculated at the body one has

$$p_x = -\rho_e u_e u_{ex} . \qquad (27)$$

Finally, by expressing the temperature as function of H, Eq.(26) can be written as follows

$$\rho(H_t + uH_x + vH_Y) = \frac{V_0^2}{H_0} p_t + \frac{1}{Pr} (\lambda H_Y)_Y + \frac{V_0^2}{H_0} (\mu u u_Y)_Y \left(1 - \frac{1}{Pr}\right) . \qquad (28)$$

The boundary conditions require that at $t = 0$ all the unknowns be given as functions of the spatial variable.

At the body $u = v = 0$. For $Y \to \infty$ one has

$$u(x, \infty) = u_e , \qquad H(x, \infty) = H_e .$$

A condition on H must be given at the body: the simplest assigns the value of H or of its derivative with respect to Y.

Chapter 1

THE THERMO-FLUID-DYNAMIC EQUATIONS

1.1 Introduction

We can assume as basic unknowns for thermo-fluid-dynamic problems velocity $\underline{V}$, pressure p, density ρ and temperature T; they are determined by the continuity, momentum, energy and state equations and by suitable boundary conditions.

When a fluid flows along a body the boundary conditions are easily given by assuming that velocity vanishes at the body and takes on a given value very far from it. More difficult is to give the boundary condition for temperature at the body. The simplest way is to assign the temperature at the solid-fluid interface, but this type of condition is of little interest for applications because in general the temperature at the interface is unknown.

The case of insulated bodies, corresponding to vanishing heat flux at the interface, occurs more frequently.

In order to solve problems of practical interest one must determine together with the temperature field in the solid and the thermo-fluid-dynamic field in the fluid.

These problems are very difficult for the elliptic character of the solution, even

in the case of high Reynolds number flow that enables us to reduce the elliptic Navier-Stokes equations to the approximate parabolic Prandtl ones. In fact the elliptic character of the Laplace equation that governs temperature in the solid makes the whole coupled problem elliptic. Boundary conditions can be given in a simpler way if one considers elongated solid bodies and neglects axial thermal conduction. In this case it is possible to obtain the temperature distribution in the solid by means of an expansion in a Taylor series and to solve the fluid equations with a suitable relation between temperature and heat flux at the interface. By studying this problem, which does not lead to similarity solutions even for simple geometries, one sees that it is characterized by coupling parameters between solid and fluid properties. Useful solutions can be obtained for small and large values of these parameters, but the exact solution is also important: Padé approximants give a good representation of such exact solution.

The relation between temperature and heat flux at the interface depends on regime (steady or unsteady), geometry of the body, type of thermal condition at the body surface that is not wetted by the fluid.

In this part we consider steady problems both for forced convection and for natural convection, the solution of which was obtained by Luchini, Lupo and Pozzi (1990) and Pozzi and Lupo (1988, 1989, 1990, 1991).

2.1 Temperature in the solid

The temperature T in the solid, in steady regime, is governed by the Laplace

equation

$$\Delta_2 T = 0 . \tag{1}$$

We shall denote quantities calculated at the fluid-solid interface by the subscript w.

When the geometry of the body is elongated, in the sense that its transverse dimension is small compared to the longitudinal one, it is possible to express heat flux at the interface in terms of T_w and its axial derivatives, as we shall do in several situations.

Let us study Eq.(1) in a strip of height b in a cartesian system $(x',\ y')$ (Fig.1) with two types of boundary conditions $T = T_b = const.$ on the lower part and $T = T_w$ on the upper part, case (a); $T_{y'} = 0$ on the lower side and $T = T_w$ on the upper part, case (b): x' and y' denote dimensional coordinates.

In case (a), if L is a characteristic length in the x' direction, it is convenient to introduce the dimensionless coordinates $X = x'/L$ and $Y = y'/b$. Then Eq.(1) may be written as

$$T_{yy} = -(b/L)^2 T_{xx} \tag{2}$$

and the temperature may be expanded in a MacLaurin series in power of the parameter $(b/L)^2$, when such a parameter is less than 1.

The leading term T° of this expansion, governed by the equation $T^\circ_{YY} = 0$, is given by

$$T^{\circ} = T_w + (T_w - T_b)Y \,. \tag{3}$$

Then

$$T^{\circ}_{y',w} = (T_w - T_b)/b \,. \tag{4}$$

Also in case (b) $T_{y'}$ may be expanded into a Taylor series in terms of y'. Taking Eq.(1) into account one has, for the leading term

$$T_{y',w} = -T_{x'x',w}b \,. \tag{5}$$

Let us now study Eq.(1) in polar coordinates (r, θ) in a wedge of half angle α (Fig.2) with two types of boundary conditions: $T(\alpha, r) = T_w(r)$ and $T(o, r) = T_b = const.$, case (c), $T(\alpha, r) = T_w(r)$ and $T_\theta(0, r) = 0$, case (d). Equation (1) in polar coordinates becomes

$$T_{\theta\theta} + r(rT_r)_r = 0 \,. \tag{6}$$

In this case the temperature may be expanded into a MacLaurin series in power of α^2. An analysis similar to that of case (a), valid for small values of α^2, leads in case (c) to the following temperature distribution in the solid at leading order

$$T = T_b + (T_w - T_b)\theta/\alpha \,. \tag{7}$$

For the temperature derivative in the direction normal to the wall, at wall, $T_{n,w}$ one has, always at leading order

$$T_{n,w} = r^{-1}T_{\theta,w} = (T_w - T_b)/\alpha r \ . \tag{8}$$

For case (d) we find

$$T_{n,w} = r^{-1}T_{\theta,w} = -\alpha(rT_r)_{r,w} \ . \tag{9}$$

3.1 Equations and boundary conditions for thermo-fluid-dynamic problems

The thermo-fluid-dynamic field in the fluid for high Reynolds numbers, is governed by the boundary layer equations, which in dimensionless two-dimensional form may be written as

$$(\rho u)_x + (\rho v)_y = 0 \tag{10}$$

$$\rho(uu_x + vu_y) = (\mu u_y)_y + p_x + F \tag{11}$$

$$\rho(uT_x + vT_y) = (\lambda T_y)_y/Pr + (\gamma - 1)M^2\mu u_y^2 \tag{12}$$

where F denote volume forces, Pr and M are respectively the Prandtl and Mach numbers of the external flow, γ is the ratio of specific heats; u and v are the components of velocity along the axes x and y, p and ρ denote pressure and density and μ and λ denote the viscosity and thermal conductivity coefficients respectively.

When a fluid flows along a body the boundary conditions associated with Eqs. (10)-(12) are $u = v = 0$ at the body; $u(x, \infty) = u_e$, $T(x, \infty) = T_e$, where u_e and T_e are the external velocity and temperature respectively. The last condition, given by the coupling of thermal field of the fluid with that of the solid, requires the continuity of temperature and of heat flux at the solid-fluid interface. In dimensional form the heat-flux coupling condition may be written as

$$\lambda T_{n,w} = \lambda_s T_{s,n} \tag{13}$$

where "s" denotes properties of the solid and $T_{n,w}$ and $T_{s,n}$ are the normal derivatives at wall of the temperature of the fluid and the solid. The expressions of $T_{s,n}$ were given in the previous section in terms of the wall temperature and its derivatives for the four cases considered.

4.1 Stewartson-Dorodnitzin transformation

When we can assume that the coefficients of viscosity μ and of thermal conductivity λ depend linearly on absolute temperature the products $\mu\rho$ and $\lambda\rho$ do not depend on temperature for perfect gases. In this case it is convenient to use the

Stewartson-Dorodnitzin transformation [6] to obtain the fluid equations in a simpler quasi-incompressible form, by introducing new dependent (U, V) and independent (ξ, η) variables. In particular for constant pressure fields the transformation, in dimensionless variables, can be written as

$$\xi = x; \qquad \eta = \int_0^y \rho dy; \qquad U = u; \qquad V = \rho v + u\eta_x \,. \tag{14}$$

In this case Eqs. (10)-(12) can be reduced to the following form

$$U_\xi + V_\eta = 0 \tag{15}$$

$$UU_\xi + VU_\eta = U_{\eta\eta} + F/\rho \tag{16}$$

$$U\theta_\xi + V\theta_\eta = \theta_{\eta\eta}/Pr + (\gamma - 1)M^2 U_\eta^2/\Delta T \tag{17}$$

where $\theta = (T - T_\infty)/\Delta T$ and ΔT is a suitable reference temperature.

When p_x is different from zero the transformation (always in non-dimensional form) is

$$X = \int_0^x a_e^m dx \,; \qquad Y = \int_0^y a_e \rho \nu_s^{-1/2} dy \tag{18}$$

$$U = U/a_e \,; \qquad V = (UY_x + \rho v \nu_s^{-1/2})/a_e^m \tag{19}$$

where the reference quantities for the outer velocity of sound a_e and for density are the corresponding stagnation ones; the reference quantity for the stagnation kinetic viscosity ν_s is that used in the definition of Reynolds number.

In terms of these new variables Eqs. (15)-(17) become

$$U_X + V_Y = 0 \tag{20}$$

$$UU_X + VU_Y = U_{YY} + (1 + S)U_eU_{eX} \tag{21}$$

$$US_X + VS_Y = S_{YY}/Pr + (\gamma - 1)(M^2/H_{es})(Pr - 1)(uu_Y)_Y/Pr \tag{22}$$

where $S = H/H_e - 1$, $H = c_pT + u^2/2$ is the total enthalpy, H_e is the outer value of H, $H_{es} = H_e/c_pT_r$ where T_r is a temperature of reference.

References to Chapter 1

[1] P. Luchini, M. Lupo, A. Pozzi, "The coupling of conduction with forced convection in Graetz problems" *J. Heat Transfer*, 112, (1990), 572-578

[2] A. Pozzi, M. Lupo, "The coupling of conduction with laminar natural convection along a flat plate" *Int. J. Heat and Mass Transfer*, 31, (1988), 1807-1814

[3] A. Pozzi, M. Lupo, "The coupling of conduction with forced convection over a flat plate" *Int. J. Heat and Mass Transfer*, **32**, (1989), 1207-1214

[4] A. Pozzi, M. Lupo, "Variable-property effects in free convection" *Int. J. Heat and Fluid Flow*, **11**, (1989), 135-141

[5] A. Pozzi, M. Lupo, "Variable-property effects in supersonic wedge flow" *AIAA J.*, **29**, (1991), 686-687

[6] H. Schlichting, Boundary Layer Theory, Mc Graw-Hill, (1968).

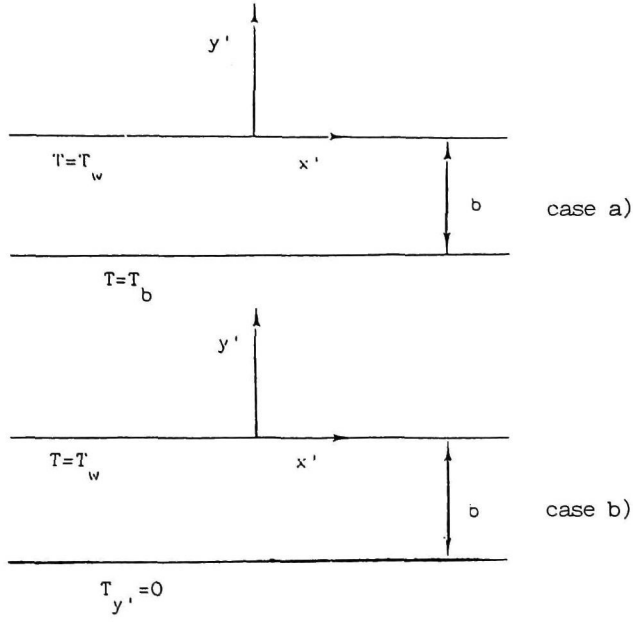

Fig.1 Flow cases:
a) strip with isothermal condition on the lower side;
b) strip with adiabatic condition on the lower side.

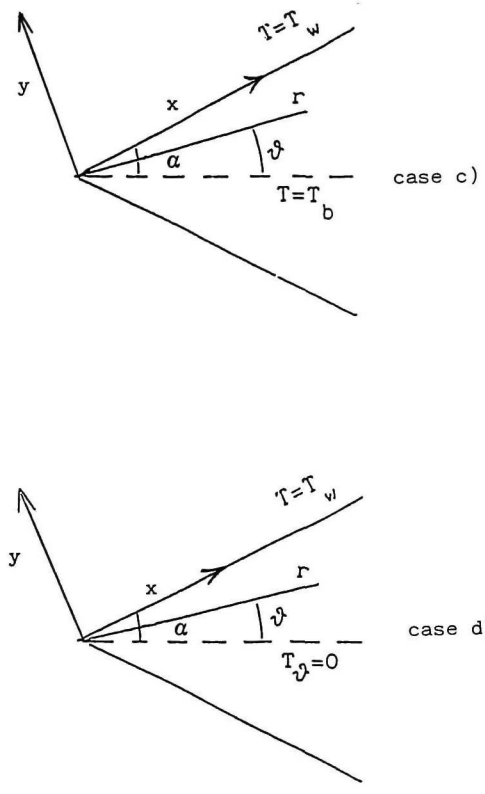

Fig.2 Flow cases:
c) wedge with isothermal condition on the axis;
d) wedge with adiabatic condition on the axis.

Chapter 2

FLOWS OVER BODIES IN FORCED CONVECTION: THE FLAT PLATE CASE

1.2 Introduction

We shall determine the thermo-fluid-dynamic field around bodies wetted by a fluid stream, using the equations and the boundary conditions recalled in chapter 1. We begin from the flat plate case.

The presence of a coupling parameter in the boundary condition at interface for the energy equation does not allow similarity solution in general. In these cases we found the solution of the problem for the plate, the wedge and the stagnation flow by putting the incompressible, or quasi incompressible stream function (such that $\psi_x = -V$, $\psi_y = U$) and $\theta = (T - T_\infty)/\Delta T$, where ΔT is a suitable reference temperature, in the following form

$$\psi = \xi^a \sum_{i=0}^{\infty} m_1^i f_i(z) ; \qquad \theta = \sum_{i=0}^{\infty} m_1^i h_i(z) \tag{1}$$

where $z = \eta/\xi^b$, $m_1 = \xi^c/p$, a, b, c are numbers depending on the geometry and

p is the coupling parameter. The functions $f_i(z)$ and $h_i(z)$, that constitute the coefficients of MacLaurin expansions (1), can be found by substituting Eqs.(1) into the momentum and energy equations and by writing these equations in the form

$$\sum_{i=0}^{\infty} m_1^i A_i(z) = 0 ; \qquad \sum_{i=0}^{\infty} m_1^i B_i(z) = 0 \tag{2}$$

$A_i = 0$ and $B_i = 0$ give all equations we need.

We consider positive values of c: therefore the series (1) converge in the range $(0, r)$ of m_1, where r is the radius of convergence.

The series (1) do not hold for any values of m_1 because r is finite. In order to calculate r and to obtain expansions valid for all values of m_1 we use the technique of Padé approximants.

2.2 Forced convection over a flat plate

The reference work for the problem of laminar forced convection along a flat plate (see Fig.1) with a boundary condition that couples the thermo- fluid-dynamic flow over the plate with the thermal field in the solid (conjugated problem) is due to Luikov et al. in 1971 [1].

The authors solved the problem by means of the generalized Fourier sine transformation and an expansion in series in terms of the Fourier variable. The results of such an analysis were presented in two figures for two examples. This solution cannot be easily used and Luikov in 1974 [2] has given an approximate solution of

the problem assuming a linear temperature distribution in the plate.

An extension of these results was obtained by Payvar in 1977 [3] for high Prandtl numbers. An improvement of the Payvar analysis was studied by Karvinen in 1978 (ref. [4] and [5]) who also presented an iterative technique for solving the conjugated heat transfer problem in a flat plate in the presence of internal heat sources.

Gosse in 1980 [6] presented an analytic solution which held at high values of the abscissa x.

We now describe the thermo-fluid-dynamic field generated by a forced flow on one side of a flat plate of small thickness b (see Fig.1), insulated on the edge, and with a temperature T_b maintained on the other side.

In Eqs.(10,1)-(12,1) of chap.1, in which $F = 0$, we take as reference lengths the wall thickness b and $bRe^{-1/2}$ along x and y directions, respectively, where $Re = u_\infty b/\nu_\infty$. The heat flux condition (13,1), taking into account Eq.(4,1) can be written as

$$\lambda Re^{1/2} t_y(\xi, 0) \;=\; \lambda_s(t_w - t_b)\,. \tag{3}$$

In this case pressure is constant.

Therefore by using Eqs.(14,1) one finds that in Stewartson-Dorodnitzin plane the velocity components are independent of temperature and it is

$$U \;=\; Z'\,; \qquad V \;=\; (zZ' - Z)/2\xi^{1/2} \tag{4}$$

where $z = \eta/\xi^{1/2}$ and $Z(z)$ is the function that solved Blasius equation $(2Z''' +$

$ZZ'' = 0$) with the boundary conditions $Z(0) = Z'(0) = 0$, $Z'(\infty) = 1$. In terms of the variables ξ and η energy equation (12,1) may be written as

$$Pr(U\theta_\xi + V\theta_\eta) \;=\; \theta_{\eta\eta} \;+\; aU_\eta^2 \tag{5}$$

where $\theta = (T - T_\infty)/(T_b - T_\infty)$, $a = Pr(\gamma - 1)M^2/\Delta t_\infty$ and $\Delta t_\infty = (T_b - T_\infty)/T_\infty$.

The coupling condition (17,1) assumes the form

$$p\theta_\eta(\xi, 0) \;=\; \theta_w - 1 \tag{6}$$

where $\theta_w = \theta(\xi, 0)$ and $p = \gamma_\infty Re^{1/2}/\lambda_s$. The other two thermal conditions are

$$\theta(0, \eta) \;=\; 0\,; \qquad \theta(\xi, \infty) \;=\; 0\,. \tag{7}$$

By substituting Eq.(1b) into Eqs.(5), (6) and (7) one finds, with $m_1 = \xi^{1/2}/p$ the following leading-order equation and boundary conditions

$$h_0'' + PrZh_0' + aZ''^2 \;=\; 0 \tag{8}$$

$$h_0' \;=\; 0\,; \qquad h_0(\infty) \;=\; 0 \tag{9}$$

and the following for the ith order

$$2h_i'' - Pr(Z'ih_i - Zh_i') = 0 \tag{10}$$

$$h_i'(0) = h_{i-1}(0) - \delta_{ij}, \qquad h_i(\infty) = 0 \tag{11}$$

where δ_{ij} is the Kronecker symbol ($\delta_{ij} = 0$ for $i \neq j$ and $\delta_{ij} = 1$ for $i = j$).

By using the Padé approximants technique we find the temperature distribution for any value of m_1.

The solution, holding for small values of $m_1 = \xi^{1/2}/p$, (initial solution) and described by equation (1b), has been found with 21 terms of expansion using a standard method. In table 1 the values of $h_i(0)$, giving the interface temperature θ_w for $Pr = 0.7$ (air), for $M \simeq 0$ and $M = 3$, and for $Pr = 7.02$ (water) have been listed.

By means of these coefficients it was possible to determine the Padé approximants: we assume the diagonal sequence and consider several values of N.

No significant difference was noted between the results obtained for $N = 10$ and those for $N > 10$.

In Fig.2 the interface temperature θ_w represented by the initial solution Eq.(1b) and the Padé approximants plotted against m_1 is drawn for $Pr = 0.7$, $M \simeq 0$, for $Pr = 7.02$ and $M \simeq 0$ and for $Pr = 0.7$ and $M = 3$ (*curves).

This figure shows that for $m_1 \leq m_1^+$ (where $m_1^+ \simeq 0.5$ for $Pr = 0.7$ and $m_1^+ \simeq 0.9$ for $Pr = 7.02$) the two representations give very similar results, while for $m_1 > m_1^+$, are completely different. If we denote by L_{in} the length of the strip

in which the initial solution holds, $L_{in} = (m_1^+ p)^2 b$.

3.2 Accuracy of the solution for the flat plate flow

In order to check the accuracy of the solution obtained in sect.2 we shall consider the asymptotic solution and we shall show that the initial solution, represented by Padé approximants, tends to the asymptotic solution when ξ tends to infinity.

To study the behaviour of the solution for $\xi \to \infty$ it is convenient to introduce the variable m as follows

$$m = p/\xi^{1/2} . \tag{12}$$

It is not possible to expand the function θ in a MacLaurin series with respect to m ($m \to 0$ corresponds to $\xi \to \infty$). In fact if we write

$$\theta = \sum_{i=0}^{\infty} m^i \theta_i(z) \tag{13}$$

the initial condition (7a) cannot be satisfied because m diverges for vanishing ξ. Moreover, the linearized problem presents eigenvalues: this circumstance, although it does not permit us to utilize an expansion, in terms of m, of the form of Eq.(13), does enable us to solve the problem of the initial condition.

If one wishes to obtain a representation of the solution that holds for high values of ξ it is necessary to modify Eq.(13) and to give the boundary condition

at $\overline{m}$ ($\overline{m} = p/\xi_0^{1/2}$, where ξ_0 is a suitable positive value ξ) according to boundary condition (7a).

We are not interested in this complicated expansion: we are only seeking the asymptotic behaviour of the solution in order to compare it with the results of the representation obtained by means of Padé approximants.

First we find the eigenvalues linked with the expansion (13). If one substitutes this expansion into Eqs.(5), (6) and (7b) he finds the following equation and boundary conditions at leading-order

$$2\theta_0'' + PrZ\theta_0' + 2aZ''^2 = 0 \tag{14}$$

$$\theta_0(0) = 1\,; \qquad \theta_0(\infty) = 0 \tag{15}$$

and the following at ith order

$$2\theta_i'' + Pr(Z'i\theta_i + Z\theta_i') = 0 \tag{16}$$

$$\theta_i(0) = \theta_{i-1}'(0)\,; \qquad \theta_i(\infty) = 0 \tag{17}$$

Eq.(16) presents eigensolutions when associated with the boundary conditions $\theta_i(0) = \theta_i(\infty) = 0$. The first one appears for $1 < \beta_1 = i < 2$ and depends on Pr. For instance, $\beta_1 = 1.60$ for $Pr = 0.7$ and $\beta_1 = 1.51$ for $Pr = 7.02$.

The first two terms in expansion (13) may then be determined by means of Eqs.(14)-(17) and the solution may be written in the form

$$\theta = \sum_{i=0}^{1} m_i \theta_i(z) + m^{\beta_1} R(m,z) \tag{18}$$

where the function $R(m,z)$ is not analytic with respect to m. Therefore neglecting terms of order m^{β_1} the asymptotic solution can be written as follows

$$\theta = \theta_0(z) + m\theta_1(z) \tag{19}$$

Table 2 compares the values of $\theta_z(m_1,0)$ obtained by means of the Padé summation and the asymptotic solution (19) for $Pr = 0.7$ and $M \simeq 0$.

In Fig.3, the interface temperature θ_w represented by the Padé summation and by the asymptotic solution with two terms is plotted against m_1 for $Pr = 0.7$ and $M \simeq 0$, for $Pr = 7.02$ and $M \simeq 0$ and for $Pr = 0.7$ and $M = 3$. Table 2 and Fig.3 show that for $m_1 \geq 8$ the values given by the Padé representation practically coincide with those given by the asymptotic solution. Therefore, while the MacLaurin initial expansion holds for $0 \leq m_1 \leq m_1^{\dagger}$ the Padé representation holds in the entire field.

References to Chapter 2

[1] A.V. Luikov, V.A. Aleksashenko and A.A. Aleksashenko, Analytical methods

of solution of conjugated problems in convective heat transfer, *Int. J. Heat Mass Transfer* **14**, (1971), 1047-1056

[2] A.V. Luikov, Conjugate convective heat transfer problems, *Int. J. Heat Mass Transfer* **17**, (1974), 257-265

[3] P. Payvar, Convective heat transfer to laminar flow over a plate of finite thickness, *Int. J. Heat Mass Transfer* **20**, (1977), 431-433

[4] R. Karvinen, Note on conjugated heat transfer in a flat plate, *Lett. Heat Mass Transfer* **5**, (1978), 197-202

[5] R. Karvinen, Some new results for conjugated heat transfer in a flat plate, *Int. J. Heat Mass Transfer* **21**, (1978), 1261-1264

[6] J. Gosse, Analyse simplifieé du couplage conduction-convection pour un ecoulement a couche limite laminaire sur une plaque plane, *Rev. Gen. Therm.* **228**, (1980), 967-971

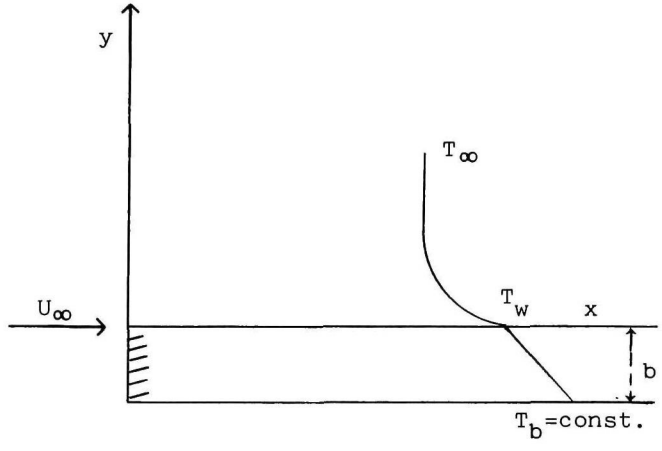

Fig.1 Thermal model of a flat plate.

Table 1

Coefficients $h_i(0)$ of expansion (1b) (initial solution)

i	$Pr = 0.7$, $M = 0$	$Pr = 0.7$, $M = 3$	$Pr = 7.02$, $M = 0$
0	0	5.8853303	0
1	2.4636984	−12.035983	1.1280761
2	−5.1291153	25.057417	−1.0799054
3	9.5413968	−46.612845	9.2572774E−1
4	−16.313412	79.696306	−7.3030601E−1
5	26.073775	−127.3783	5.3904464E−1
6	−39.399996	192.48139	−3.7639352E−1
7	56.744427	−277.21406	2.5060616E−1
8	−78.362526	382.82461	−1.6004882E−1
9	104.25337	−509.30837	9.8498975E−2
10	−134.12117	655.22015	−5.8632192E−2
11	167.36393	−817.61883	3.3859516E−2
12	−203.09191	992.15765	−1.9017861E−2
13	240.17474	−1173.3142	1.0411339E−2
14	−277.31236	1354.7373	−5.5655834E−3
15	313.12236	−1529.6733	2.9098012E−3
16	−346.23453	1691.4286	−1.4899360E−3
17	375.38318	−1833.8199	7.4809335E−4
18	−399.48843	1951.5720	−3.6872367E−4
19	417.71981	−2040.6281	1.7857745E−4
20	−429.53754	2098.3516	−8.5057695E−5

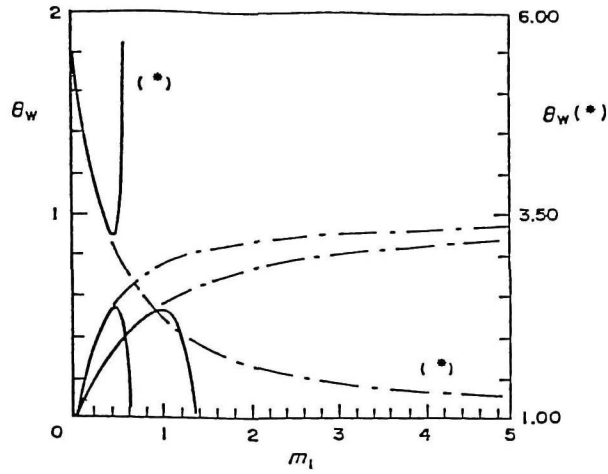

Fig.2 The interface temperature represented by the initial solution (———) and by Padé summation (— · —) for Pr=7.02 and M=0 (lower curves), Pr=0.7 and M=0 (middle curves), Pr=0.7 and M=3 (upper curves).

Table 2. Comparison between Padé summation and the asymptotic solution with two terms

m_1	Padé summation	Asymptotic solution two terms (eq.(19))
0.5	−0.2088	−0.2927
1.0	−0.2530	−0.2927
1.5	−0.2692	−0.2927
2.0	−0.2769	−0.2927
3.0	−0.2839	−0.2927
4.0	−0.2870	−0.2927
6.0	−0.2897	−0.2927
8.0	−0.2909	−0.2927
10.0	−0.2915	−0.2927

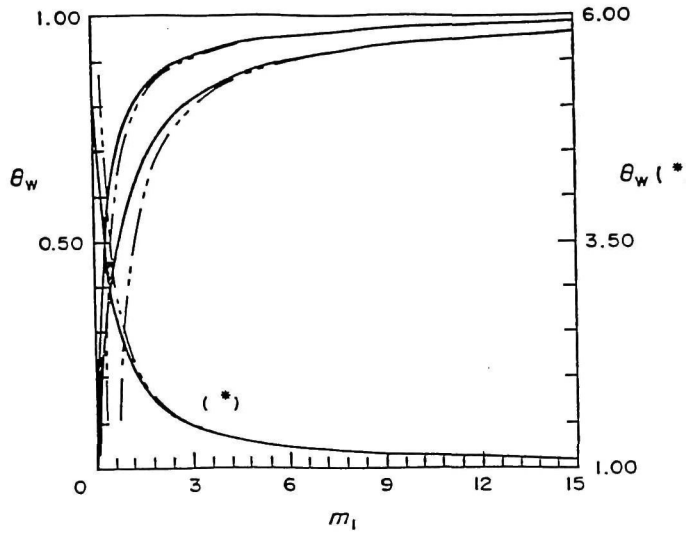

Fig.3 The interface temperature in the asymptotic (— – – —) and Padé representation (———) for Pr=0.7 and M=0 (upper curves), Pr=7.02 and M=0 (middle curves), Pr=0.7 and M=3 (lower curves).

The figures are reprinted from Int. J. of Heat and Mass Transfer Vol.32, A. Pozzi and M. Lupo, "The coupling of conduction with forced convection over a flat plate", 1207-1214, Copyright 1989 with permission from Pergamon Press Ltd., Headington Hill Hall, Oxford OX3 OBW, UK.

Chapter 3

FORCED CONVECTION IN STAGNATION FLOW

1.3 Incompressible flow against a slab: constant temperature on the lower side of the slab

In the analysis of the incompressible stagnation flows bounded by the geometries shown in cases a) and b) of Fig.1 of chap.1 the stream function ψ is given by $\psi = xf(y)$ and f is the solution of the differential equation

$$f''' + ff'' + 1 - f'^2 = 0 \tag{1}$$

with the boundary conditions $f(0) = f'(0) = 0$, $f'(\infty) = 1$. The energy equation in terms of f can be written as follows

$$x\theta_x f' - f\theta_y = \theta_{yy}/Pr + (\gamma - 1)M_0^2 x^2 f''^2 \tag{2}$$

where $\theta = (T - T_e)/T_0$. The reference quantities are L, $LRe^{-1/2}$, V_0, $V_0 Re^{-1/2}$, ρ_0, μ_0, and λ_0 for x, y, u, v, ρ, μ and λ respectively. V_0, μ_0, and λ_0 are the

characteristic velocity, density, viscosity and thermal conductivity of the flow, M_0 is the Mach number referred to temperature T_0, L is a characteristic length in the direction of the x axis, T_e is the external temperature and T_0 is equal to $T_b - T_e$. Boundary conditions associated with Eq.(2) are

$$\theta(x,\infty) = 0\,; \qquad p\theta_{y,w} = \theta_w - 1 \tag{3}$$

where $p = Re^{1/2} b\lambda_0 / L\lambda_s$. The solution of Eqs.(2) and (3) is determined as the sum of $\theta_h(y)$, a solution of the homogeneous part of Eq.(2), and $(\gamma-1)M_0^2 x^2 \theta_p(y)$, a particular solution of the same equation. The equations and the boundary conditions for θ_h and θ_p are

$$\theta_h''/Pr + f\theta_h' = 0 \tag{4}$$

$$\theta_h(\infty) = 0\,; \qquad p\theta_h'(0) = \theta_h(0) - 1 \tag{5}$$

$$\theta_p''/Pr + f''^2 - 2f'\theta_p + f\theta_p = 0 \tag{6}$$

$$\theta_p(\infty) = 0\,; \qquad p\theta_p'(0) = \theta_p(0). \tag{7}$$

The solution of Eq.(4) with boundary conditions (5) is given by

$$\theta_h = \int_\infty^y exp\left[-Pr\int_0^y f\,dy\right]dy/\left[\int_\infty^0 exp\left(-Pr\int_0^y f\,dy\right)dy - p\right]. \quad (8)$$

The curves of $\theta_h(0)$ and $\theta_p(0)$ versus p are plotted in Fig.1.

The value of $\theta_p(0)$ as $p \to \infty$ (dotted line) is also plotted in the figure, obtained with the adiabatic boundary condition at the interface.

2.3 Incompressible flow against a slab: adiabatic condition on the lower side of the slab

When $T_y = 0$ on the lower side of the slab the stream function ψ is the same as in previous section. The boundary conditions associated with Eq.(2) are

$$\theta(x,\infty) = 0\,; \qquad p\theta_{y,w} = -\theta_{xx,w} \quad (9)$$

where

$$p = Re^{1/2}L\lambda_0/b\lambda_s. \quad (10)$$

In this case the solution can be found by means of a procedure that respects the elliptic character of the boundary condition (9b). In fact this condition couples the solution valid for small values of x with that valid for high values of x, so that

the temperature at the stagnation point $\theta(0,0)$ becomes an unknown. In general a problem of this kind, given its linearity, can be solved writing θ in the following form

$$\theta \;=\; C\theta_h(x,y) \;+\; (\gamma-1)M_0^2x^2\theta_p(x,y) \tag{11}$$

where C is $\theta(0,0)$, whose value should be calculated by requiring that the correct asymptotic behavior be obtained for $x \to \infty$.

The functions $\theta_h(x,y)$ and $\theta_p(x,y)$ can be expressed by means of the following MacLaurin series in the variable $m_1 = px^2$

$$\theta_h \;=\; \sum_{i=0}^{\infty} m_1^i\theta_{h,i}(y)\,; \qquad \theta_p \;=\; \sum_{i=0}^{\infty} m_1^i\theta_{p,i}(y)\,. \tag{12}$$

By substituting Eq.(11) into Eq.(2) and into its associated homogeneous, taking into account Eqs.(12), one has for the homogeneous part

$$\theta''_{h,0}/Pr \;+\; f\theta'_{h,0} \;=\; 0 \tag{13}$$

$$\theta_{h,0}(\infty) \;=\; 0\,; \qquad \theta_{h,0}(0) \;=\; 1 \tag{14}$$

for the leading term, and

$$\theta''_{h,i}/Pr \;-\; 2i\theta_{h,i}f' \;+\; f\theta'_{h,i} \;=\; 0 \tag{15}$$

$$\theta_{h,i}(\infty) = 0\,; \qquad \theta_{h,i}(0) = \theta'_{h,i-1}(0)/(4i^2 - 2i) \tag{16}$$

for $i > 0$.

For the particular integral

$$\theta''_{p,0}/Pr + f''^2 - 2\theta_{p,0}f' + f\theta'_{p,0} = 0 \tag{17}$$

$$\theta_{p,0}(\infty) = 0\,; \qquad \theta_{p,0}(0) = 0 \tag{18}$$

for the leading term and

$$\theta''_{p,i}/Pr - 2(1+i)\theta_{p,i}f' + f\theta'_{p,i} = 0 \tag{19}$$

$$\theta_{p,i}(\infty) = 0\,; \qquad \theta_{p,i} = -\theta'_{p,i-1}(0)/(2 + 6i + 4i^2) \tag{20}$$

for $i > 0$.

To calcultate the constant C we need to determine the asymptotic solution as $x \to \infty$. This solution may be obtained by expanding θ_p in an asymptotic series in the variable $m_2 = 1/m_1$ and considering the leading term $h_0(y)$ of this expansion. The equation and the boundary conditions determining $h_0(y)$ are

$$h''_0/Pr + f''^2 - 2h_0f' + fh'_0 = 0 \tag{21}$$

$$h_0(\infty) \;=\; 0\,; \qquad h_0'(0) \;=\; 0. \tag{22}$$

Now the constant C can be determined by matching the solution (11) with the asymptotic solution $(\gamma-1)M_0^2x^2h_0(y)$ calculated, for instance, at $y=0$. One has

$$\frac{C}{(\gamma-1)M_0^2} \;=\; \lim_{x\to\infty}\; x^2\,[h_0(0)-\sum_{i=0}^{\infty} m_1^i\theta_{p,i}(0)]/\sum_{i=0}^{\infty} m_1^i\theta_{h,i}(0)\,. \tag{23}$$

So far we have described the general procedure. However, in the particular case of Eqs.(2) and (9), characterized by the appearance of x in integral powers, an exact solution having a polynomial dependence on x turns out to exit. On expressing an expression of the form

$$\theta \;=\; \theta_0(y) \;+\; x^2\theta_2(y) \tag{24}$$

into Eqs.(2) and (9), it may be verified that these equations are satisfied provided that θ_0 and θ_2 obey the equations and boundary conditions

$$\theta_{2yy}/Pr \;+\; (\gamma-1)M_0^2f''^2 \;=\; 2\theta_2f' \;-\; f\theta_{2yy}\;; \qquad \theta_{2y,w} \;=\; 0 \tag{25}$$

$$\theta_{0yy}/Pr \;=\; -f\theta_{0y}\;; \qquad p\theta_{0y,w} \;=\; -2\theta_{2,w}. \tag{26}$$

The same result would, of course, be recovered if Eq.(23) were evaluated numerically.

In Fig.2 $p\theta_w/(\gamma-1)M_0^2$ is plotted versus m_1 together with the function $m_1 h_0(0)$ (dotted curve) up to $m_1 = 50$ whereas in Fig.3 $h_0(0)$ (dotted curve) and $p\theta_w/m_1(\gamma-1)M_0^2$ are plotted versus m_1.

3.3 Compressible flow against a flat plate: non viscous flow

We study the thermo-fluid-dynamic field generated by a fast stream impinging on an isothermal plane. The Mach number of the stream is less than one but not so small that compressibility can be neglected.

The analysis requires first the non viscous solution of the basic equation and then the viscous solution in the boundary layer approximation. The results of this research are reported in ref. [1].

The compressible stream function ψ for the inviscid subsonic flow can be determined in the hodograph plane, i.e. by assuming the cartesian component u and v of the velocity as independent variables. In this plane the equation for ψ becomes linear and can be solved by separation of variables in terms of simple solutions [2].

By introducing the compressible stream function ψ (such that $\psi_y = \rho u/\rho_s$, $\psi_x = -\rho v/\rho_s$, where u and v are the velocity components along the cartesian axes x and y and the subscript "s" indicates stagnation conditions) the two-dimensional motion equations can be written as

$$\psi_{xx}(1-u^2/a^2) - 2\psi_{xy}uv/a^2 + \psi_{yy}(1-v^2/a^2) = 0 \qquad (27)$$

$$a^2 + (\gamma - 1)V^2/2 = a_s^2 \qquad (Bernoulli\ equation) \tag{28}$$

where a is the sound velocity, $V^2 = u^2 + v^2$ and γ is the ratio between the specific heat coefficients.

If one assumes V and θ, angle between the velocity vector and x-axis, as independent variables, Eq.(27), becomes (see Appendix)

$$V^2[1 - (\gamma - 1)V^2/(2a_s^2)]\psi_{VV} + [1 - (\gamma + 1)V^2/(2a_s^2)]\psi_{\theta\theta}$$

$$+ V[1 - (\gamma - 3)V^2/(2a_s^2)]\psi_V = 0\,. \tag{29}$$

It is convenient to introduce the variable $\tau = (\gamma-1)V^2/(2a_s^2)$, where $a_s[2/(\gamma-1)]^{1/2}$ is the limiting velocity V_L (the critical velocity V_C is related to V_L by the equation $V_C = V_L[(\gamma - 1)/(\gamma + 1)]^{1/2}$; therefore $V = a$ when $\tau = (\gamma - 1)/(\gamma + 1)$. In this way Eq.(28) in a non-dimensional (a is nondimensionalized with respect to a_s) form becomes

$$a^2 + \tau = 1 \tag{30}$$

and the density and the pressure can be written as

$$\rho/\rho_{s'} = (1 - \tau)^{1/(\gamma-1)}\,; \qquad p/p_s = (1 - \tau)^{\gamma/(\gamma-1)}. \tag{31}$$

Solutions of Eq.(29) can be written in the form

$$\psi_n = -sin(n\theta + d_n)V^n f_n(\tau) \tag{32}$$

where d_n is an arbitrary constant and f_n is the Gaussian hypergeometric function $F(a_n, b_n, n+1, \tau)$ [3] with

$$a_n,\ b_n = \{(\gamma-1)n - 1 \pm [(\gamma^2-1)n^2 + 1]\}/[2(\gamma-1)]$$

for $\gamma = 1.4$ and $n = 2$ f_n becomes a polynomial: in this case, the stream function can be written in a non-dimensional form as

$$\psi = -sin2\theta\ V^2 f_2(\tau)/2 \tag{33}$$

where $f_2 = 1 - 5\tau/2 + 35\tau^2/16 - 21\tau^3/32$ and V is nondimensionalized with respect to a suitable reference velocity V_r: therefore it is $\tau = k^2V^2$, where $k = V_r/V_L$.

This function vanishes when $\theta = 0$ and $\theta = \pi/2$ and therefore it represents the stream function of a flow symmetrical with respect to the x-axis impinging on a plane: the inflow and outflow can be obtained from Eq.(33). The last streamline that we consider can be assumed to represent a wall.

The potential function can be determined from the irrotationality equation $\varphi_\theta = V\psi_V \rho_s/\rho$. One has

$$\varphi = V^2(1 - 5\tau + 105\tau^2/16 - 21\tau^3/8)cos2\theta/2(1-\tau)^{5/2}\ .$$

The expression giving $x(V,\theta)$ and $y(V,\theta)$ can be obtained from the following equations

$$\begin{aligned} x_V &= (\varphi_V cos\theta - sin\theta\varphi_V\rho_s/\rho)/V \\ y_V &= (\varphi_V sin\theta + cos\theta\psi_V\rho_s/\rho)/V \end{aligned} \tag{34}$$

or

$$\begin{aligned} x_\theta &= (\varphi_\theta cos\theta - sin\theta\psi_\theta\rho_s/\rho)/V \\ y_\theta &= (\psi_\theta sin\theta + cos\theta\psi_\theta\rho_s/\rho)/V \ . \end{aligned} \tag{35}$$

From Eq.(35) in nondimensional form one has

$$x = Vcos\theta\left[3 - \frac{15}{2}\tau + \frac{105}{16}\tau^2 - \frac{63}{32}\tau^3 - cos^2\theta\left(5\tau - \frac{35}{4}\tau^2 + \frac{63}{16}\tau^3\right)\right]/3(1-\tau)^{5/2} \tag{36a}$$

$$y = -Vsin\theta\left[3 - \frac{15}{2}\tau + \frac{105}{16}\tau^2 - \frac{63}{32}\tau^3 - sin^2\theta\left(5\tau - \frac{35}{4}\tau^2 + \frac{63}{16}\tau^3\right)\right]/3(1-\tau)^{5/2} \tag{36b}$$

and in particular from Eq.(36a) it is

$$x_w = V(3 - 25\tau/2 + 245\tau^2/16 - 189\tau^3/32)/3(1-\tau)^{5/2} \tag{37}$$

where the subscript "w" indicates the wall.

The streamlines of such a flow are drawn in Fig.4.

Any two of these streamlines can be considered as walls of a duct discharging against a plane plate. The non-dimensional modulus of velocity, V, and its inclination θ with respect to the x-axis at $y = -1$ are plotted in Fig.5: in this way the initial conditions of this flow are known. V and θ at $x = 0.2$ and $x = 0.5$ are plotted in Fig.6. Figure 7 gives Kx versus τ.

4.3 Compressible flow against a flat plate: viscous flow

The boundary layer equation in a non-dimensional form can be written as

$$(\rho u)_x + (\rho v)_v = 0 \tag{38}$$

$$\rho(uu_x + vu_y) = \rho_e u_e u_{ex} + (\mu u_y)_y \tag{39}$$

$$\rho(uS_x + vS_y) = (\lambda S_y)_y/Pr + (Pr-1)[\mu V_r^2 uu_y]_y/PrH_e \tag{40}$$

where the subscript "e" indicates external inviscid condition calculated on the wall; μ and λ are the viscosity and thermal conductivity coefficients, $S = h_{tot}/h_{tot,e} - 1$ and h_{tot} is the total enthalpy $h + V^2/2$. The boundary conditions associated with Eqs.(38)-(40) are $u(x,0) = v(x,0) = 0$; $u(x,\infty) = u_e$; $S(x,0) = S_w$, $S(x,\infty) = 0$.

Equations (38)-(40) by means of the Dorodnitzin-Stewartson transformation (a_e and ρ are nondimensionalized with respect to the respective stagnation quantities) become

$$U_X + V_Y = 0 \tag{41}$$

$$UU_X + VU_Y = U_{YY} + (1+S)U_eU_{eX} \tag{42}$$

$$US_X + VS_Y = S_{YY}/Pr + (Pr-1)a^2V_r^2UU_Y/(PrH_e)\,. \tag{43}$$

By introducing the stream function ψ (such that $\psi_Y = U$ and $\psi_X = -V$) and the variable $\tau(X)$ given by Eq.(37), Eqs.(42) and (43) can be written as

$$\psi_Y\psi_{Y\tau} - \psi_\tau\psi_{YY} = \psi_{YYY}X_\tau + (1+S)U_eU_{e\tau} \tag{44}$$

$$\psi_Y S_\tau - \psi_\tau S_Y = S_{YY}X_\tau/Pr + (Pr-1)(1-\tau)X_\tau\psi_y\psi_{yy}V_r^2/(PrH_e)\,. \tag{45}$$

These equations can be solved by putting

$$k\psi = [\tau/(1-\tau)]^{1/2}\sum_{i=0}^{\infty}\tau^i f_i(Y)\,; \qquad S = \sum_{i=0}^{\infty}\tau^i S_i(Y) \tag{46}$$

with $f_i(0) = f_i'(0) = 0$; $f_0'(\infty) = 1$; $f_i'(\infty) = 0$ for $i > 0$; $S_0(0) = S_w$; $S_i(0) = 0$ for $i > 0$ and $S_i(\infty) = 0$.

By substituting Eqs.(46) into Eqs.(44) and (45) one has the equations for the unknowns f_i and S_i. In particular the leading order of the expansion gives

$$f_0''' + f_0'' f_0 - f_0'^2 = -1 - S_0$$

$$S_0''/Pr + f_0 S_0' = 0 \tag{47}$$

while f_n and S_n, with $n > 0$, are given by

$$f_n''' + f_0 f_n'' - 2(n+1) f_0' f_n' + (2n+1) f_0'' f_n = -S_n + F_n$$

$$S_n''/Pr + f_0 S_n' - 2n S_n f_0' = G_n \tag{48}$$

where

$$g(\tau) = (1 - 17\tau/2 + 275\tau^2/16 - 441\tau^3/32 + 63\tau^4/16)/2 = \sum g_i \tau^i$$

$$F_n = -2f_0''(g_n - 2g_{n-1} + g_{n-2}) + 2(n-1) f_0'' f_{n-1} - 2(n-1) f_0' f_{n-1}'$$

$$-2\sum_{i=1}^{n-1}[f'''_{n-1}(g_i - 2g_{i-1} + g_{i-2}) + f''_{n-1}[(i+1/2)f_i$$

$$-(i-1)f_{i-1}] - f'_{n-1}((i+1/2)f'_i - (i-1)f'_{i-1})]$$

$$G_n = -\sum_{i=1}^{n}[S''_{n-i}(g_i - 2g_{i-1} + g_{i-2}) + (n-i)S_{n-i}(f'_i - f'_{i-1})$$

$$-S'_{n-i}[(f_i(i+1/2) - (i-1)f_{i-1})]] - 2(Pr-1)h_n/Pr$$

where

$$h_n = \sum_{i=0}^{n}\left(\sum_{j=0}^{n-i} f'_j f''_{n-i-j}\right)(g_{i-1} - 2g_{i-2} + g_{i-3})\,.$$

The representation of ψ and S given by Eqs.(46) is not valid for any value of τ. In order to evaluate the range of validity of such expansion and to obtain a representation valid for higher values of τ we use the Padé representation. The numerical solution of Eqs.(47) and (48), found using the Runge-Kutta method, has been obtained by considering 13 terms of Eqs.(46). The radius of convergence r of MacLaurin expansion has been determined by the Padé approximants technique: we found $r = 0.06$. The Padé approximants also allow to obtain a representation of the functions ψ and S valid for values of $\tau > r$.

The second derivative of $\Sigma f_i \tau^i$ and the first of $\Sigma S_i \tau^i$ at $y = 0$ are drawn in Figs.8, 9, 10 and 11; dashed curves represent expansion (46) while solid curves

represent Padé approximants. The curves of $u_{y,0}$ and S are drawn for $Pr = 1$ and $Pr = 0.74$, for both $S_w = -0.8$ and $S_w = -0.4$. We can see that the two representations practically coincide when $\tau < r$; when $\tau > r$ the MacLaurin series diverges while the Padé representation is regular. Non-dimensional shear stress $u_{Y,0}$ and heat flux $S_{Y,0}$ are therefore exactly given by the Padé approximants in the entire field of interest. The same quantities are drawn (for $M = 0.5$ and $M = 0.75$) versus x in Figs.12 and 13.

References to Chapter 3

[1] A. Pozzi, A. Bianchini, A.R. Teodori: "Some new test cases in compressible thermo-fluid-dynamics" *Int. J. Heat and Fluid Flow* (1993), 14, 201-205.

[2] R. Von Mises, H. Geiringer, G.S.S. Ludford: "Mathematical Theory of Compressible Fluid Flow", Academic Press, (1958).

[3] M. Abramowitz, I.A. Segun: "Handbook of Mathematical Functions" Dover Pub., (1968).

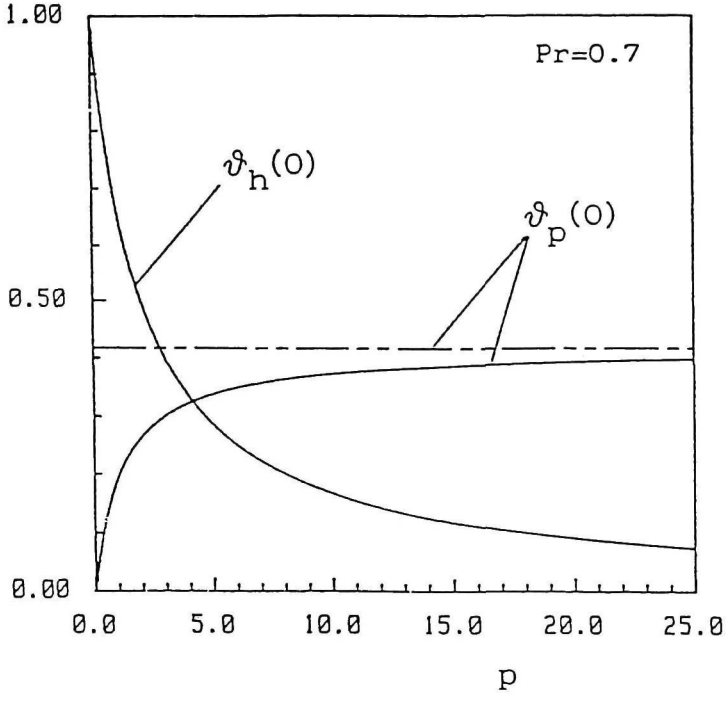

Fig.1 Stagnation flow with isothermal condition on the lower side of the slab; constants necessary for calculation of the wall temperature, as $\vartheta_w=\vartheta_h(0)+(\gamma-1)M^2x^2\vartheta_p(0)$, versus coupling parameter p.

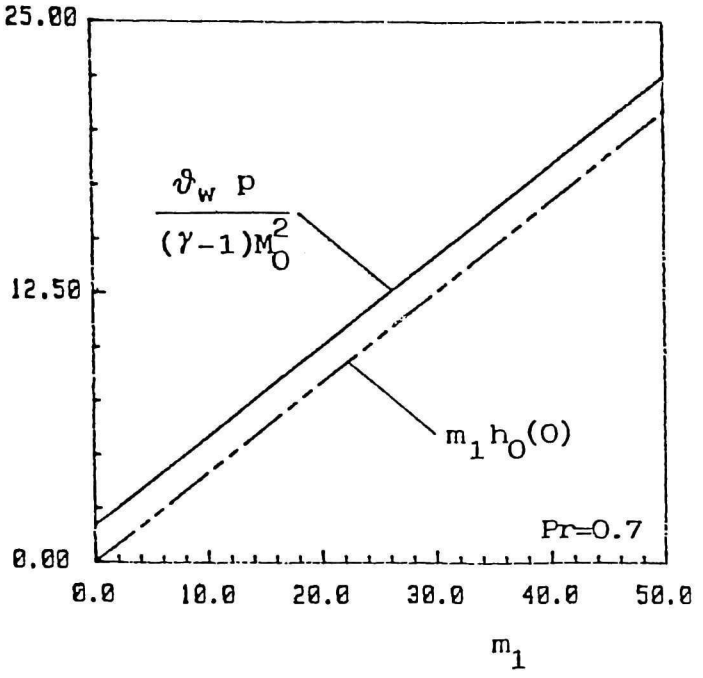

Fig.2 Stagnation flow with adiabatic condition on the lower side of the slab. Universal plot of wall temperature, rescaled as indicated, versus generalized axial coordinate m_1 in the presence (———) and absence (----) of wall conduction.

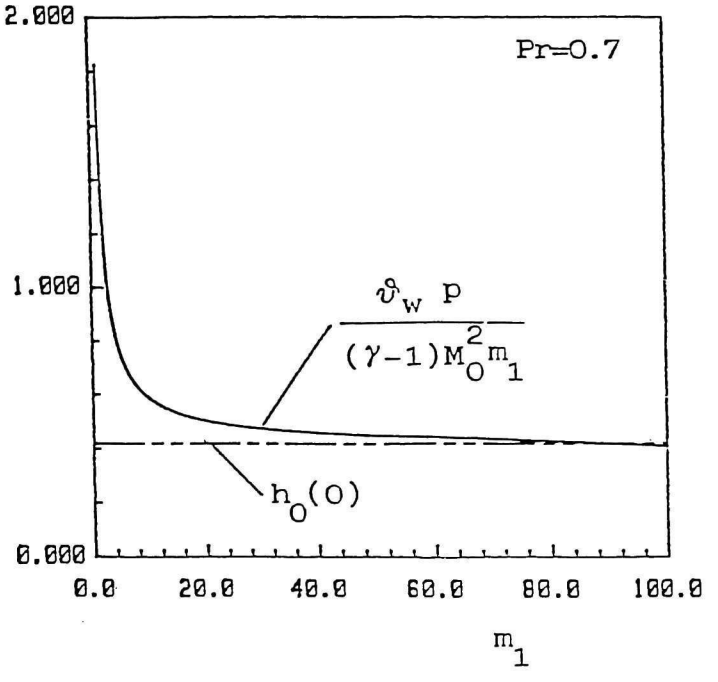

Fig.3 Stagnation flow with adiabatic condition on the lower side of the slab: same results as in Fig.2 plotted in a different scaling in which the dimensionless temperature is finite at infinity.

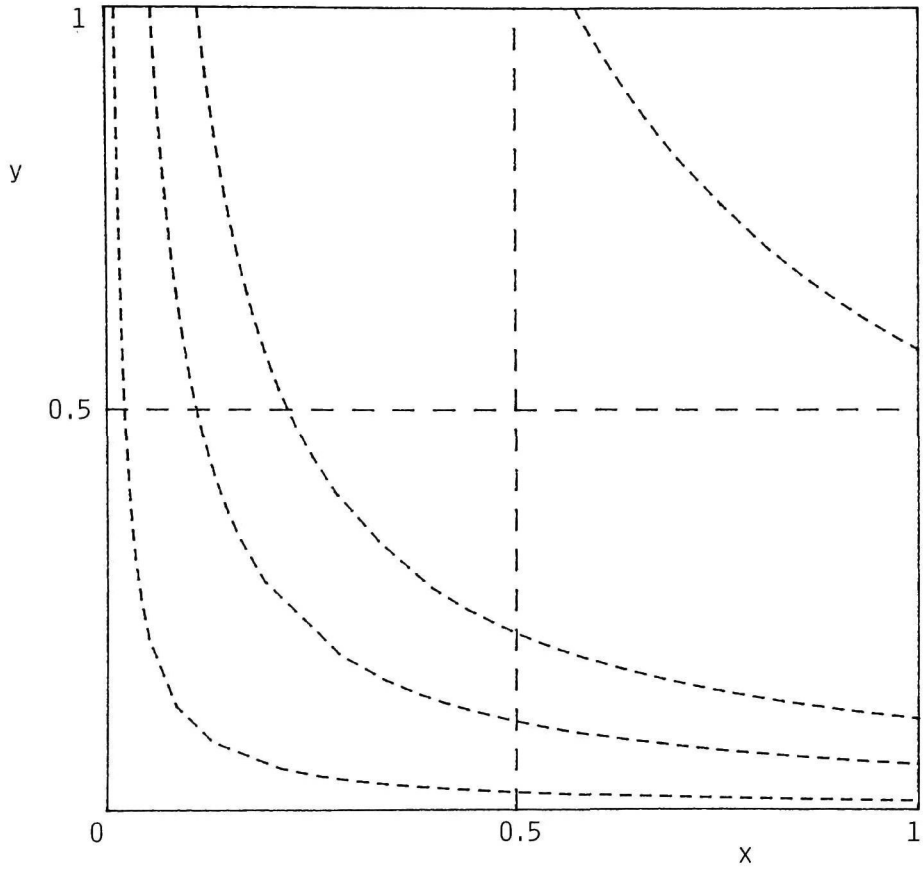

Fig.4 Streamlines; $\psi = 0.01,\ 0.05,\ 0.1,\ 0.5$.

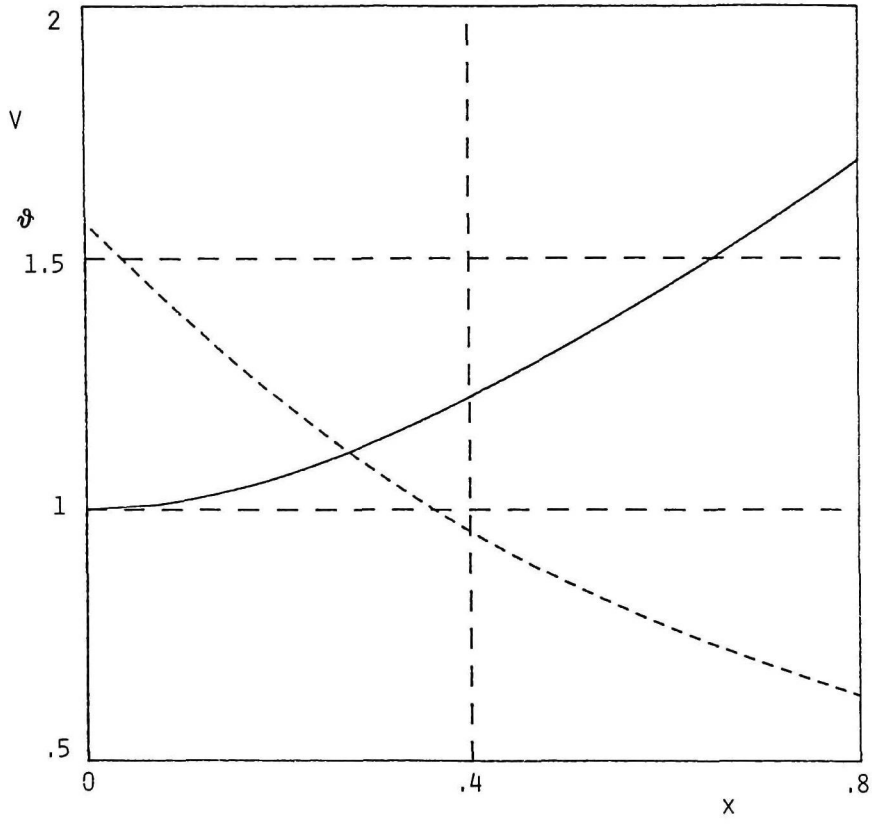

Fig.5 V(x) ——— and ϑ(x) ----- at y=-1.

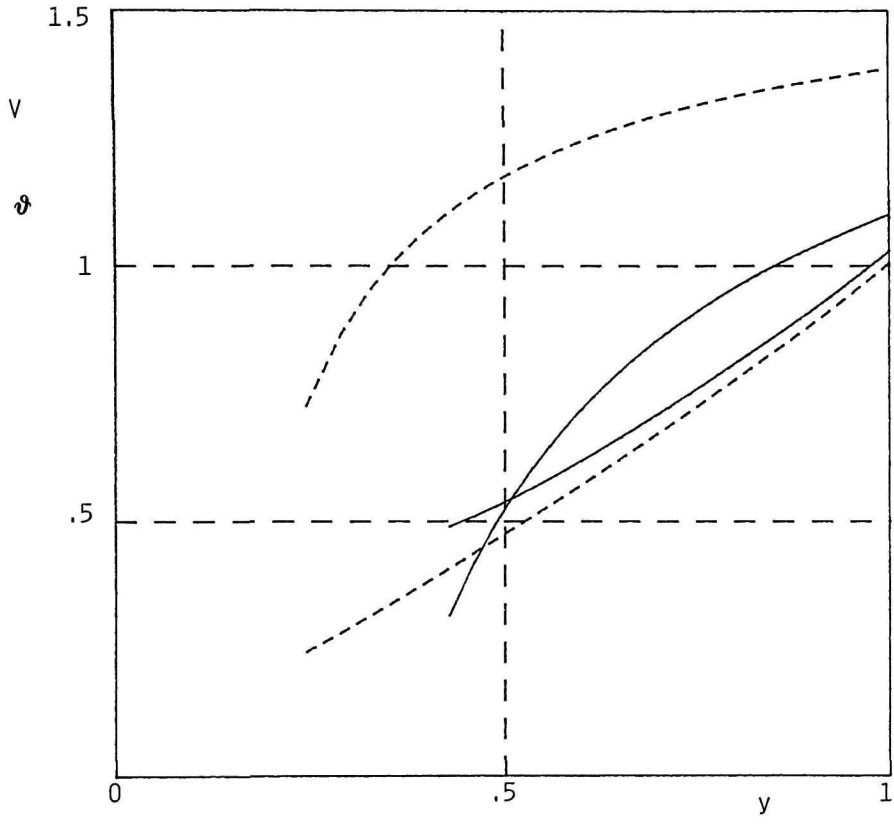

Fig.6 $V(y)$ and $\theta(y)$ at $x = 0.2$ – – – – – and $x = 0.5$ _____.

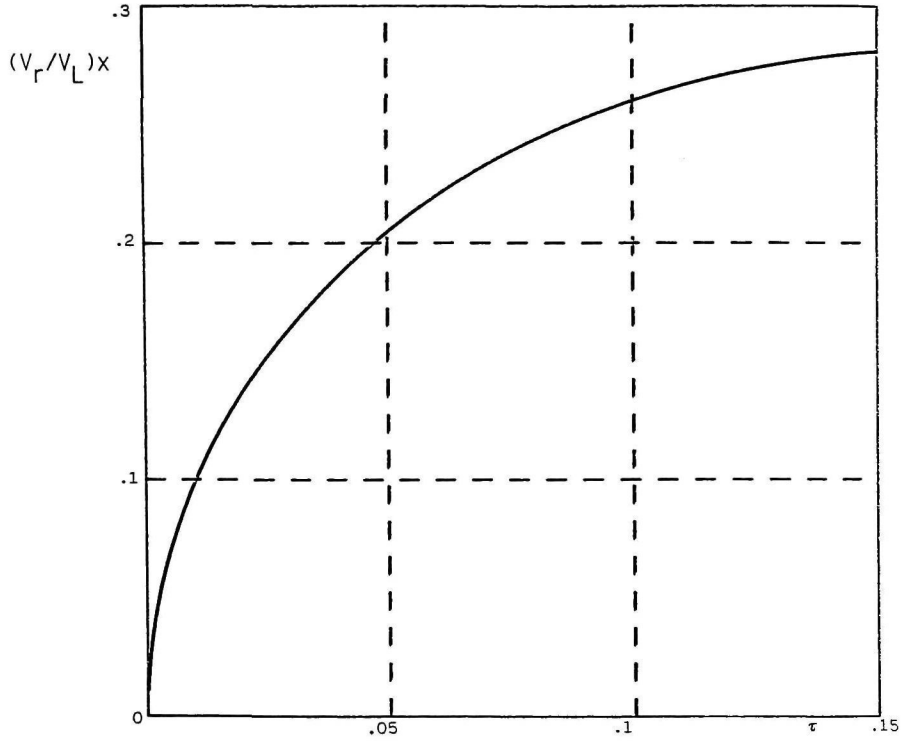

Fig.7 Abscissa versus velocity.

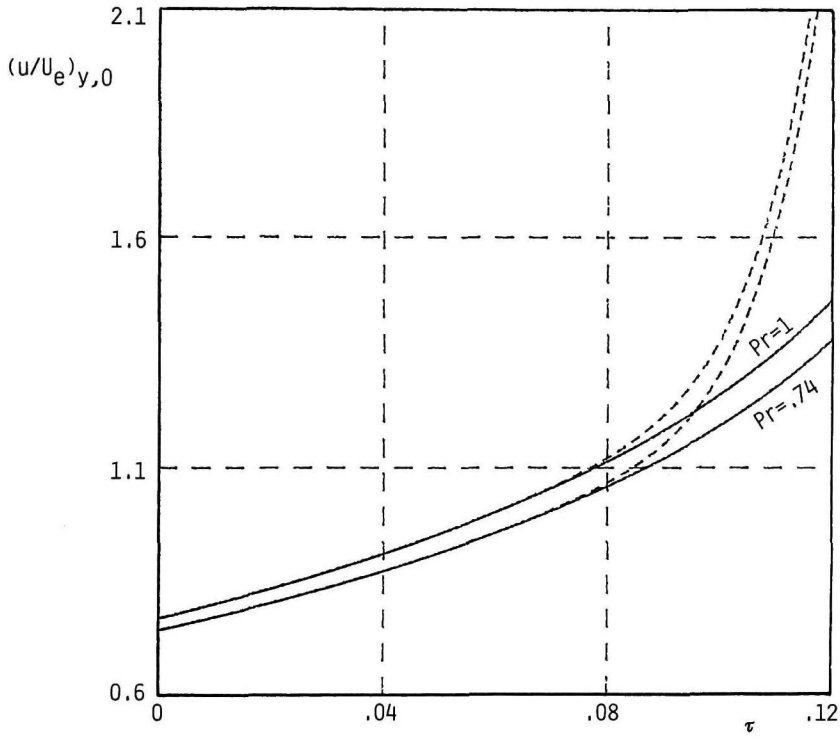

Fig.8 Comparison between MacLaurin expansion – – – – – $\Sigma f_i''\tau^i$ and their Padé approximants _____ of $(u/U_e)_{Y,0}$ for $Pr = 1$, $Pr = 0.74$ and $S_w = -0.8$.

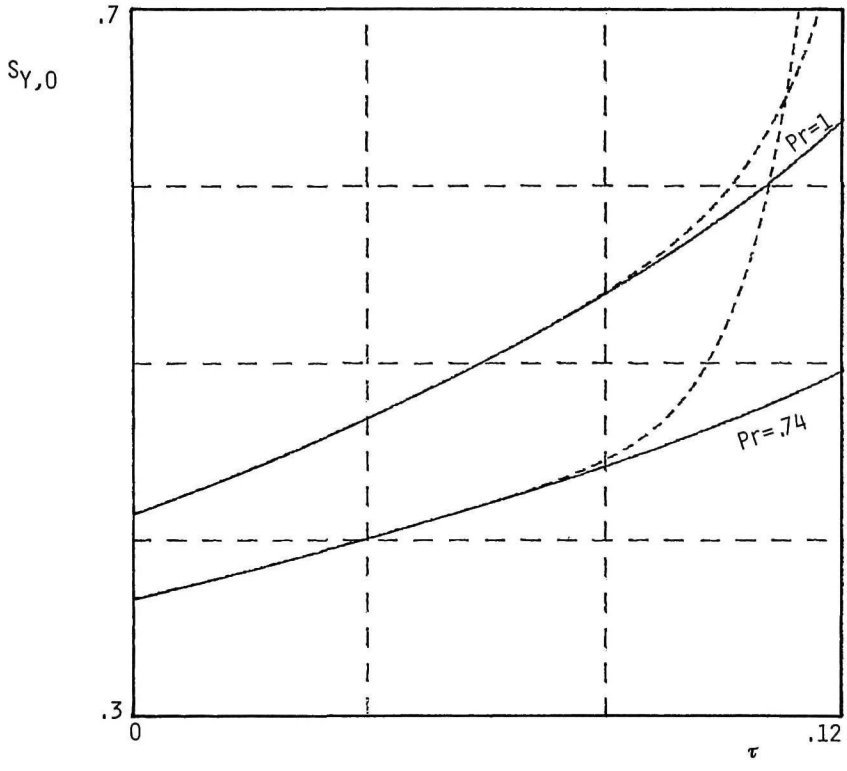

Fig.9 Comparison between MacLaurin expansion – – – – – $\Sigma S_i' \tau^i$ and their Padé approximants _____ of $S_{Y,0}$ for $Pr = 1$, $Pr = 0.74$ and $S_w = -0.8$.

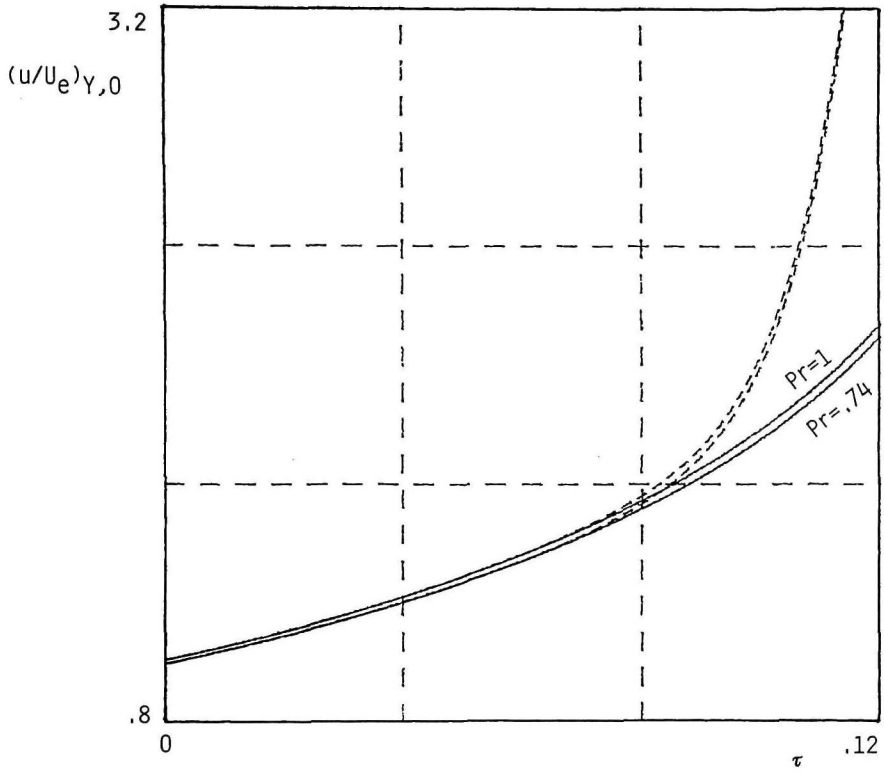

Fig.10 Comparison between MacLaurin expansion – – – – – $\Sigma f_i'' \tau^i$ and their Padé approximants _____ of$(u/U_e)_{Y,0}$ for $Pr = 1$, $Pr = 0.74$ and $S_w = -0.4$.

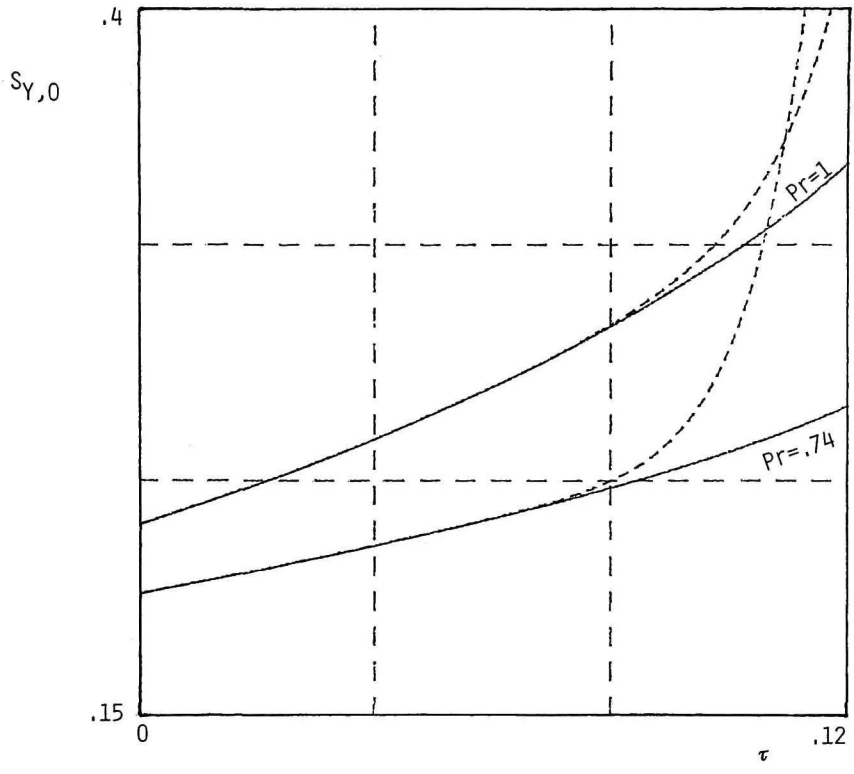

Fig.11 Comparison between MacLaurin expansion – – – – – $\Sigma S_i' \tau^i$ and their Padé approximants _____ of $S_{Y,0}$ for $Pr = 1$, $Pr = 0.74$ and $S_w = -0.4$.

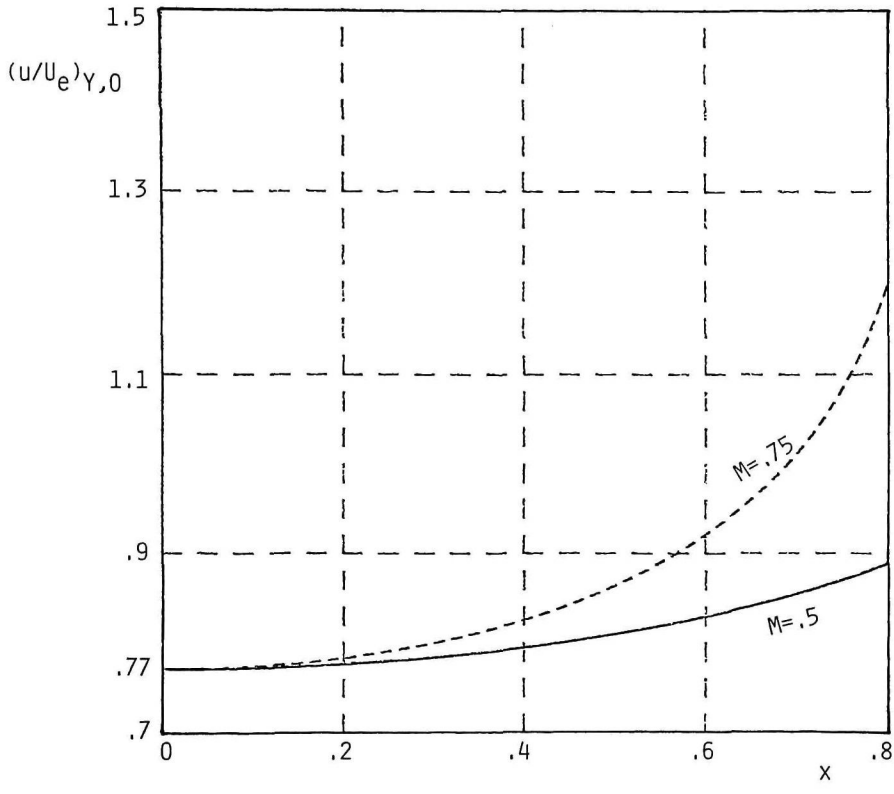

Fig.12 $(u/U_e)_{Y,0}$ versus x for $M = 0.5$ and $M = 0.75$, $Pr = 1$, $S_w = 0.8$.

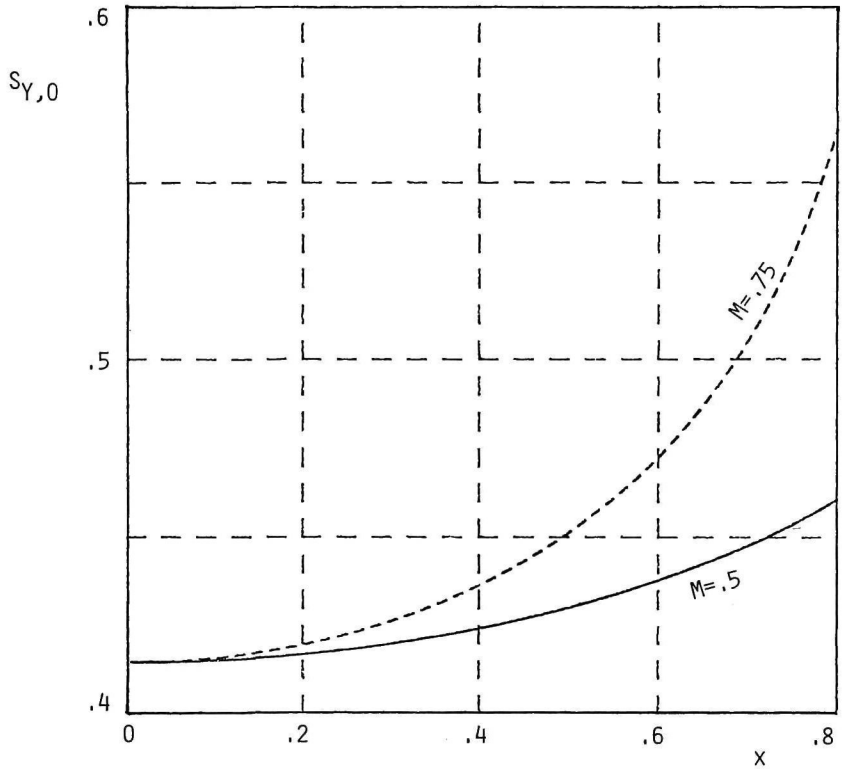

Fig.13 $S_{Y,0}$ versus x for $M = 0.5$ and $M = 0.75$, $Pr = 1$, $S_w = -0.8$.

Appendix to Chapter 3

MOTION EQUATIONS IN THE ODOGRAPH PLANE

Compressible two-dimensional irrotational steady equations of motion can be written in a linear form assuming V (modulus of velocity $\underline{V}$) and θ (angle that $\underline{V}$ forms with a reference axis x) as independent variables. From irrotationality of motion we have

$$\underline{V} = grad\varphi \tag{A.1}$$

where φ is the scalar potential function.

The potential vector $\underline{A}$ gives velocity by means of the following equation

$$\rho\underline{V} = rot\,\underline{A} \tag{A.2}$$

where ρ is the density. We assume a cartesian system of reference (x, y) and denote by u and v the components of $\underline{V}$ in this system. One has

$$u = Vcos\theta\,; \qquad v = Vsin\theta\,. \tag{A.3}$$

In two-dimensional plane case $\underline{A}$ only has non zero value for the third component; we denote by ψ (stream function) such a component. Therefore we have

$$\psi_x = -\rho v \; ; \qquad \psi_y = \rho u \; . \tag{A.4}$$

By differentiating φ and ψ we have

$$d\varphi = udx + vdy \; ; \qquad d\psi = -\rho v dx + \rho u dy \; . \tag{A.5}$$

These equations, taking into account Eqs. (A.3), give for dx and dy the following expressions:

$$\begin{aligned} dx &= (cos\theta d\varphi - (1/\rho) sin\theta d\psi)/V \\ dy &= (sin\theta d\varphi + (1/\rho) cos\theta d\psi)/V \; . \end{aligned} \tag{A.6}$$

If we assume V and θ as independent variables we have

$$dx = x_V dV + x_\theta d\theta \; ; \qquad dy = y_V dV + y_\theta d\theta \tag{A.7}$$

$$d\varphi = \varphi_V dV + \varphi_\theta d\theta \qquad d\psi = \psi_V dV + \psi_\theta d\theta \; . \tag{A.8}$$

By substituting Eqs.(A.7) and (A.8) into Eqs.(A.6) it results

$$x_V = (cos\theta\varphi_V - sin\theta\psi_V/\rho)/V$$

$$x_\theta = (cos\theta\varphi_\theta - sin\theta\psi_\theta/\rho)/V \qquad (A.9)$$

$$y_V = (sin\theta\varphi_V + cos\theta\psi_V/\rho)/V$$

$$y_\theta = (sin\theta\varphi_\theta + cos\theta\psi_\theta/\rho)/V\ . \qquad (A.10)$$

By equating $x_{V\theta}$ to $x_{\theta V}$ (obtained from Eqs. (A.9)), and $y_{V\theta}$ to $y_{\theta V}$ (obtained from Eqs. (A.10)) we have two equations that can be written in the form

$$Asin\theta + Bcos\theta = 0$$

$$Acos\theta + Bsin\theta = 0\ . \qquad (A.11)$$

Therefore it is $A = B = 0$, i.e.

$$\varphi_\theta = V\psi_V/\rho \qquad (A.12)$$

$$\varphi_V = (1/\rho)_V\psi_\theta - (1/\rho)_\theta\psi_V - (1/\rho V)\psi_\theta\ . \qquad (A.13)$$

From Bernoulli equation

$$(\gamma - 1)V^2/2 + a^2 = a_s^2 \qquad (A.14)$$

where a_s is the stagnation velocity of sound, the isoentropic one

$$p/\rho^\gamma = const \qquad (A.15)$$

and state equation for perfect gases

$$p = \rho RT \qquad (A.16)$$

($a^2 = p_\rho = \gamma RT$, where γ is the ratio of heat coefficients) it results that a, p and ρ only depend on V. Moreover from Eqs. (A.14)-(A.16) one has

$$dp = -\rho V dV \qquad (A.17)$$

i.e.

$$p_V = -\rho V \, . \qquad (A.18)$$

Therefore it is

$$(1/\rho)_V = -\rho_V/\rho^2 = -\rho_p p_V/\rho^2 = -p_V/a^2\rho^2 = V/\rho a^2 \, . \qquad (A.19)$$

Thus Eq.(A.13) becomes

$$\varphi_V = (V/\rho a^2 - 1/\rho V)\psi_\theta \,. \tag{A.20}$$

By differentiating φ_θ with respect to V and φ_V with respect to θ and equating these two equations one has

$$V^2\psi_{VV} + V\psi_V(1+M^2) + (1-M^2)\psi_{\theta\theta} = 0 \tag{A.21}$$

where M is the Mach number ($M = V/a$). From Eq. (A.14) one has

$$1/M^2 = a_s^2/V^2 - (\gamma-1)/2 \tag{A.22}$$

and Eq. (A.21) becomes

$$V^2[1-(\gamma-1)V^2/a_s^2]\psi_{VV} + V[1-(\gamma-3)V^2/2a_s^2]\psi_V$$

$$+ [1-(\gamma+1)V^2/2a_s^2]\psi_{\theta\theta} = 0 \,. \tag{A.23}$$

Chapter 4

FLOWS OVER BODIES IN FORCED CONVECTION: THE WEDGE CASE

1.4 Introduction

In this chapter we analyze two situations of coupled heat transfer in a fluid and the adjacent solid wall that are of interest in supersonic and hypersonic flight, where care must be taken to dissipate the heat generated by friction and compression of the gas and transferred to the walls of the aircraft. A part of the analysis is based on a generalization of the previous solution (flat plate case) to boundary-layer flow over a wedge, behind the leading shock wave, considering, however, different boundary conditions with respect to conduction in the solid. We shall study two cases, quite different from each other: a solid wedge refrigerated, and thus held at constant temperature, on its axis, and a nonrefrigerated wedge, where heat is removed by axial conduction only.

Therefore we shall consider a solid wedge surrounded by a supersonic stream that forms a shock at its wedge and held in either isothermal, case (c), or adiabatic

(symmetric), case (d), conditions on its axis. (see Fig.1).

2.4 Equations and boundary conditions

Also in this case pressure is constant. Therefore by using Eqs.(14,1) one finds that in Stewartson-Dorodnitzin plane the velocity components are independent of temperature and are those of the flat-plate case; it is

$$U = Z' ; \qquad V = (zZ' - Z)/2\xi^{1/2} \tag{1}$$

where $z = \eta/\xi^{1/2}$ and $Z(z)$ is the function that solves Blasius equation, $2Z''' + ZZ'' = 0$.

In terms of Z the energy equation becomes

$$\xi\theta_\xi Z' - Z\theta_z/2 = \theta_{zz}/Pr + (\gamma - 1)M_0^2 Z''^2 \tag{2}$$

where $\theta = (T - T_e)/T_0$, M_0 is the Mach number referred to the temperature T_0 that is equal to $T_b - T_e$ in case (c) and to the stagnation temperature in case (d).

We consider a supersonic stream of Mach number M_1 and temperature T_1 that encounters a wedge aligned with the flow of half-angle α. After the shock wave that forms at the front the Mach number and temperature are M_2 and T_2.

The dimensionless temperature θ may be written as

$$\theta = \theta_h + (\gamma - 1)M_0^2\theta_p \tag{3}$$

where $(\gamma - 1)M_0^2\theta_p$ is a particular solution of Eq.(2) and θ_h is a solution of the homogeneous part of Eq.(2).

The boundary conditions associated with Eq.(2) are

$$\theta(\xi, \infty) = 0 \tag{4}$$

and

$$p\theta_{z,w} = (\theta_w - 1)/\xi^{1/2}\,; \qquad p = Re^{1/2}\alpha\lambda_0/\lambda_{so} \tag{5}$$

for case (c) and

$$p\theta_{z,w} = -\xi^{1/2}(\xi\theta_\xi)_{\xi,w}\,; \qquad p = Re^{1/2}\lambda_0/\alpha\lambda_{so} \tag{6}$$

for case (d).

3.4 Isothermal condition on the axis

When the axis of the wedge is at constant temperature, case (c), as the Mach number M_0 has been referred to the temperature $T_0 = T_b - T_2$, we can write $M_0^2 = M_2^2/\Delta t$, where $\Delta t = (T_b - T_2)/T_2$.

In this case it is convenient to solve the problem in terms of the variables z and

$$m_1 = p\, x^2 \tag{7}$$

by expressing θ_h and θ_p of Eq.(3) by means of the following MacLaurin series in the variable m_1

$$\theta_h = \sum_{i=0}^{\infty} m_1^i \theta_{h,i}(z) \tag{8}$$

$$\theta_p = \sum_{i=0}^{\infty} m_1^i \theta_{p,i}(z)\,. \tag{9}$$

It is possible to follow a unified procedure for the determination of the equations and the boundary conditions for the terms $\theta_{h,i}$ and $\theta_{p,i}$ of Eqs.(8) and (9).

In fact, from Eqs.(2) and (5) one obtains

$$\theta_0''/Pr + Z\theta_0' + \epsilon Z''^2 = 0 \tag{10}$$

$$\theta_0(0) = 1 - \epsilon\,; \qquad \theta_0(\infty) = 0 \tag{11}$$

where $\epsilon = 0$ for $\theta_{h,0}$ and $\epsilon = 1$ for $\theta_{p,0}$, for the leading term and

$$\theta_i''/Pr + Z\theta_i' - iZ'\theta_i = 0 \tag{12}$$

$$\theta_i(0) = \theta_{i-1}'(0)\,; \qquad \theta_i(\infty) = 0 \tag{13}$$

for $i > 0$.

By using the Padé approximation technique we obtain a representation that is valid even when MacLaurin series does not converge.

The comparison between the MacLaurin (dash and dot lines) and the Padé (solid lines) representations is shown in Fig.2 for 14-term expansions. For $0 \leq m_1 \leq 1$ the two representations coincide because the radius of convergence of the MacLaurin series is 1. For $m_1 > 1$ the MacLaurin curves diverge while the Padé representation still converge.

To verify the validity of the solutions given by Padé representation for θ_h and θ_p, we have studied the asymptotic behavior of these two functions. As in the previous chapter, we expand θ_h and θ_p in terms of the variable $m_2 = 1/m_1$ and consider the zero-order term of these expansions. It can be seen that the asymptotic solution for θ_h is identically zero, whereas the one for θ_p, denoted by $h_0(z)$, is the solution of the differential equation

$$h_0''/Pr + Zh_0' + Z''^2 = 0 \tag{14}$$

with the boundary conditions

$$h_0'(0) = 0\,; \qquad h_0(\infty) = 0\,. \tag{15}$$

The curves of $\theta_h(0)$ and $\theta_p(0)$, obtained from the Padé technique, and the asymptotic value $h_0(0)$ (dotted line) are plotted versus m_1 in Fig.3. This figure shows that for $m_1 \to \infty (x \to \infty)$, θ_h indeed vanishes and θ_p tends to the asymptotic solution h_0.

We are now in a position to draw the curve of θ_w and of the non-dimensional heat flux at wall Nu (Nusselt number). We consider a wedge of half-angle $\alpha = 5deg.$; $T_1 = 270\ K$, $T_b = 1000\ K$ and $M_1 = 2, 3, 4, 5, 6$. M_2 can be obtained from the shock waves equations. The curves of θ_w and Nu are plotted versus m_1 in Figs. 4 and 5.

It must be noted, in Fig.5, that $Nu/Re_x^{1/2}$ tends to zero for $m_1 \to \infty$, because the asymptotic solution is the one obtained with the adiabatic condition at the interface. Figure 4 shows how θ_w, starting from 1, reaches the adiabatic wall temperature (broken lines) at infinity, which presents the usual dependence on the Mach number. At $M_1 = 4$ the solution coincides both with the asymptotic one and with the one obtained with the isothermal condition at the interface. Under this condition the wedge is at constant temperature.

The dependence on p of the solution has been concealed by the choice of scales in Figs. 4 and 5. Changing p is equivalent to stretching the scale of m_1 in these figures; in particular for $p \to 0$ the solution corresponding to an isothermal boundary condition and for $p \to \infty$ the one corresponding to an adiabatic condition is attained.

4.4 Adiabatic condition on the axis

We consider the case of adiabatic condition on the axis (symmetric case).

The solution of this case is trivial. In fact, as θ turns out to be a function of the variable z only, because the variable x does not appear explicitly either in the

equation or in the boundary condition, the coupling condition (6) is satisfied by simply letting $\theta'(0) = 0$. Hence the solution of equation (2) with the boundary condition (6) is the function θ satisfying the following equation and boundary conditions:

$$\theta''/Pr + Z\theta' + Z''^2 = 0$$

$$\theta'(0) = 0\,; \qquad \theta(\infty) = 0\,.$$

The similarity solution thus obtained is at the same time adiabatic and isothermal at the wall and satisfies equation (6) for any value of p.

Notice that the accidental situation that an adiabatic solution is at the same time isothermal makes this solution valid even when no approximation is made in the treatment of the thermal field in the solid wall, as in this case temperature inside the solid is simply constant.

References to Chapter 4

[1] P. Luchini, M. Lupo, A. Pozzi: "The Effects of Wall Thermal Resistance on Forced Convection Around Two-Dimensional Bodies", Journal of Heat Transfer (1990), 112, 572-578.

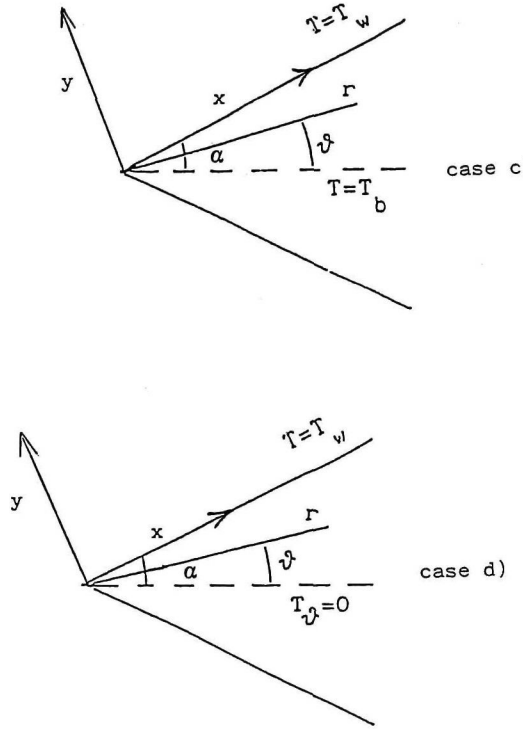

Fig.1 Flow cases:
c) wedge with isothermal condition on the axis;
d) wedge with adiabatic condition on the axis.

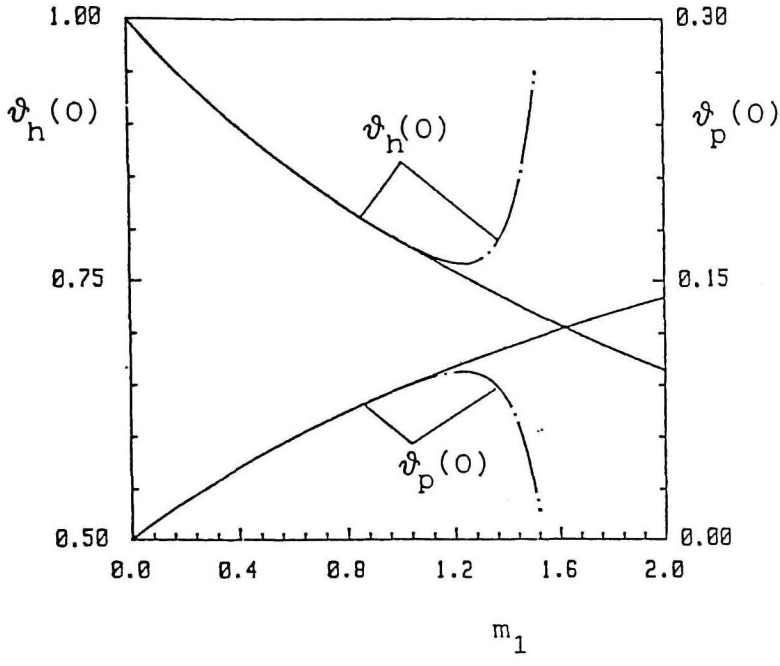

Fig.2 Wedge flow with isothermal condition on the axis: convergence of Padé approximations (solid lines) and Taylor series (dotted lines).

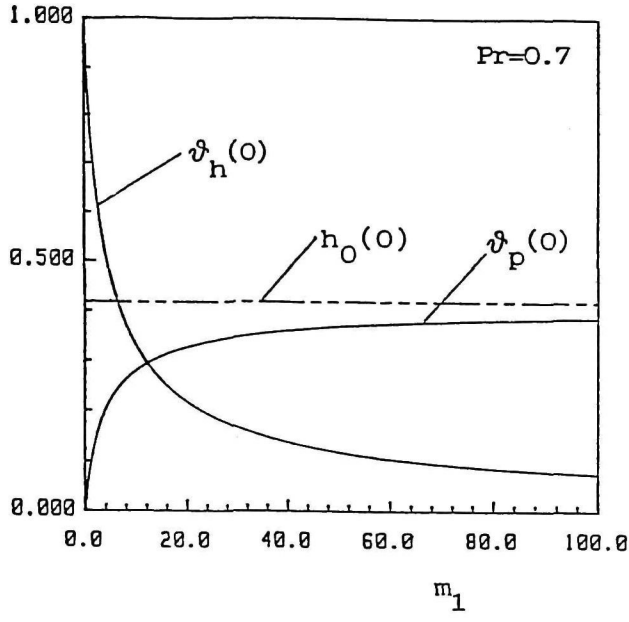

Fig.3 Wedge flow with isothermal condition on the axis: universal plot of the functions necessary for calculation of the wall temperature as $\vartheta_w(0)=\vartheta_h(0)+(\gamma-1)M^2\vartheta_p(0)$.

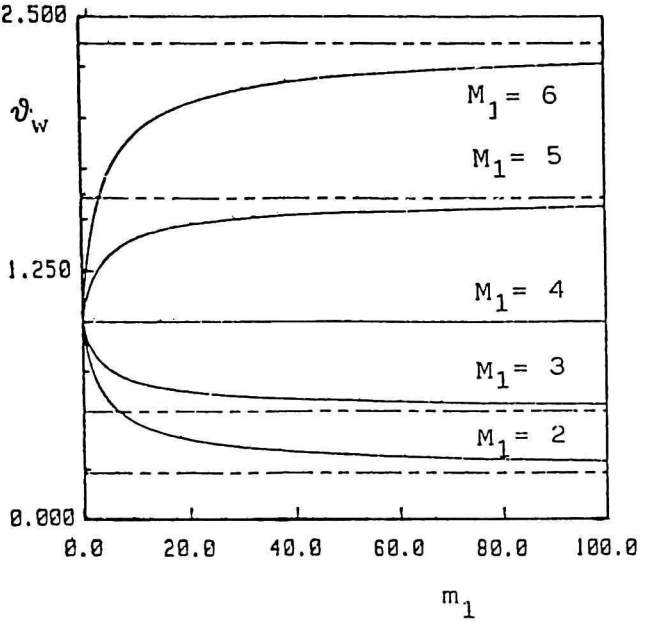

Fig.4 Variation of wall temperature ϑ_w versus generalized axial coordinate m_1 for wedge flow with isothermal boundary condition at several Mach numbers.

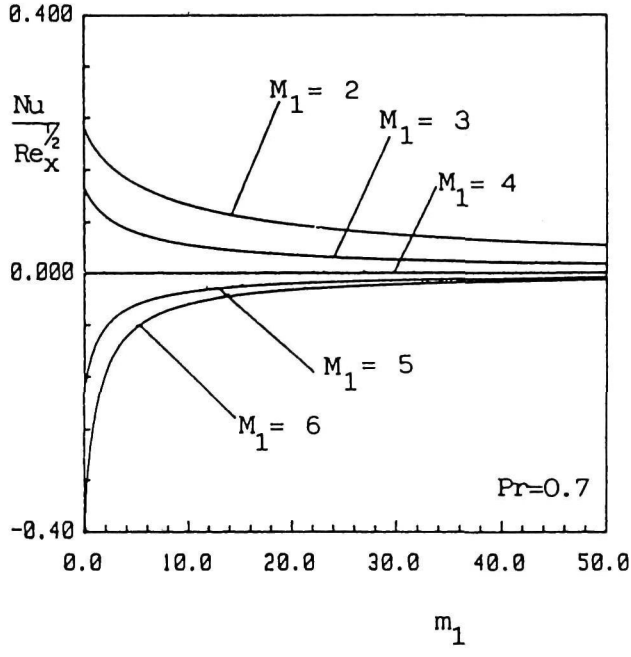

Fig.5 Variation of local Nusselt number $Nu/Re^{1/2}$ with m_1 for wedge flow with isothermal boundary condition at several Mach numbers.

Chapter 5

THE COUPLING OF CONDUCTION WITH LAMINAR NATURAL CONVECTION ALONG A VERTICAL FLAT PLATE

1.5 Introduction

As pointed out in ref.[1], when convective heat transfer depends strongly on the thermal boundary conditions, natural convection must be studied as a mixed problem if one needs an accurate analysis of the thermo-fluid-dynamics field. The phenomenon depends on several parameters: therefore in many cases this strong dependence does exist.

In ref.[1] an analysis is given of the relative importance of the parameters of the problem in particular with reference to axial heat conduction. In ref.[2], by extending the analysis of Gosse [3], a technique is shown which improves the results given by the first term of an asymptotic expansion of the solution. In the same paper a new correlation for the evaluation of the heat transfer coefficient is also presented.

This analysis holds for high values of the abscissa x; the value of the point x_0 from which the expansion is valid depends on the parameters that govern the

problem.

In this chapter we study coupled natural convection by identifying the region where point x_0 is located, improving the results concerning the asymptotic expansion by adding terms of higher order with respect to the first one, discussing the general form of the asymptotic expansion, which is singular for the presence of eigen-solutions, and determining the expansion holding for small values of x in an accurate way, by evaluating many terms of the series and its radius of convergence by means of Padé approximants technique. This analysis was published in ref.[4].

2.5 Equations and boundary conditions

The equations that govern the steady two dimensional flow due to the free convection along a side of a vertical flat plate of thickness b, insulated on the edges and with a temperature T_b on the other side (Fig.1) in non-dimensional form may be written as

$$u_x + v_y = 0 \tag{1}$$

$$uu_x + vu_y = u_{yy} + \theta \tag{2}$$

$$u\theta_x + v\theta_y = \theta_{yy}/Pr \tag{3}$$

where $\theta = (T - T_\infty)/(T_b - T_\infty)$. The reference quantities are: $L = \nu^{2/3}/g^{1/3}$ for x, $L/d^{1/4}$ for y and $\nu d^{1/4}$ for the stream function ψ, where $d = (T_b - T_\infty)\beta$, β is the volume thermal expansion coefficient and g is the acceleration due to gravity.

The boundary conditions that must be associated with Eqs.(1)-(3) are

$$u(x,0) \;=\; v(x,0) \;=\; u(0,y) \;=\; u(x,\infty) \;=\; 0 \tag{4}$$

$$\theta(0,y) \;=\; \theta(x,\infty) \;=\; 0 \tag{5}$$

$$\theta(x,0) - 1 \;=\; p\theta_y(x,0) \tag{6}$$

where

$$p \;=\; d^{1/4} b\lambda / L\lambda_s \; . \tag{7}$$

3.5 Solution for small x: initial expansion

Let $s = y/(px)^{1/5}$, $\psi = x^{4/5} g(x,s)/p^{1/5}$, $\theta = x^{1/5} h(x,s)/p^{4/5}$.

Then Eqs.(1)-(3) may be written as

$$3g_s^2 \;-\; 4gg_{ss} \;+\; 5x(g_s g_{sx} - g_x g_{ss}) \;=\; 5(h + g_{sss}) \tag{8}$$

$$hg_s - 4gh_s + 5x(g_s h_x - h_s g_x) = 5h_{ss}/Pr \tag{9}$$

and Eq.(6) becomes

$$h_s(x,0) = m_1 h(x,0) - 1 \tag{10}$$

where

$$m_1 = x^{1/5}/p^{4/5} . \tag{11}$$

By assuming m_1 and s as independent variables it is possible to expand the functions g and h in a MacLaurin series with respect to m_1 ($m_1 = 0$ corresponds to $x = 0$) in this way

$$g = \sum_{i=0}^{\infty} m_1^i g_i(s) ; \qquad h = \sum_{i=0}^{\infty} m_1^i h_i(s) . \tag{12}$$

The following are the expansion of functions g_i and h_i from (12)

$$\begin{aligned} &5g_i''' - 6g_0' g_i' + 4(g_i g_0'' + g_0 g_i'') - i(g_0' g_i' - g_i g_0'') + 5h_i = M_i \\ &5h_i''/Pr - h_0 g_i' - h_i g_0' + 4g_0 h_i' + 4g_i h_0' - i(g_0' h_i - h_0' g_i) = N_i \end{aligned} \tag{13}$$

where

$$M_i = \sum_{j=1}^{i-1} [3g'_j g'_{i-j} - 4g_j g'_{i-j} + j(g'_j g'_{i-j} - g_j g''_{i-j})]$$

$$N_i = \sum_{j=1}^{i-1} [h_j g'_{i-j} - 4g_j h'_{i-j} + j(h_j g'_{i-j} - g_j h'_{i-j})].$$

The boundary conditions are

$$g_i(0) = g'_i(0) = g'_i(\infty) = h_i(\infty) = 0$$

$$h'_0(0) = -1\,; \quad h'_i(0) = h_{i-1}(0) \qquad (i > 0)\,. \tag{14}$$

Equations (13) and (14) represent a standard boundary-value problem which can be easily solved numerically. The only difficulty with this expansion is the evaluation of its radius of convergence $r(Pr)$. Such a function can be obtained by means of the technique of Padé approximants.

We choose the diagonal sequence by assuming $M = N$.

We have checked the reliability of the results by analyzing the two expansions related to the wall temperature and to the drag coefficient (i.e. $u_y(x,0)$), for N varying between 4 and 28 in increments of 2. The two sequences for $Pr = 0.733$ give the following values for the radius of convergence r : 0.97, 1.05, 1.09, 1.11, 1.13, 1.14, 1.15, 1.15, 1.16, 1.16, 1.15, for the wall temperature expansion and 1.17, 1.17, 1.16, 1.16, 1.16, 1.17, 1.16, 1.16, 1.15 for the drag coefficient expansion. Both sequences give a value of nearly 1.15 for r. For $Pr = 2.97$ we find $r = 1.65$.

The behaviour of expansion (12) in the range $(0, r)$ of m_1 confirms the value of r found in this way. In Table 1 the values of θ are listed for N terms of the expansion and for $Pr = 2.97$: $m_1 = 1.3$ corresponds to $0.8r$. For small values of m_1 a few terms are sufficient to obtain convergence, as m_1 approaches r the number of terms necessary to reach a good accuracy increases rapidly.

Hence in the range $(0, r)$ for m_1 expansion (12) represents the solution of the problem well.

4.5 Solution for large x: asymptotic expansion

The solution for $m_1 > r$ assumes a form different from that expressed by expansion (12).

In fact if one substitutes the following expansions

$$f = \sum_{i=0}^{\infty} m^i f_i(z) ; \qquad \theta = \sum_{i=0}^{\infty} m^i \theta_i(z) \tag{15}$$

where $z = y/x^{1/4}$, $\psi = x^{3/4} f(x, z)$ and

$$m = p x^{-1/4} \tag{16}$$

into Eqs.(1), (2), (3) and (6), that lead to

$$2f_z^2 - 3ff_{zz} + 4x(f_{zx} - f_x f_{zz}) = 4(\theta + f_{zzz})$$

$$4x(\theta_x f_z - f_x \theta_z) - 3f\theta_z = 4\theta_{zz}/Pr \tag{17}$$

$$\theta(x,0) - 1 = m\theta_z(x,0) \tag{18}$$

one finds at the leading order the following system:

$$\begin{gathered} 2f_0'^2 - 3f_0 f_0'' = 4(\theta_0 + f_0''') \\ - 3f_0\theta_0' = 4\theta_0''/Pr \end{gathered} \tag{19}$$

$$f_0(0) = f_0'(0) = f_0'(\infty) = 0$$

$$\theta_0(0) = 1 \qquad \theta_0(\infty) = 0$$

and at the ith order

$$\begin{gathered} 4(f_i''' + \theta_i) - 4f_0' f_i' + 3f_0 f_i'' + 3f_0'' f_i + i(f_i' f_0' - f_i f_0'') = S_i \\ 4\theta_i''/Pr + 3f_0\theta_i' + 3f_i\theta_0' + i(f_0'\theta_i - \theta_0' f_i) = T_i \end{gathered} \tag{20}$$

$$f_i(0) = f_i'(0) = f_i'(\infty) = 0$$

$$\theta_i(0) = \theta_{i-1}'(0)\,; \qquad \theta_i(\infty) = 0$$

where

$$S_i = \sum_{j=1}^{i-1} [2f_j'f_{i-j}' - 3f_jf_{i-j}'' - j(f_j'f_{i-j}' - f_jf_{i-j}'')]$$

$$T_i = \sum_{j=1}^{i-1} [-j(\theta_j f_{i-j}' - f_j\theta_{i-j}') - 3f_j\theta_{i-j}']. \tag{21}$$

Equations (20) represent the eigensolutions.

The first one appeared in expansion (10) for $i = 4$, for linearized Eqs.(20) admit an eigensolution. In fact Eqs.(1)-(3) are unchanged by a translation of the origin of the x-axis and their solutions do not change in form when x is substituted for $x - x_0$. If one expands $\psi(x, y, x_0)$ and $\theta(x, y, x_0)$ in powers of x_0, by writing $\psi(x, y, x_0) = x^{3/4}[\psi_0(x, y) + x_0\psi_1(x, y)]$ and $\theta = \theta_0(x, y) + x_0\theta_1(x, y)$, one finds that ψ_1 and θ_1 may be written as $(1/x)F_1(z)$ and $(1/x)G_1(z)$. As this solution holds for any x_0, F_1 and G_1 represent an eigensolution. In particular one finds

$$F_1 = (3/4)f_0 - (1/4)zf_0'\,; \qquad G_1 = -(1/4)z\theta_0'$$

where f_0 and θ_0 are given by the leading-order term in expansion (10). Functions F_1 and G_1 satisfy Eqs.(20) with $i = 4$ and $S_i = T_i = 0$.

Then the first four terms in expansion (15) can be determined by means of Eqs.(20) (the presence of the first eigenvalue does not permit the solution of Eqs.(20) for $i = 4$) and the solution can be written in the form

$$f = \sum_{i=0}^{3} m^i f_i(z) + m^4 Q(m,z)$$

$$\theta = \sum_{i=0}^{3} m^i \theta_i(z) + m^4 R(m,z) \qquad (10')$$

where functions $Q(m,z)$ and $R(m,z)$ are not analytic.

Both Q and R may be represented by suitable expansions. The eigenfunctions have the form $(1/x)^q\ f_q(z)$, $(1/x)^q\ \theta_q(z)$ where q is a real parameter which takes on eigenvalues.

The first eigenvalue of q for any Pr is 1; the second one for $Pr = 2.97$ is 2.2 and for $Pr = 0.73$ is 2.4.

The results have shown that the number of terms necessary to represent the initial solution satisfactorily in the range $(0, x_0)$, with x_0 corresponding to a value of m equal to $0.8r$ (r being the radius of convergence), is 17. At $x = x_0$, in the considered case, the asymptotic solution is represented well by means of four terms.

For $Pr = 0.733,\ 1.15,\ 2.97,\ 7.2,\ 13.6$ the radii of convergence of the initial expansion are 1.16, 1.36, 1.65, 2.03, 2.29, respectively.

The values at $y = 0$ of the first few terms of the initial and asymptotic expansions are listed in Tables 2 and 3.

In order to compare our results with those of ref.[2] we consider a plate with length ℓ and define a Grashof number according to its length; moreover, letting

$K = \lambda_s \ell / \lambda_f b$, we can write $m = Gr^{1/4}/(x/\ell)^{1/4} K$ and $m_1 = K^{4/5}(x/\ell)^{1/5}/Gr^{1/5}$. We assume for Gr the value of 10^9. We define the Grashof number as follows

$$\frac{g\ell^3 d}{\nu^2} .$$

In Figs. 2 and 3, θ, evaluated by means of the asymptotic expansion, is plotted vs. x/ℓ for $K = 500$ and 1000 and $Pr = 2.97$ together with the results of ref.[2]. One can see that the first approximation is not very accurate for the lower value of K: an improvement is obtained by means of the technique of ref.[2]. As K increases, the differences between the first and the third approximation become smaller.

To compare the two expansions we have considered θ and u_y at the wall as a representation of the thermal field and of the fluid-dynamic field. The number of terms of the initial expansion is 17. In Figs. 4 and 5 the case $K = 500$, $Pr = 2.97$ is drawn. In Fig. 4 the dashed curve, corresponding to the asymptotic solution for θ, diverges for $x \to 0$ and differs appreciably from the initial one up to $x/\ell = 0.05$. For higher values of x/ℓ one sees that the two curves are very close to each other. The value of x/ℓ corresponding to the largest abscissa of convergence of the initial expansion is roughly 0.19; hence in the range (0.05, 0.19) both expansions seem to hold. A similar behaviour is displayed in Fig.5, but for the considered number of terms the two curves stay very close in a shorter range.

In both cases the value of $x_0/\ell = 0.06$, corresponding to a value of $m_1 = 0.8r$, is a suitable starting point for the asymptotic expansion.

In Figs. 6 and 7 the curves for the case of $K = 250$ and $Pr = 2.97$ are drawn. For these values $x_0/\ell > 1$. Therefore, in the whole range $(0, 1)$ the thermo-fluid-

dynamic field is governed by the initial solution. The figures show an appreciable difference between the dashed curve (asymptotic solution) and the solid curve (initial solution) for both functions.

In Figs. 8 and 9 the curves relating to $K = 250$ and $Pr = 0.733$ are drawn. In this case $x_0/\ell = 0.26$. The comparison with Figs. 6 and 7 shows that the lower value of Pr makes the difference between the two solutions very small, except for vanishing values of x.

The previous analysis enables one to obtain the solution of the problem in the entire field using the initial solution for $0 < x < x_0$ and asymptotic solution for $x > x_0$. x_0 is the starting point of the asymptotic solution and the velocity and temperature profiles obtained from the initial solution represent the initial conditions for the asymptotic solution.

According to the analysis presented in the previous sections the difference between the two solutions at $x = x_0$ must be of the order of magnitude m^4: in fact we have taken into account the terms of the asymptotic expansion up to the third order. Figures 4-9 confirm such behaviour.

Therefore, when $m(x_0)$ is not too high, as in the considered cases, the approximation in which terms of order m^4 are neglected is satisfactory.

To obtain higher approximations one must consider a new expansion in terms of eigenfunctions, starting from order m^4.

References to Chapter 5

[1] M. Miyamoto, J. Sumikawa, T. Akiyoski and T. Nakamura, Effects of axial heat conduction in a vertical flat plate of free convection heat transfer, *Int. J. Heat Mass Transfer* **23**, 1545-1533 (1980).

[2] J. Timma, J.P. Padet, Etude théorique du couplage convection-conduction en convection libre laminaire sur une plaque verticale, *Int. J. Heat Mass Transfer* **28**, 1097-1104 (1985).

[3] J. Gosse, Analyse simplifiée du couplage conduction-convection pour un ecoulement a' couche limite laminaire sur une plaque plane, *Rev. Gen. Therm.* **228** (1980).

[4] A. Pozzi, M. Lupo, The coupling of conduction with laminar natural convection along a flat plate, *Int. J. Heat Mass Transfer* **31**, 1807-1814 (1988).

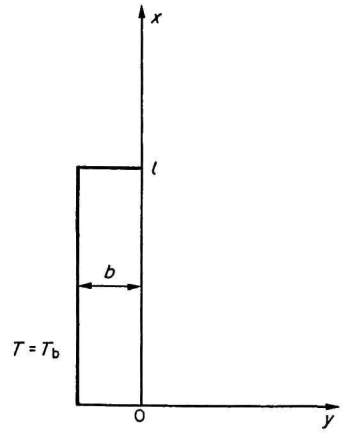

Fig.1 A vertical flat plate and coordinate system.

Table 1.

Values of ϑ, for Pr=2.97, for several terms of the expansion.

	$m_1 = 0.574$	$m_1 = 0.910$	$m_1 = 1.045$	$m_1 = 1.20$	$m_1 = 1.302$	$m_1 = 1.44$	$m_1 = 1.56$
$N = 4$	0.498	0.732	0.905	1.235	1.568	2.25	3.137
$N = 6$	0.490	0.630	0.687	0.780	0.876	1.101	1.441
$N = 8$	0.490	0.618	0.650	0.664	0.650	0.570	0.394
$N = 10$	0.490	0.620	0.657	0.690	0.704	0.703	0.661
$N = 12$	0.490	0.620	0.659	0.699	0.730	0.802	0.946
$N = 14$	0.490	0.620	0.658	0.693	0.712	0.728	0.723
$N = 16$	0.490	0.620	0.658	0.693	0.711	0.717	0.667
$N = 17$	0.490	0.620	0.658	0.693	0.714	0.739	0.762

Table 2.

Initial expansion: values of $g_n''(0)$ and $h_n(0)$.

	$Pr = 0.733$		$Pr = 2.97$	
n	$g_n''(0)$	$h_n(0)$	$g_n''(0)$	$h_n(0)$
0	1.540	2.042	9.194×10^{-1}	1.411
1	-1.641	-3.083	-6.799×10^{-1}	-1.481
2	1.624	3.789	4.698×10^{-1}	1.271
3	-1.371	-3.886	-2.787×10^{-1}	-9.147×10^{-1}
4	9.453×10^{-1}	3.322	1.360×10^{-1}	5.512×10^{-1}
5	-4.840×10^{-1}	2.298	-4.992×10^{-2}	-2.704×10^{-1}
6	1.210×10^{-1}	1.172	9.470×10^{-3}	9.896×10^{-2}
7	7.296×10^{-2}	-2.853×10^{-1}	3.295×10^{-3}	-1.827×10^{-2}
8	-1.095×10^{-1}	-1.844×10^{-1}	-3.895×10^{-3}	-6.959×10^{-3}
9	5.699×10^{-2}	2.681×10^{-1}	1.570×10^{-3}	7.875×10^{-3}
10	7.548×10^{-3}	-1.632×10^{-1}	2.823×10^{-5}	-3.093×10^{-3}
11	-3.774×10^{-2}	-2.162×10^{-2}	-4.462×10^{-4}	-1.190×10^{-4}
12	2.901×10^{-2}	9.333×10^{-2}	2.770×10^{-4}	9.216×10^{-4}
13	-3.509×10^{-3}	-6.994×10^{-2}	-4.674×10^{-5}	-5.541×10^{-4}
14	-1.454×10^{-2}	7.013×10^{-3}	-5.389×10^{-5}	8.412×10^{-5}
15	1.534×10^{-2}	3.632×10^{-2}	4.985×10^{-5}	1.142×10^{-4}
16	-4.697×10^{-3}	-3.719×10^{-2}	-1.571×10^{-5}	-1.011×10^{-4}
17	-5.632×10^{-3}	1.069×10^{-2}	-5.706×10^{-6}	3.016×10^{-5}

Table 3. Asymptotic expansion: values of $f''_n(0)$ and $\vartheta'_n(0)$

n	$Pr = 0.733$		$Pr = 2.97$	
	$f''_n(0)$	$\theta'_n(0)$	$f''_n(0)$	$\theta'_n(0)$
0	9.532×10^{-1}	-3.591×10^{-1}	7.522×10^{-1}	-5.749×10^{-1}
1	-2.908×10^{-1}	1.315×10^{-1}	-3.693×10^{-1}	3.414×10^{-1}
2	1.143×10^{-1}	-3.593×10^{-2}	2.392×10^{-1}	-1.545×10^{-1}
3	-4.128×10^{-2}	3.845×10^{-8}	-1.515×10^{-1}	8.482×10^{-7}

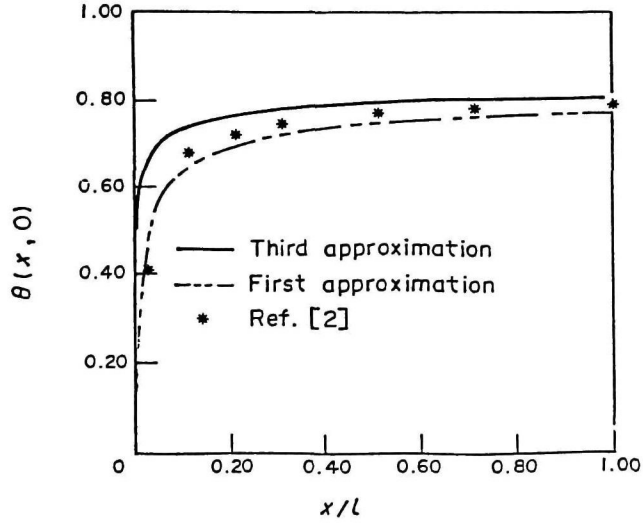

Fig.2 Non-dimensional temperature at the wall $\vartheta(x,0)$ in the asymptotic solution for Pr=2.97, K=500, $Gr=10^9$.

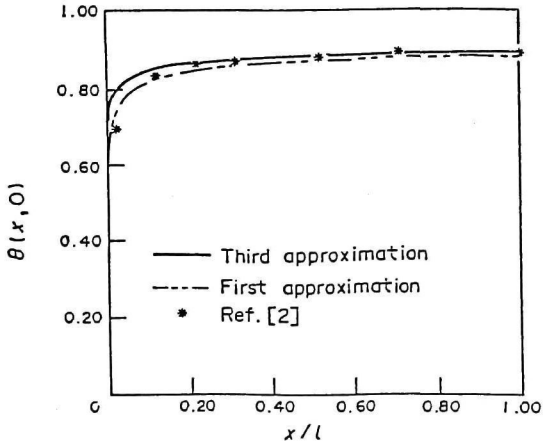

Fig.3 Non-dimensional temperature at the wall $\vartheta(x,0)$ in the asymptotic solution for Pr=2.97, K=1000, $Gr=10^9$.

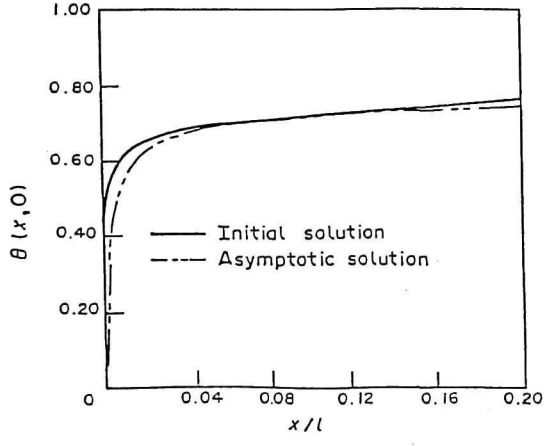

Fig.4 Non-dimensional temperature at the wall $\vartheta(x,0)$ for Pr=2.97, K=500.

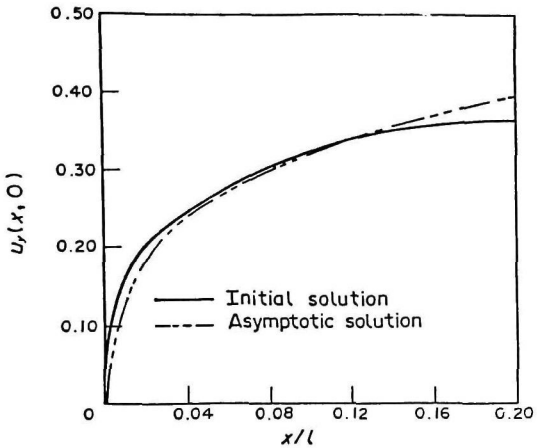

Fig.5 $u_y(x,0)$ for Pr=2.97, K=500.

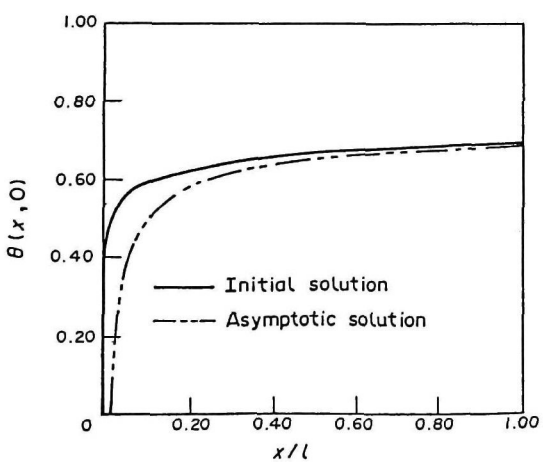

Fig.6 Non-dimensional temperature at the wall $\vartheta(x,0)$ for Pr=2.97, K=250.

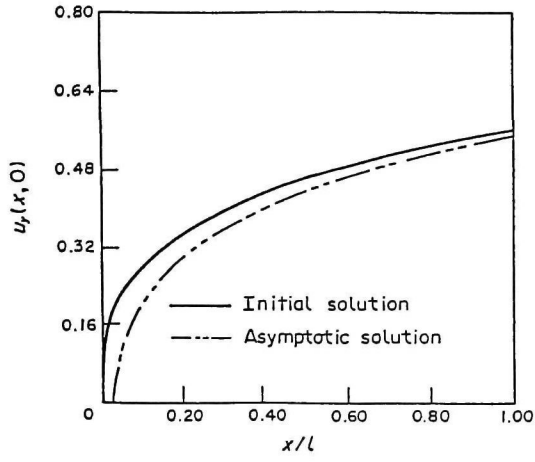

Fig.7 $u_y(x,0)$ for Pr=2.97, K=250.

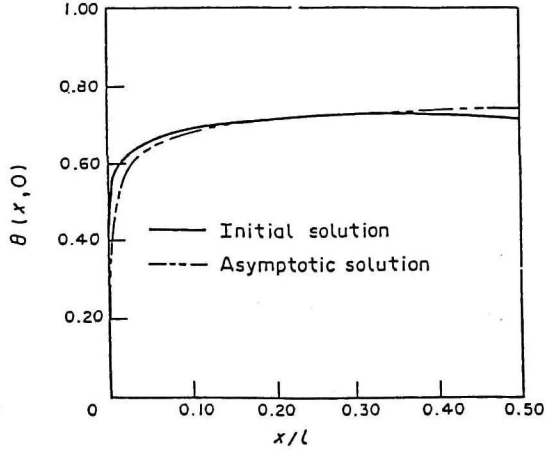

Fig.8 Non-dimensional temperature at the wall $\vartheta(x,0)$ for Pr=0.733, K=250.

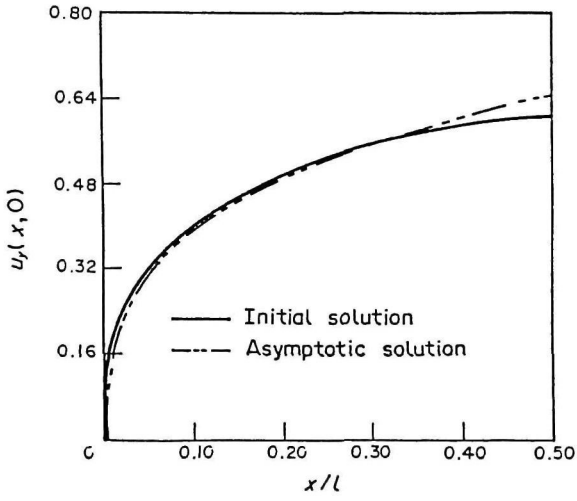

Fig.9 $u_y(x,0)$ for Pr=0.733, K=250.

The figures are reprinted from Int. J. of Heat and Mass Transfer Vol.31, A. Pozzi and M. Lupo, "The coupling of conduction with laminar natural convection along a flat plate", 1807-1814, Copyright 1988 with permission from Pergamon Press Ltd., Headington Hill Hall, Oxford OX3 OBW, UK.

Chapter 6

VARIABLE-PROPERTIES EFFECTS: SUPERSONIC WEDGE FLOW

1.6 Introduction

The first studies on variable-property effects were based on empirical methods, such as the "reference-temperature method" and the "property-ratio method" [1]. In the reference-temperature method, the properties are calculated at a reference temperature T_r different for each property. In the property-ratio method, the variable-property results are obtained by multiplying the corresponding constant-property results by a factor in the form

$$\prod_i [\alpha_i(T_w)/\alpha_i(T_\infty)]^{n_i}$$

where $\alpha_1 = \mu$, $\alpha_2 = \lambda$, $\alpha_3 = \rho$ and the exponents n_i are determined empirically. Subsequently, the problem of variable-property effects has been studied, for walls of zero thickness, in the case of small temperature differences. In particular, Carey and Mollendorf [2] have presented a first-order perturbation analysis for liquids assuming a linear dependence of viscosity on temperature. Gray and Giorgini [3]

have analyzed the limits of applicability of the Boussinesq approximation in the natural convection. Merker and Mey [4], studying the natural convection in a shallow cavity, have found that the reference temperature can be assumed to be the arithmetic mean between the highest and lowest temperatures, if the difference of these temperatures is on the order of 30 K or less.

In this chapter we consider the variable-property effects on supersonic flow along a wedge, taking into account wall thermal resistance. The axis of the wedge is maintained either at a constant temperature or under adiabatic conditions.

Viscosity and thermal conductivity coefficients are assumed to depend on temperature in a polynomial form by generalizing the analysis performed in chapter 4.

The problem governed by the isothermal condition on the axis does not admit similarity solutions and is solved by using two expansions, an initial one and an asymptotic one, and applying the Padé approximants technique. The solution of the second problem can be obtained in similarity form. A discussion of the variable-property effects ends this chapter.

The results of this analysis were published in ref.[5].

2.6 Equation and boundary conditions

As in chap.4, a supersonic stream of Mach number M_1, velocity u_1 and temperature T_1 encounters a wedge whose axis is maintained at a constant temperature T_a in case a) or under adiabatic conditions in case b). Mach number, velocity

and temperature behind the shock wave caused by the wedge are M_2, u_2 and T_2 respectively (Fig.1).

The equations governing the thermo-fluid-dynamic field are the boundary layer equations that in non-dimensional form may be written as

$$(\rho u)_x + (\rho v)_y = 0 \tag{1}$$

$$\rho(uu_x + vu_y) = (\mu u_y)_y \tag{2}$$

$$\rho(ut_x + vt_y) = (\lambda t_y)_y/Pr + [(\gamma - 1)M_2^2/\Delta t]\mu u_y^2 \tag{3}$$

where u and v are the velocity components along the x and y cartesian axes, ρ, μ and λ denote density, viscosity and thermal conductivity coefficients of the fluid and t is the dimensionless temperature defined as $(T - T_2)/(T_a - T_2)$ in case a) and $(T - T_2)/T_2$ in case b).

The reference quantities are L, $LRe^{-1/2}$, u_2, $u_2Re^{-1/2}$, ρ_2, μ_2, λ_2 for x, y, u, v, ρ, μ and λ respectively, where the subscript 2 denotes free stream conditions downstream of the shock wave and L is a characteristic length in the direction of the x-axis. Re and Pr are the Reynolds and Prandtl numbers of the fluid and $\Delta t = (T_a - T_2)/T_2$ in case a) and $\Delta t = 1$ in case b).

The boundary conditions associated with Eqs. (1)-(3) are

$$u(x,0) = v(x,0) = 0 \tag{4}$$

$$u(x,\infty) = 1\,; \qquad t(x,\infty) = 0 \tag{5}$$

The continuity of heat flux at the solid fluid interface in dimensionless form may be written as

$$\lambda t_{y,w} = [t_w - 1]/Ix \tag{6}$$

in case a) and

$$\lambda t_{y,w} = -(xt_x)_{x,w}/I \tag{7}$$

in case b), where the coupling parameter I is

$$I = Re^{1/2}\lambda_2\alpha/\lambda_{so} \tag{8}$$

in case a) and

$$I = Re^{1/2}\lambda_2/(\lambda_{so}\alpha) \tag{9}$$

in case b).

In order to take into account the influence of variability of the fluid properties on the flow it is convenient to introduce the Stewartson-Dorodnitzin transformation in the isobaric form, by utilizing the new independent variables:

$$\xi = x\ ; \qquad \eta\ =\ \int_0^y \rho dy\ . \tag{10}$$

In terms of these variables Eqs. (1)-(3) become

$$u_\xi\ +\ V_\eta\ =\ 0 \tag{11}$$

$$uu_\xi\ +\ Vu_\eta\ =\ [(\rho\mu)u_\eta]_\eta \tag{12}$$

$$ut_\xi\ +\ Vt_\eta\ =\ [(\rho\lambda)t_\eta]_\eta/Pr\ +\ [(\gamma-1)M^2/\Delta t](\rho\mu)u_\eta^2 \tag{13}$$

where

$$V\ =\ \rho v\ +\ u\eta_x\ . \tag{14}$$

In the case of $\rho\mu$ constant, Eqs.(11) and (12) may be solved independently of the energy equation (13) and the stream function ψ is obtained in similar form in terms of the variable

$$z\ =\ \eta/\xi^{1/2}\ .$$

If viscosity and thermal conductivity coefficients are assumed to depend on temperature in a polynomial form, Eqs.(11) and (12) must be solved together with Eq.(13).

In particular we assume the following dependence of μ and λ on absolute temperature T:

$$\mu = \sum_{i=1}^{n} \alpha_i T_i \; ; \qquad \lambda = \sum_{i=1}^{n} \beta_i T_i \tag{15}$$

so that, in dimensionless form, products, $\rho\mu$ and $\rho\lambda$ ($\rho = 1/T$ for a perfect gas) are expressed by means of polynomials in terms of t:

$$\rho\mu = 1 + \sum_{i=1}^{n-1} a_i t_i \; ; \qquad \rho\lambda = 1 + \sum_{i=1}^{n-1} b_i t_i \; . \tag{16}$$

If we consider $n = 2$ it is

$$\begin{aligned} \rho\mu &= 1 + a_1 t \\ \\ \rho\lambda &= 1 + b_1 t \end{aligned} \tag{17}$$

where $a_1 = \alpha_2(T_a - T_2)/(\alpha_1 + \alpha_2 T_2)$ and $b_1 = \beta_1 + \beta_2(T_a - T_2)/(\beta_1 + \beta_2 T_2)$ in case a), whereas $a_1 = \alpha_2 T_2/(\alpha_1 + \alpha_2 T_2)$ and $b_1 = \beta_2 T_2/(\beta_1 + \beta_2 T_2)$ in case b).

By introducing Eqs.(17) into conditions (6) and (7) we obtain the following conditions

$$(1 + b_1 t_w) t_{z,w} = [t_w - 1]/I\xi^{1/2} \tag{18}$$

$$(1 + b_1 t_w) t_{z,w} = -(\xi t_\xi)_{\xi,w} \xi^{1/2} / I$$

for case a) and b) respectively.

3.6 The method of solution for case a)

Owing to the coupling condition (18a) the problem does not admit similar solutions; in fact the solution has a different character for small and high values of ξ ($\xi = x$).

For small values of ξ the solution tends to that obtained with the isothermal condition at the interface and it is convenient to assume $m_1 = I\xi^{1/2}$ and z as independent variables. In this case it is possible to expand the unknowns in a MacLaurin series with respect to m_1. This expansion, whose leading term represents the solution with the isothermal condition at the interface, has a finite radius of convergence and does not allow us to describe the entire thermo-fluid-dynamic field. However we shall see that it is possible, using the Padé approximants technique, not only to calculate the radius of convergence of the initial expansion, but also to obtain a representation valid in the whole field.

For high values of ξ the solution tends to that obtained with the adiabatic condition at the interface and it is convenient to assume $m_2 = 1/m_1$ and z as independent variables. In this case it is possible to expand the unknowns in a MacLaurin series with respect to m_2 because, while no problem is encountered in calculating the first two coefficients of the expansion, the third one cannot be calculated for the presence of eigensolutions. Therefore to take into account terms of $O(m_2^2)$ the asymptotic expansion must be modified so as to include non integral

powers and logarithmic terms. Nevertheless, since terms of this kind do not appear below order 2, they can be neglected in the proposed procedure.

Each term of the two expansions is obtained by solving numerically a system of ordinary differential equations obtained in the usual way from Eqs.(11)-(13) applying the Cauchy's rule for multiplication of power series. In particular we assume in the following, for the sake of simplicity, Eqs.(17) ($n = 2$) for $\rho\mu$ and $\rho\lambda$.

4.6 Expansions for small and high values of ξ for case a)

In order to determine the equations and the boundary conditions which allow us to calculate the terms of expansion for small (initial expansion) and high (asymptotic expansion) values of ξ, we shall follow a unified procedure assuming $z = \eta/\xi^{1/2}$ and $m = (I\xi^{1/2})^{\delta}$ as independent variables where $\delta = 1$ for the initial expansion ($m = m_1$), and $\delta = -1$ for the asymptotic expansion ($m = m_2$). Then, letting $\psi = \xi^{1/2} f(\xi, z)$ ($u = \psi_\eta$ and $V = -\psi_\xi$) and $t = h(\xi, z)$ and assuming z and m as independent variables, Eqs.(12), (13) and (17) give:

$$(1/2)(\delta m f_z f_{zm} - f f_{zz} - \delta m f_m f_{zz}) = (1 + a_1 h) f_{zzz} + a_1 h_z f_{zz} \qquad (19)$$

$$(1/2)(\delta m f_z h_m - f h_z - \delta m f_m h_z) = (1 + b_1 h) h_{zz}/Pr \qquad (20)$$

$$+ b_1 h_z^2/Pr \; + \; ((\gamma - 1)m_2^2/\Delta T)(1 + a_1 h) f_{zz}^2$$

whereas the coupling condition (18a) becomes

$$m^\delta (1 + b_1 h(x,0)) h_z(x,0) \; = \; h(x,0) - 1 \; . \tag{21}$$

Now if one expands the functions f and h in a MacLaurin series with respect to m one has

$$f \; = \; \sum_{i=0}^{\infty} m^i f_i(z) \; ; \qquad h \; = \; \sum_{i=0}^{\infty} m^i h_i(z) \; . \tag{22}$$

Substituting the expansions (22) into Eqs.(4), (5), (19), (20) and (21) gives at the leading order the following system

$$(1 + a_1 h_0) f_0''' \; + \; a_1 h_0' f_0'' \; + \; (1/2) f_0 f_0'' \; = \; 0 \tag{23a}$$

$$(1 + b_1 h_0) h_0''/Pr \; + \; b_1 h_0'^2/Pr \; + \; (1/2) f_0 \theta_0'$$

$$+ \; ((\gamma - 1)M^2/\Delta t)(1 + a_1 \theta_0) f_0''^2 \; = \; 0 \tag{23b}$$

$$f_0(0) \; = \; f_0'(0) \; = \; 0 \; ; \qquad f_0'(\infty) \; = \; 1 \; ; \qquad h_0(\infty) \; = \; 0 \tag{23c}$$

and

$$h_0(0) \;=\; 1 \tag{23d}$$

for the initial expansion (representing the solution with the isothermal boundary condition at the interface), and

$$h_0'(0) \;=\; 0 \tag{23e}$$

for the asymptotic expansion (representing the solution with the adiabatic boundary at the interface), whereas at the i-th order one has

$$\begin{aligned}(1+a_1h_0)f_i''' \;+\; a_1(h_if_0''' + h_i'f_0'' + h_0'f_i'') \;-\; (i\delta/2)f_0'f_i' \\ +\; (1/2)f_0f_i'' \;+\; ((1+i\delta)/2)f_if_0'' \;=\; M_i\end{aligned} \tag{24a}$$

$$\begin{aligned}(1+b_1h_0)\theta_i''/Pr \;+\; b_1(h_ih_0'' + 2h_i'h_0')/Pr \;-\; (i\delta/2)h_if_0' \;+\; (1/2)f_0h_i' \\ +\; ((1+i\delta)/2)f_ih_0' \;+\; (\gamma-1)M_2^2(2(1+a_1h_0)f_0''f_i'' + a_1A_0h_i) \;=\; N_i\end{aligned} \tag{24b}$$

$$f_i(0) \;=\; f_i'(0) \;=\; f_i'(\infty) \;=\; h_i(\infty) \;=\; 0 \tag{24c}$$

$$h_i(0) = h'_{i-1}(0) + b_1 B_{i-1} \tag{25}$$

for the initial expansion, and

$$(1 + b_1 h_0(0))h'_1(0) + b_1 h_1(0)h'_0(0) = h_0(0) - 1 \tag{26a}$$

for the first order of the asymptotic expansion, and

$$(1 + b_1 h_0(0))h'_i(0) + b_1 h_i(0)h'_0(0) = h_{i-1}(0) - b_1 B_{i-1} \tag{26b}$$

for the successive terms of the asymptotic expansion, where

$$M_i = \sum_{j=1}^{i-1} [(j\delta/2)f'_j f'_{i-j} - ((1 + j\delta)/2)f_j f''_{i-j} - a_1(h_j f'''_{i-j} + h'_j f''_{i-j})]$$

$$N_i = \sum_{j=1}^{i-1} [(j\delta/2)h_j f'_{i-j} - ((1 + j\delta)/2)f_j h'_{i-j} - b_1(h_j h''_{i-j} + h'_j h'_{i-j})/Pr$$

$$- (\gamma - 1)M_2^2((1 + a_1 h_0) + f'_j f''_{i-j} + a_1 A_j h_{i-j})]$$

$$A_j = \sum_{k=0}^{j} f''_k f''_{j-k}$$

$$B_i = \sum_{j=0}^{i} h_j(0) h'_{i-j}(0) .$$

The expansion for small values of ξ ($m = I\xi^{1/2}$) is regular and its radius of convergence can be calculated by means of Padé approximants technique.

In this way it is possible to obtain a rapid convergence by using only a few terms of the original Taylor series but above all the utility of Padé approximants lies in the fact that they work well also when the Taylor series does not converge, obtaining a representation valid in the entire thermo-fluid-dynamic field.

On the contrary the expansion for high values of ξ ($m = 1/(I\xi^{1/2})$) is not regular and the terms of this expansion may be calculated without any difficulties only for $i = 0, 1$; for $i > 1$ the system (24) with $\delta = -1$ admits eigensolutions, the first of which results for $i = 2$. Therefore it is necessary to modify the form of the asymptotic expansion including the eigensolutions, and to give initial conditions at $\xi = \xi_0 > 0$. However we shall see that it is sufficient to consider only the first two terms of the asymptotic expansion because the Padé approximant technique will permit us to obtain a representation valid in the entire thermo-fluid-dynamic field.

Thus the asymptotic solution will check only the accuracy of the Padé representation at high of ξ.

5.6 Solution for case b)

When the axis is under adiabatic conditions, case b), the thermal boundary con-

dition at the solid-fluid interface may be expressed as

$$(1 + b_1 t_w) t_{z,w} \;=\; -(\xi t_\xi)_{\xi,w} \xi^{1/2} / I \,. \tag{18b}$$

Then, the boundary layer equations (11)-(13) with condition (18b) may be solved assuming t and f ($\psi = \xi^{1/2} f$) as functions of the similarity variable z only. In fact Eqs.(12b) and (12c) become

$$(1 + a_1 t) f''' + \; a_1 t' f'' + \; (1/2) f f'' \;=\; 0 \tag{27a}$$

$$(1 + b_1 t) t''/Pr \;+\; b_1 t'^2/Pr \;+\; (1/2) f t' + \; (\gamma - 1) M_2^2 (1 + a_1 t) f''^2 \;=\; 0 \tag{27b}$$

with the boundary conditions

$$f(0) \;=\; f'(0) \;=\; 0\,; \qquad f'(\infty) \;=\; 1\,; \qquad t(\infty) \;=\; 0 \tag{27c}$$

whereas Eq.(18b), as the r.h.s. equals zero, gives

$$t'(0) \;=\; 0\,. \tag{27d}$$

6.6 Results and discussion

The previous analysis will be applied to the case of air ($Pr = 0.7$) assuming for the Mach number upstream of the shock wave M_1 the values of 3 and 6, and for T_1 the value of 300 K; moreover we have assumed $\alpha = 5°$ and $T_a = 1000$ K. For $M_1 = 3$, $T_1 = 270$ K and $\alpha = 5°$ one obtains, from the shock wave theory, $M_2 = 2.75$ and $T_2 = 301$ K ($\Delta t = (T_a - T_2)/T_2 = 2.32$), whereas for $M_1 = 6$ and for the same values of T_1 and α one has $M_2 = 5.32$ and $T_2 = 332$ K ($\Delta t = 2.01$).

In the temperature range $300 - 1700$ K the variation of viscosity and thermal conductivity can be well described by utilizing Eqs.(15) with $n = 2$ and calculating the coefficients α_1, α_2, β_1, β_2 so that they pass through $\mu(T = 400\ \text{K}) = 2.27 \cdot 10^{-4} P$ and $\mu(T = 1600\ \text{K}) = 5.63 \cdot 10^{-4} P$ and through $\lambda(T = 400\ \text{K}) = 3.27 \cdot 10^{-2} W/mK$ and $\lambda(T = 1600\ \text{K}) = 1.00 \cdot 10^{-1} W/mK$. In this way the maximum error obtained for $\mu(T)$ and $\lambda(T)$ is of the order of a few per cent. Finally we may calculate the coefficients a_1 and b_1 of Eqs.(17); these values, together with the values of $h_0(0)$ and $f_0''(0)$ for the solution with the adiabatic boundary condition (solution for $x \to \infty$) are reported in Table 1.

As noted in the previous section, Padé approximants technique has been used for the representation of results in the case of the solution with the isothermal boundary condition. The remarkable improvement obtainable by using Padé approximants with respect to the MacLaurin expansion and the convergence to the

asymptotic expansion is shown in Figs. 2 and 3 where $t_w = t(m_1, 0)$ is plotted versus m_1 for $M_2 = 5.32$. Figure 2 shows that the initial expansion with 16 terms, that coincides with Padé representation for $m_1 < 1$, diverges when $m_1 > 1$; this results is in complete agreement with that obtained by means of Padé technique that provides a value for the radius of convergence equal to about 1. Figure 3 shows the convergence of the results, obtained by Padé approximants, to those given by the asymptotic expansion calculated up to the first order. Thus Padé representation is valid also when the MacLaurin original expansion does not converge.

In Figure 4 the curves of t_w versus m_1 are drawn for $M_1 = 3$ ($M_2 = 2.75$) and $M_1 = 6$ ($M_2 = 5.32$); the curves obtained by choosing $a_1 = b_1 = 0$ (dotted curves), that is $\rho\mu = \rho\lambda = 1$, are also shown in Figs.4 and 5. For $M_1 = 3$ the approximation $\rho\mu = \rho\lambda = 1$ provides very good results; whereas for $M_1 = 6$ the per cent difference is about 10.

Figure 4 shows the influence of wall thermal resistance. At $m_1 = 0$ is $t_w = 1$ and hence for small values of Re, α, λ_2 and x or for high values of λ_{s_o} the solution is close to that obtained with the isothermal boundary condition, while for high values of m_1 the solution tends to that obtained with the adiabatic condition.

The curves of $Nu/Re_x^{1/2}$ for $M_1 = 3$ and $M_1 = 6$ are plotted versus m_1 in Fig.5 where the Nusselt number Nu is defined as the dimensionless heat flux, that is

$$q_w = \frac{Nu\lambda_2(T_w - T_2)}{x}.$$

It must be noted that, since the asymptotic solution is obtained with the adiabatic condition, the curves of $Nu_x \cdot Re_x^{-1/2}$ tend to zero for $m_1 \to \infty$ ($x \to \infty$). In order to appreciate better the difference with respect to the case $a_1 = b_1 = 0$,

these curves are reported in Fig.6 up to $m_1 = 5$ by using two different scales for $M_1 = 3$ and $M_1 = 6$. As before the approximation $\rho\mu = \rho\lambda = 1$ (dotted curves) is good for $M_1 = 3$ whereas for $M_1 = 6$ the per cent difference is about 15.

The friction coefficient c_f, defined as

$$c_f = \frac{\tau_w}{\rho_2 u_2^2}$$

is plotted in Fig.7 versus m_1. It must be noted that, if we assume $a_1 = b_1 = 0$, c_f does not depend on the variable m_1; in fact in this case the velocity field may be solved independently of the thermal field in terms of the similarity variable z. Figure 8 shows that for the evaluation of c_f the assumption $\rho\mu = \rho\lambda = 1$ is not satisfactory even for $M_1 = 3$. The per cent difference with respect to the case $a_1 = b_1 = 0$ is about 9 for $M_1 = 3$ and about 30 for $M_1 = 6$.

The solution with the adiabatic boundary condition has been obtained in a similar form in terms of the variable z. The initial values $t(0)$ and $f''(0)$ depend on the values of a_1 and b_1.

In order to analyze the influence of the variable property of the fluid on flow the curves of $t_w = t(0)$ and c_f are plotted versus a_1 in Figs. (8) and (9), assuming $M_1 = 3$ and $b_1 = -0.4, 0, 0.4$. These figures show that both t_w and c_f increase almost linearly with a_1.

References to Chapter 6

[1] W.M. Kays, Convective Heat and Mass Transfer, McGraw-Hill, New York, 1966.

[2] Van P. Carey and J.C. Mollendorf, Variable viscosity effects in several natural convection flows, Int. J. Heat Mass Transfer (1980), 23, 95-109.

[3] D.D. Gray and A. Giorgini, The validity of the Boussinesq approximation for liquids and gases, Int. J. Heat Mass Transfer (1976), 19, 545-551.

[4] G.P. Merker and S. Mey, Free convection in a shallow cavity with variable properties - 1. Newtonian fluid, Int. J. Heat Mass Transfer (1987), 30, 1825-1832.

[5] A. Pozzi and M. Lupo, Variable-properties effects in supersonic wedge flow, AIAA J. (1991), 29, 686-687.

Table 1

Values of the characteristic quantities for $M_1 = 3$ and $M_1 = 6$ ($\alpha = 5\ deg$)

	a_1	b_1	Δt	$h_0(0)$	$f_0''(0)$
$M_1 = 3$	-0.215	-0.134	2.32	0.535	0.359
$M_1 = 6$	-0.207	-0.129	2.01	2.145	0.489

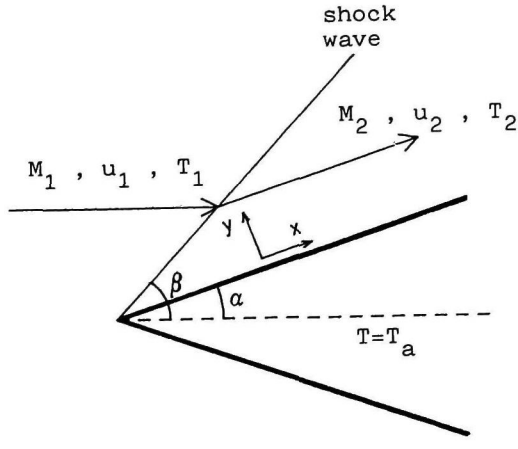

case a)

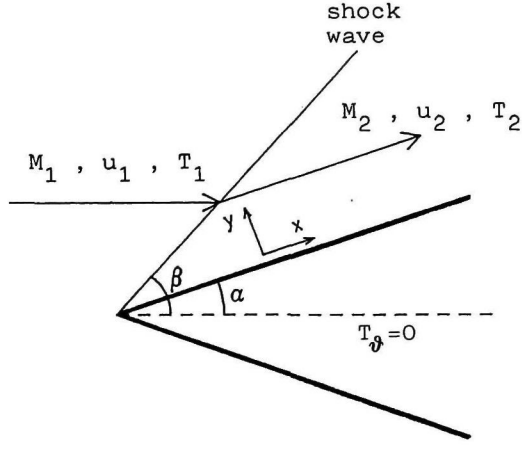

case b)

Fig.1 Schematic view of the problem.

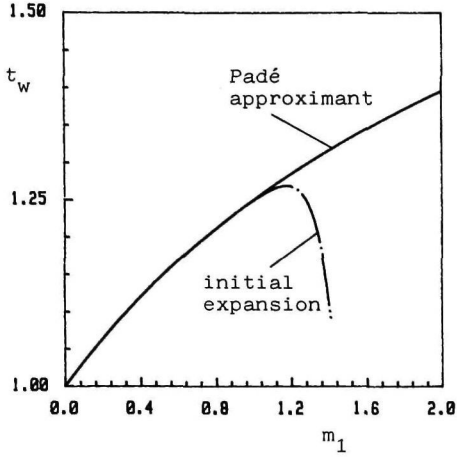

Fig.2 t_w obtained by means of initial expansion and Padé approximants technique (M_1=6).

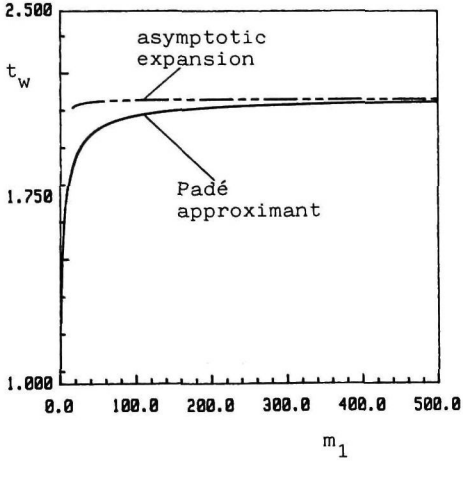

Fig.3 Matching between the Padé approximant and the asymptotic solution (M_1=6).

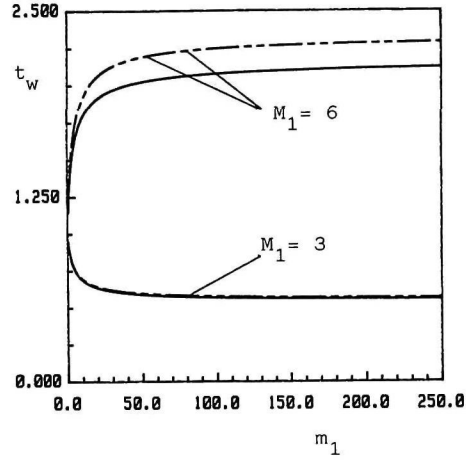

Fig.4 Curves of t_w for M_1=3 and M_1=6.

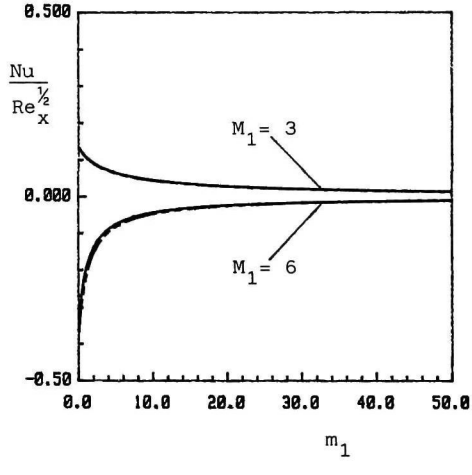

Fig.5 Curves of $Nu/Re_x^{1/2}$ for M_1=3 and M_1=6.

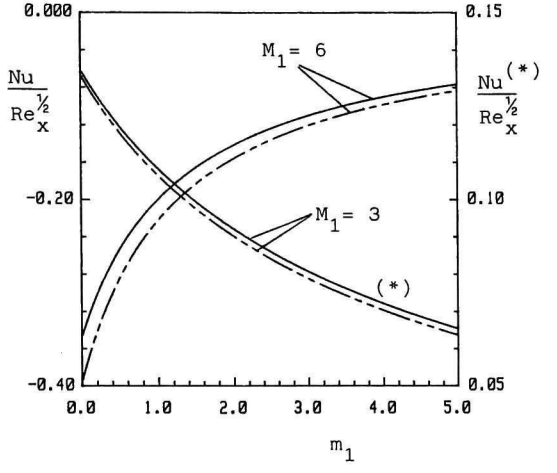

Fig.6 Curves of $Nu/Re_x^{1/2}$ for M_1=3 and M_1=6.

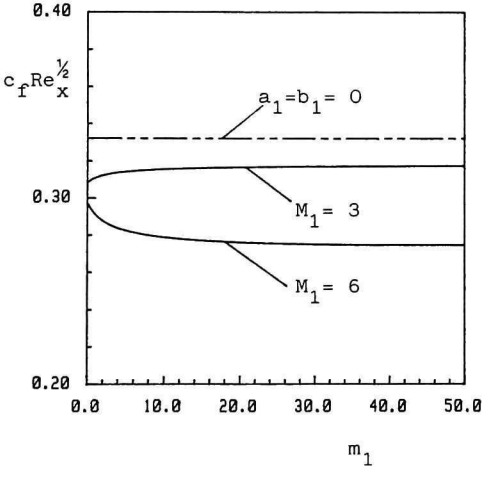

Fig.7 Curves of $c_f Re_x^{1/2}$ for M_1=3 and M_1=6 and for a_1=b_1=0.

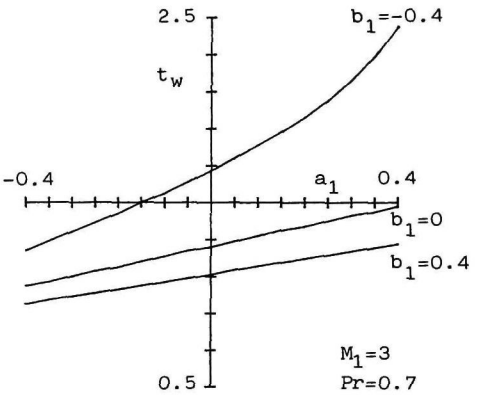

Fig.8 Variation of $t_w=t(0)$ with a_1 and b_1.

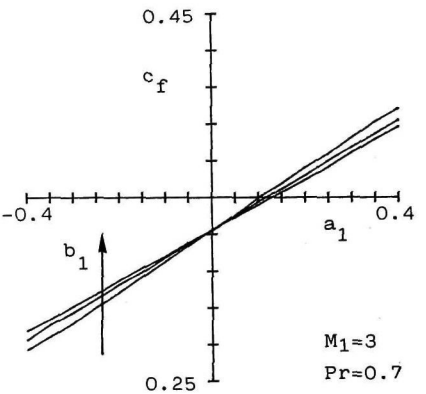

Fig.9 Variation of c_f with a_1 and b_1.

Chapter 7

VARIABLE-PROPERTIES EFFECTS: FREE CONVECTION

1.7 Introduction

The analysis of natural convection problem is usually performed by applying the Boussinesq approximation which consists of considering all the properties constants and writing the momentum equation in the following form [1]

$$\rho(uu_x + vu_y) \;=\; \mu u_{yy} \;+\; \rho\beta_\infty g(T - T_\infty) \tag{1}$$

where g is the acceleration due to gravity and β is the coefficient of thermal expansion, defined as the specific variation of volume at constant pressure. It is given by

$$\beta \;=\; \rho\,\frac{\partial(1/\rho)}{\partial T}\,. \tag{2}$$

For perfect gases, from the equation of state, one has

$$\beta = \frac{1}{T} . \tag{3}$$

The last term of Eq.(1) is the buoyancy term.

In order to consider the variable-property effects in free convection we start from the momentum equation in the boundary layer approximation in the following form

$$\rho(uu_x + vu_y) + p_x = (\mu u_y)_y + F \tag{4}$$

where F denotes the component of volume force along the vertical direction.

In the natural convection case the volume forces cannot be neglected because they are the only driving force.

Let p_∞ be the pressure that exists when the velocity $\underline{V}$ vanishes ($T = T_\infty$); as $F = -\rho g$ (F has the dimension of a force divided by a volume), it is

$$\frac{\partial p_\infty}{\partial x} = g\rho_\infty . \tag{5}$$

It results that $p = p_\infty$ even when $\underline{V}$ is different from zero. Therefore Eq.(4) becomes

$$\rho(uu_x + vu_y) = (\mu u_y)_y + g(\rho_\infty - \rho) . \tag{6}$$

For perfect gases one has

$$\rho_\infty - \rho \;=\; \rho(\frac{\rho_\infty}{\rho} - 1) \;=\; \rho(\frac{T}{T_\infty} - 1) \tag{7}$$

and Eq.(6) gives

$$\rho(uu_x + vu_y) \;=\; (\mu u_y)_y \;+\; g\rho(\frac{T}{T_\infty} - 1)\,. \tag{8}$$

This analysis was published in ref.[2].

2.7 Basic equations

Taking into account Eq.(8) the dimensionless boundary layer equations governing the problem are

$$(\rho u)_x \;+\; (\rho v)_y \;=\; 0 \tag{9}$$

$$\rho(uu_x + vu_y) \;=\; (\mu u_y)_y \;+\; \rho\theta \tag{10}$$

$$\rho(u\theta_x + v\theta_y) \;=\; \frac{(\lambda\theta_y)_y}{Pr} \tag{11}$$

where

$$\theta = \frac{T - T_\infty}{T_b - T_\infty}$$

and Pr is the Prandtl number.

The reference frame is illustrated in Figure 1, where b denotes the thickness of the plate, which is insulated at the edges, and a temperature T_b is maintained on the side away from the fluid.

The reference quantities are: $L = \nu_\infty^{2/3} g^{-1/3}$ for x', $Ld^{-1/4}$ for y', ρ_∞ for ρ, μ_∞ for μ, λ_∞ for λ, and $\nu_\infty d^{1/4}$ for the stream function ψ (such that $\rho u = \psi_y \rho_\infty$, $\rho v = -\psi_x \rho_\infty$), where

$$d = \frac{(T_b - T_\infty)}{T_\infty} .$$

It is possible to take into account the variable-property effects by means of the nondimensional Stewartson-Dorodnitzin transformation:

$$\xi = x ; \qquad \eta = \int_0^y \rho dy \tag{12}$$

assuming that the viscosity and thermal conductivity coefficients are proportional to the absolute temperature, so that $\mu\rho = \lambda\rho = 1$.

This hypothesis concerning the dependence on temperature of the viscosity and thermal conductivity coefficients cannot adequate describe the thermo-fluid-dynamic field if the fluid-side plate temperature is very different from that of the outer side. Therefore we assume the following dependence of μ and λ on absolute temperature T

$$\mu = \sum_{i=1}^{n} \alpha_i T^i \tag{13}$$

$$\lambda = \sum_{i=1}^{n} \beta_i T^i \tag{14}$$

so that, in dimensionless form, the products $\mu\rho$ and $\lambda\rho$ ($\rho T = 1$) are expressed by means of polynomials in terms of θ:

$$\mu\rho = 1 + \sum_{i=1}^{n-1} a_i \theta^i \tag{15}$$

$$\lambda\rho = 1 + \sum_{i=1}^{n-1} b_i \theta^i \,. \tag{16}$$

In particular, for $n = 2$ we have

$$\begin{aligned} \mu\rho &= 1 + a_1\theta \\ \\ \lambda\rho &= 1 + b_1\theta \end{aligned} \tag{17}$$

where

$$a_1 = \alpha_2 \frac{T_b - T_\infty}{\alpha_1 + \alpha_2 T_\infty} \,; \qquad b_1 = \beta_2 \frac{T_b - T_\infty}{\alpha_1 + \alpha_2 T_\infty} \,.$$

Then Eqs.(9), (10), (11), (15) and (16) give

$$u_x + V_\eta = 0 \tag{18}$$

$$uu_x + Vu_\eta = \left[\left(1 + \sum_{i=1}^{n-1} a_i \theta^i\right) u_\eta\right]_\eta + \theta \tag{19}$$

$$u\theta_x + V\theta_\eta = [(1 + \sum_{i=1}^{n-1} b_i \theta_i)\theta_\eta]_\eta / Pr \tag{20}$$

where $V = \rho v + u\eta_x$.

The boundary conditions associated with Eqs.(18)-(20) are

$$u(x,0) = V(x,0) = u(x,\infty) = \theta(x,\infty) = 0 \tag{21}$$

$$u(0,\eta) = \theta(0,\eta) = 0\,. \tag{22}$$

The wall boundary condition associated with Eq. (20) usually involves assigning the temperature or the heat flux at the solid-fluid interface ($y = 0$). For a plate of nonzero thickness, we must solve the coupled thermal fields in both the solid and the fluid. The coupling conditions require that the temperature and the heat flux be continuous at the interface. The temperature T_{so} in the solid, neglecting the wall's longitudinal conduction, is

$$T_{so} = T_w(x') - \frac{[T_b - T_w(x')]y'}{b}$$

where $T_w(x') = T(x', 0)$ is the unknown temperature at the interface.

The heat flux continuity condition, using Eq.(16), may be written in dimensionless form as

$$p\left(1 + \sum_{i=1}^{n-1} b_i \theta_w^i\right) \theta_\eta(x, 0) = \theta_w - 1 \tag{23}$$

where

$$p = \frac{d^{1/4} b \lambda_\infty}{L \lambda_{so}} \tag{24}$$

and λ_{so} is the solid thermal conductivity. Equation (23) represents the last boundary condition associated with Eqs.(18)-(20).

3.7 Solution for low x

Let

$$s = \frac{\eta}{(px)^{1/5}}, \qquad \psi = \frac{x^{4/5} g(x, s)}{p^{1/5}}, \qquad \theta = \frac{x^{1/5} h(x, s)}{p^{4/5}},$$

and

$$m_1 = \frac{x^{1/5}}{p^{4/5}} . \tag{25}$$

We can expand the functions g and h in a MacLaurin series with respect to m_1, to get

$$g = \sum_{i=0}^{\infty} m_1^i g_i(s) ; \qquad h = \sum_{i=0}^{\infty} m_1^i h_i(s) . \tag{26}$$

In this way, if we assume that $g_i'(\infty) = h_i(\infty) = 0$, the initial condition of Eq.(22) are satisfied as well.

From Eqs.(15), (16), (19), (20) and (23) we find at the leading order the following system

$$3g_0'^2 - 4g_0 g_0'' = 5g''' \tag{27}$$

$$h_0 g_0' - 4g_0 h_0' = \frac{5}{Pr} h_0''' \tag{28}$$

with the boundary conditions

$$g_0(0) = g_0'(0) = g_0'(\infty) = 0 \tag{29}$$

$$h_0'(0) = -1 ; \qquad h_0(\infty) = 0 \tag{30}$$

and at the ith order

$$6g_0'g_i' + ig_i'g_0' - 4(g_0g_i'' + g_ig_0'') - ig_ig_0'' - 5g_i''' = H_i \tag{31}$$

$$h_0g_i' + h_ig_0' - 4(g_0h_i' + g_ih_0') - \frac{5}{Pr}h_i'' = K_i \tag{32}$$

with the boundary conditions

$$g_i(0) = g_i'(0) = g_i'(\infty) = 0 \tag{33}$$

$$h_i'(0) = h_{i-1}(0)\,; \qquad h_i(\infty) = 0 \tag{34}$$

where

$$H_i = 5h_{i-1} + a_1 \sum_{j=0}^{i-1} (h_jg_{i-1-j}''' + h_j'g_{i-1-j}'')$$

$$-3\sum_{j=1}^{i-1} g_j'g_{i-j}' + \sum_{j=1}^{i-1} jg_j'g_{i-j}' + \sum_{j=1}^{i-1} jg_jg_{i-j}'' + 4\sum_{j=1}^{i-1} g_jg_{i-j}''$$

$$K_i = b_1 \sum_{j=0}^{i-1} (h_jh_{i-1-j}'' + h_j'h_{i-1-j}'') - \sum_{j=1}^{i-1} g_j'h_{i-j} + jh_jg_{i-j}')$$

$$+ \sum_{j=1}^{i-1} (4h'_j g_{i-j} + j g_j h'_{i-j}) \, .$$

4.7 Solution for high x

To obtain the asymptotic expansion we introduce the same similarity variable used for the isothermal problem, $z = \eta / x^{1/4}$. We let $\psi = x^{3/4} f(x,z)$ and

$$m \; = \; \frac{p}{x^{1/4}} \, . \tag{35}$$

If we expand the functions f and θ in a MacLaurin series, writing

$$f \; = \; \sum_{i=0}^{\infty} m^i f_i(z) \, ; \qquad \theta \; = \; \sum_{i=0}^{\infty} m^i \theta_i(z) \tag{36}$$

from Eqs.(15), (16), (19), (20) and (23) we find at the leading order the following system:

$$(1 + a_1 \theta_0) f_0''' \; + \; \left(a_1 \theta_0' + \frac{3}{4} f_0 \right) f_0'' \; - \; \frac{1}{2} f_0'^2 \; + \; \theta_0 \; = \; 0 \tag{37}$$

$$(1 + b_1 \theta_0) \theta_0'' \; + \; b_1 \theta_0'^2 \; + \; \frac{3}{4} Pr f_0 \theta_0' \; = \; 0 \tag{38}$$

$$f_0(0) = f_0'(0) = f_0'(\infty) = 0 \tag{39}$$

$$\theta_0(0) = 1\,; \qquad \theta_0(\infty) = 0 \tag{40}$$

(representing the isothermal problem) and at the ith order

$$(1 + a_1\theta_0)f_i''' + \theta_i + a_1(\theta_i f_0''' + \theta_0' f_i'' + \theta_i' f_0'')$$

$$- f_0' f_i' + \frac{3}{4}(f_0 f_i'' + f_i f_0'') + \frac{i}{4}(f_i' f_0' - f_i f_0'') = S_i \tag{41}$$

$$(1 + b_1\theta_0)\theta_i'' + b_1(\theta_i\theta_0'' + 2\theta_i'\theta_0') + \frac{3}{4}Pr(f_0\theta_i' + f_i\theta_0')$$

$$+ \frac{i}{4}Pr(\theta_i f_0' - f_i\theta_0') = T_i \tag{42}$$

$$f_i(0) = f_i'(0) = f_i'(\infty) = 0 \tag{43}$$

$$\theta_i(0) = \theta_{i-1}'(0) + b_1 A_{i-1}\,; \qquad \theta_i(\infty) = 0 \tag{44}$$

where

$$A_i = \sum_{j=0}^{i} \theta_j(0)\theta'_{i-j}(0)$$

$$S_i = \sum_{j=1}^{i-1} \left[\frac{1}{2} f'_j f'_{i-j} - \frac{3}{4} f_j f''_{i-j} - \frac{j}{4} (f'_j f'_{i-j} - f_j f''_{i-j}) - a_1(\theta_j f'''_{i-j} + \theta'_j f''_{i-j}) \right]$$

$$T_i = \sum_{j=1}^{i-1} \left[-b_1(\theta_j \theta''_{i-j} + \theta'_j \theta'_{i-j}) - \frac{j}{4} Pr(\theta_j f'_{i-j} + f_j \theta'_{i-j}) - \frac{3}{4} Pr f_j \theta'_{i-j} \right]$$

Eqs.(41)-(44) may be solved numerically without difficulty for $i = 1$, 2 and 3; for $i = 4$, Eqs. (41) and (42), with $S_i = T_i = 0$ and with the initial conditions $f_4(0) = f'_4(0) = \theta_4(0) = 0$; $f''_4(0) = C f''_0(0)$; $\theta'_4(0) = -C\theta'_0(0)$, where C is a free constant, allows a solution by $f_4 = C(3f_0 - z f'_0)$; $\theta_4 = -Cz\theta'_0$, which satisfies the conditions at infinity $f'_4(\infty) = \theta_4(\infty) = 0$. Therefore f_4 and θ_4 represent an eigensolution of Eqs.(41)-(44).

To take into account terms of $O(m^4)$, we must modify the form of Eqs.(36) to include the eigensolutions and give initial conditions at $x = x_0 > 0$. However, we need to consider only the first four terms in Eqs.(36), because the Padé approximants technique permit us to obtain a representation valid in the entire thermo-fluid-dynamic field. Thus the asymptotic solution will check only the ac-

curacy of the Padé representation at high values of x.

5.7 Results

We will apply the preceding analysis to the case of air ($Pr = 0.7$), assuming for the ambient temperature, T_∞, the value of 300 K and for T_b the values of 700, 1000, and 1300 K ($d = \beta(T_b - T_\infty) = 1.33,\ 2.33$, and 3.33).

We consider a plate of finite thickness b and length l and define a Grashof number Gr_l according to this length. Moreover, letting $K = \lambda_{s_o} l/\lambda_\infty b$, we can write

$$p = d^{1/4}/K\ , \qquad m = Gr_l^{1/4}/(x'/l)^{1/4}K\ , \qquad m_1 = K^{4/5}(x'/l)^{1/5}/Gr_l^{1/5}.$$

All results are obtained for $Gr_l = 10^9$ and for $Pr = 0.7$.

The Padé approximants technique used to calculate the radius of convergence of the original MacLaurin expansion shows that the MacLaurin- expansion (26) have a finite radius of convergence (on the order of magnitude of unity (i.e., $m_1 = O(1)$), whereas the Padé representation is valid for the entire field.

These results are shown in Figures 2 and 3, where θ_w is plotted versus x'/l for the range $300 - 1000$ K and for K= 250. The asymptotic and initial expansion are evaluated with 4 and 11 terms, respectively.

Figure 2 shows that the initial expansion that coincides with Padé representation for $x'/l < 0.1$ diverges when $x'/l > 0.1$.

Figure 3 shows that for $x'/l > 0.1$ the Padé approximant and the asymptotic expansion give practically the same values ($x'/l = 0.1$ corresponds to a value of m_1 close to the radius of convergence). Therefore Padé representation is valid also when the MacLaurin original expansion (initial expansion) does not converge. Hence Padé approximants accurately represent the solution for both low and high values of the abscissa.

In Figures 4-10, we denote the range $300 - 700$ K by – – – – –, the range $300 - 1000$ K by ——- - - —— and the range $300 - 1300$ K by ——. ——; we denote the approximation $\mu\rho = \lambda\rho = 1$ by ————— .

We analyze the effects of the variable fluid properties and of the thickness of the plate on Nu_x, θ_w, and c_f, and temperature and velocity profiles. The Nusselt number, defined as $Nu_x = x'q_w/\lambda_\infty(T_w - T_\infty) = -x'\lambda_w T_{y,w}/\lambda_\infty(T_w - T_\infty)$, is plotted in Figure 4 versus x'/l for $K = 250$. For the evaluation of the Nusselt number, the assumption $\mu\rho = \lambda\rho = 1$ for air works well enough in the ranges of temperature considered. In fact, at $x/l = 1.0$, the difference is only about 4% in the range $300 - 700$ K and about 6% in the range $300 - 1300$ K. Considering a higher value of K, which corresponds to a smaller thermal resistance of the solid, does not modify these differences substantially.

In Figure 5 the curves of $Nu_x/Gr_x^{1/4}$ are based on $K = 1000$. The difference is about 4.5% in the range $300 - 700$ K and about 6.5% in the range $300 - 1300$ K. In this case the curves are flatter than those in Figure 4, because for high values of K the largest part of the variation in wall temperature is confined to a small region near the leading edge of the plate. Thus the wall-fluid interface can be considered almost completely isothermal.

The dimensionless wall temperature θ_w is plotted versus x'/l in Figure 6 for

$K = 250$ and $K = 1000$. Comparison of the curves of θ_w, calculated with the assumption $\mu\rho = \lambda\rho = 1$, to those in the range $300 - 1300$ K shows that the dimensionless temperature at the wall is slightly dependent on the variation of μ, λ, and ρ with temperature. We found empirically for air that, in the ranges of temperature considered, we can obtain $Nu_x/Gr_x^{1/4}$ from the constant-property solution by calculating μ and λ at the reference temperature $T_r = T_w - 0.15(T_w - T_\infty)$. The results obtained for the range $300 - 1000$ K are represented in Figure 7 by curve (*). Naturally, the most appropriate reference temperature is different for different quantities of interest (c_f, boundary layer thickness, flow rate).

The friction coefficient c_f, defined as $\tau_w/\rho_\infty(\nu_\infty/x')^2$, is plotted in Figure 8 for $d = 1.33$ and $d = 3.33$. The difference with respect to the curves obtained by using the assumption $\mu\rho = \lambda\rho = 1$ (solid curves) is about 8% for $d = 1.33$ and about 14% for $d = 3.33$.

Padé approximants technique may also be used for determining temperature and velocity profiles. In fact, if we set

$$\sum_{i=0}^{N+M} m_1^i h_i(s) = \sum_{i=0}^{N} A_i m_1^i / \sum_{i=0}^{M} B_i m_1^i ,$$

the Padé coefficients A_i and B_i would depend on s. By computing these coefficients for several values of s, we can draw temperature and velocity profiles for each value of m_1, that is, for each value of x'/l, as $m_1 = K^{4/5}(x'/l)^{1/5}/Gr_l^{1/5}$.

Figures 9 and 10 present dimensionless temperature and velocity profiles ($s = \eta/(px)^{1/5}$, the similarity variable for the initial expansion) for $K = 250$ and $T_b = 1300$ K. Figures 9 and 10 show that the approximation $\mu\rho = \lambda\rho = 1$ is acceptable for the temperature considered.

We summarize the preceding results in Table 1 by presenting some significant quantities obtained from the isothermal solution. All the results apply to the case of air and are based on the assumptions that $T_\infty = 300$ K, $T_b = 700$, 1000, and 1300 K, and $Pr = 0.7$. For different gases and for different ranges of temperature, the values of coefficients a_1 and b_1, appearing in the dimensionless products $\mu\rho$ and $\lambda\rho$ (Eq.(17)) will be different. To analyze the influence of a_1 and b_1 on the thermo-fluid-dynamic field, we plotted in Figures 11 and 12 the curves of $Nu_x/Gr_x^{1/4}$ and $(1+d)c_f/Gr_x^{3/4}$ versus b_1 for several values of a_1 for isothermal boundary conditions, assuming that $Pr = 0.7$. Both nondimensional groups vary almost linearly with a_1 and b_1 in the ranges considered.

References to Chapter 7

[1] H. Schlichting, Boundary Layer Theory, McGraw-Hill, 1968

[2] A. Pozzi, M. Lupo, Variable properties effects in free convection, Int. J. Heat and Fluid Flow, (1990) Vol. 11, No.2, 135-141.

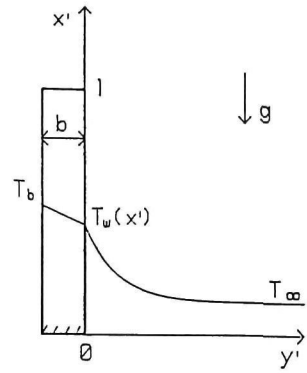

Fig.1 Thermal model of a plate.

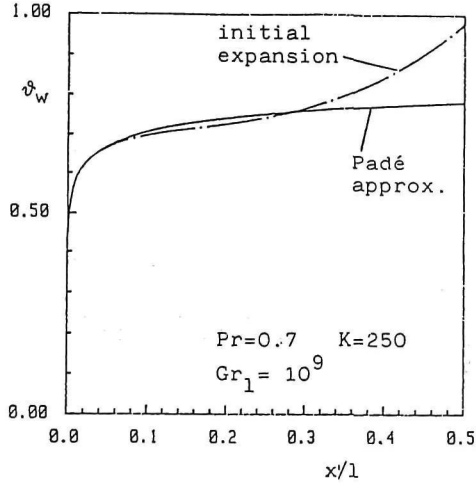

Fig.2 Non-dimensional temperature at the wall, ϑ_w, given by initial expansion and Padé approximant.

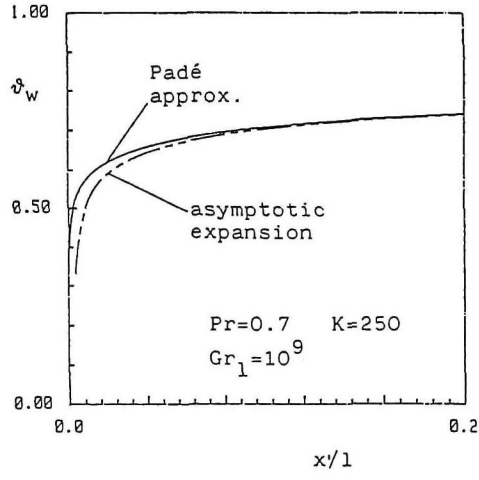

Fig.3 Non-dimensional temperature at the wall, ϑ_w, given by asymptotic expansion and Padé approximant.

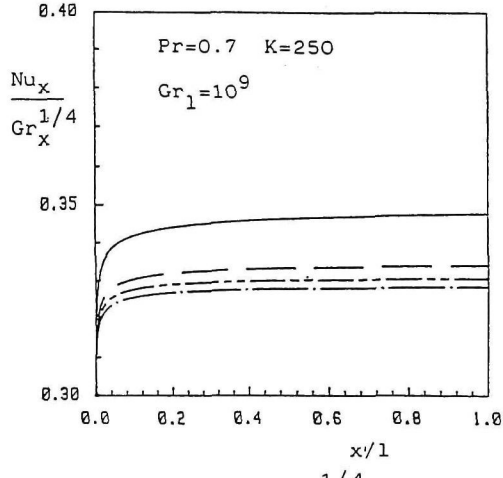

Fig.4 Comparison of $Nu_x/Gr_x^{1/4}$ for K=250, for d=1.33, 2.33, and 3.33, with that of $\mu\varrho=\lambda\varrho=1$.

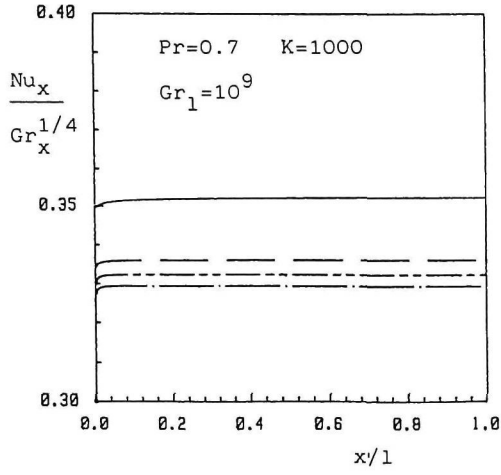

Fig.5 Comparison of $Nu_x/Gr_x^{1/4}$ for K=1000, for d=1.33, 2.33 and 3.33, with that of $\mu\varrho=\lambda\varrho=1$.

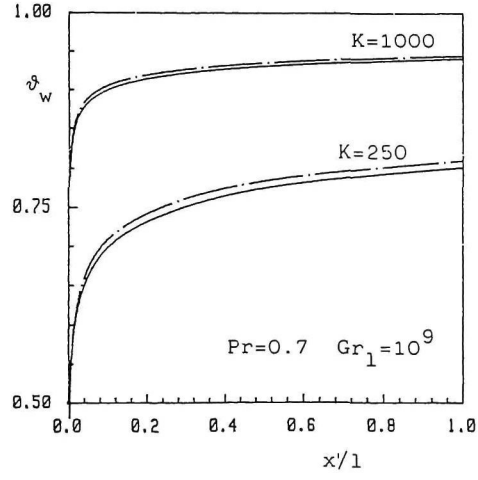

Fig.6 Comparison of ϑ_w for K=250 and K=1000, for d=3.33, with that of $\mu\varrho=\lambda\varrho=1$.

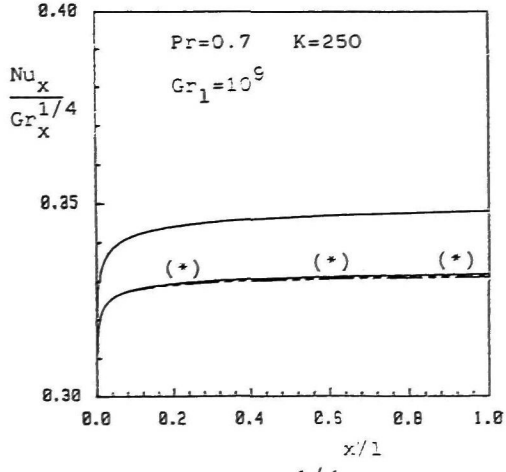

Fig.7 Comparison of $Nu_x/Gr_x^{1/4}$ (— — — —) with those obtained by the reference temperature method, (*) curve, and by the approximation $\mu\varrho=\lambda\varrho=1$.

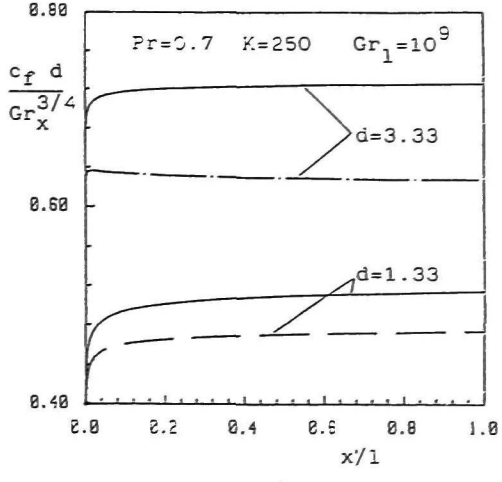

Fig.8 Comparison of $c_f d/Gr^{3/4}$ for d=1.33 and d=3.33 with that of $\mu\varrho=\lambda\varrho=1$.

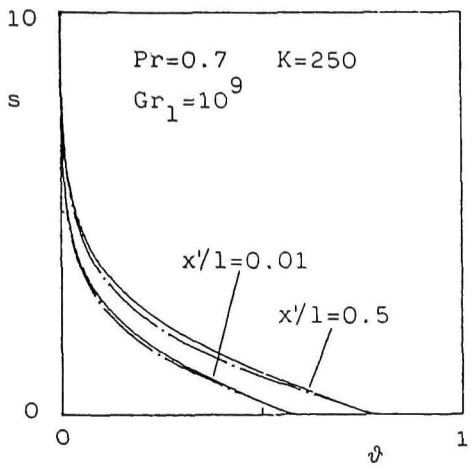

Fig.9 Plot of non-dimensional temperature ϑ versus $s=\eta/(px)^{1/5}$ for d=3.33.

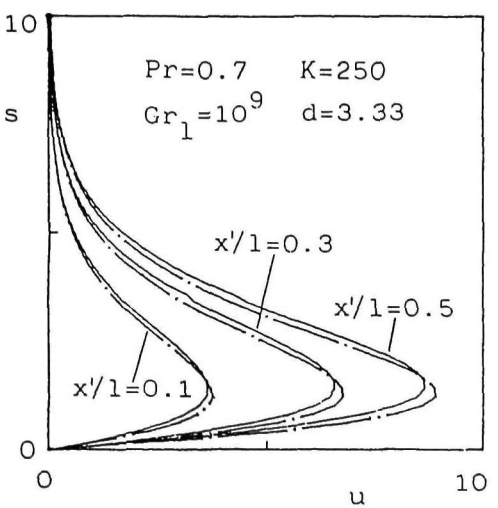

Fig.10 Plot of non-dimensional velocity component u versus $s=\eta/(px)^{1/5}$ for d=3.33.

Table 1

Quantities obtained from the isothermal solution for T_∞ =300 K.

	a_1	b_1	f''_0	ϑ'_0	$Nu_x/Gr_x^{1/4}$	$(1+d)c_f/Gr^{3/4}$
$\mu\rho=\lambda\rho=1$	0	0	0.960	−0.353	0.353	0.960
T_b=700 K	−0.229	−0.177	1.120	−0.408	0.336	0.864
T_b=1000 K	−0.316	−0.228	1.206	−0.430	0.332	0.825
T_b=1300 K	−0.380	−0.267	1.283	−0.449	0.329	0.796

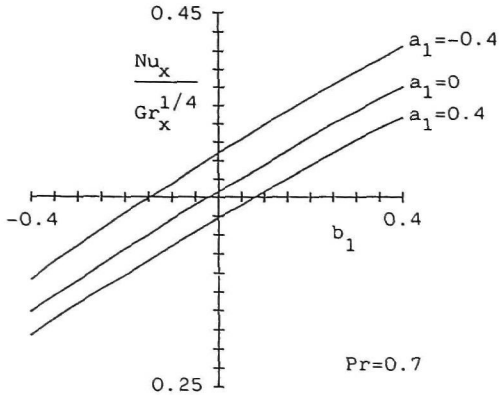

Fig.11 Plot of $Nu_x/Gr^{1/4}$ for the isothermal solution versus b_1 for a_1=-0.4, and 0.4 (Pr=0.7).

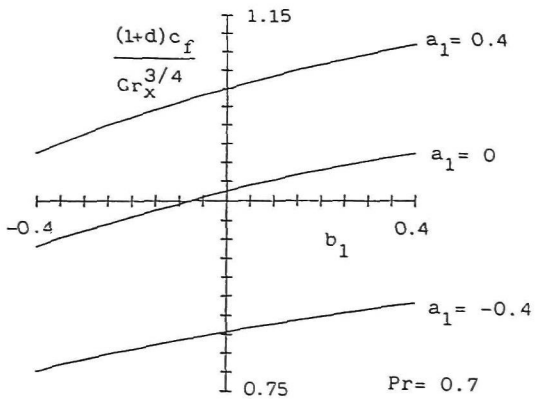

Fig.12 Plot of $(1+d)c_f/Gr^{3/4}$ for the isothermal solution versus b_1 for a_1=-0.4, 0, and 0.4 (Pr=0.7).

Chapter 8

PLANE JET INTO A MOVING MEDIUM

1.8 Introduction

In this chapter we study the flow of a fluid free from solid surfaces. We consider in fact a narrow plane jet issuing into a moving medium.

Studies about the flow of viscous jets began with the analysis by Schlichting [1] who in 1933 presented a simple model of a thin laminar jet issuing into a medium at rest. He considered vanishing initial width of the jet and an incompressible fluid. These hypotheses led to a similarity solution of the problem which can be written in closed form in terms of hyperbolic functions.

However, jets present many physical situations of primary interest that cannot be described by the Schlichting model and if one of his assumptions fails (except that of incompressibility provided that the product density-coefficient of viscosity is constant) the self-similarity of the problem is destroyed.

A first example is given by a jet issuing into a moving medium: this case appears in jet propelled vehicles where the velocity of the outer medium destroys the similarity.

A second example is given by a jet non-homogeneous with respect to the outer

medium as in the cases of the combustion chambers and of the exhausts of a combustion machine in the atmosphere. Another example is given by a jet of a conductive liquid metal or ionized gas in the presence of a magnetic field.

In ref. [2] these problems were studied as perturbations acting on the Schlichting model: the corresponding first approximations were solved in closed form by means of Legendre functions.

In this chapter we consider the case of jet issuing into a moving medium and by using the Padé approximants technique we obtain very accurate results for any value of the outer velocity and in any point of the plane.

2.8 The Schlichting solution for a jet issuing into a medium at rest

In this section we consider the efflux of a jet from a narrow orifice when it mixes with the surrounding fluid at rest.

The two-dimensional laminar boundary layer equations, when the axial pressure gradient is vanishing, in a non-dimensional incompressible form, can be written as follows

$$u_x + v_y = 0 \tag{1}$$

$$uu_x + vu_y = u_{yy} \, . \tag{2}$$

The boundary conditions concern the symmetry of the jet, its asymptotic behaviour and the initial conditions. When the outer velocity is zero one has

$$u_y(x,0) = 0 \tag{3}$$

$$v(x,0) = 0 \tag{4}$$

$$u(x,\infty) = 0 \tag{5}$$

$$u(0,y) = u_i \tag{6}$$

where u_i denotes the initial velocity of the jet.

Schlichting assumed the initial width of the jet to be vanishing: in this case the condition at $x = 0$ must be given in an integral form. Let K be the initial momentum of jet; then the initial condition can be written as

$$\int_{-\infty}^{\infty} u^2(0,y)dy = K\,. \tag{7}$$

We observe that the integration of Eq.(2) with respect to y between $-\infty$ and $+\infty$, by taking into account Eqs.(1) and (5), gives

$$\frac{d}{dx}\int_{-\infty}^{\infty} u^2 dy = 0\,. \tag{8}$$

Therefore one has

$$\int_{-\infty}^{\infty} u^2 dy = K . \tag{9}$$

By introducing the stream function ψ (such that $u = \psi_y$, $v = -\psi_x$) Eq.(1) is identically satisfied. By putting

$$\psi = x^{1/3} f(z) ; \qquad z = \frac{y}{3x^{2/3}} \tag{10}$$

one finds

$$u = \frac{1}{3x^{1/3}} f' ; \qquad v = \frac{1}{3x^{2/3}} (2zf' - f) \tag{11}$$

and from Eq.(2) one has

$$f''' + f'^2 + ff'' = 0 . \tag{12}$$

Equations (3), (4) and (5) lead to the following boundary conditions

$$f(0) = f''(0) = f'(\infty) = 0 . \tag{13}$$

Moreover from Eq.(9) one has

$$\int_{-\infty}^{\infty} f'^2 dz = 3K . \tag{14}$$

Equations (12), (13) and (14) constitute the Schlichting problem.

It must be noted that once a solution for a particular K has been found, any solution for a different value of K can be obtained, by a suitable change of variable, from the first one. In fact Eqs.(12) and (13) are invariant with respect to the substitution

$$f = \alpha f^* ; \qquad z* = \alpha z \tag{15}$$

where α is an arbitrary constant and f^* and $z*$ are two new variables.

From Eqs.(12) and (13) one has

$$f = (2C)^{1/2} Tan(C/2)^{1/2} z \tag{16}$$

where Tan denotes hyperbolic tangent. C is an arbitrary constant equals $f'(0)$. Equation (14) relates C to K as

$$K = (4/9)C(2C)^{1/2} . \tag{17}$$

3.8 Jet into a moving medium: initial solution

We consider now the flow generated by a thin jet issuing into a medium whose velocity has the constant value u_e (see Fig. 1). The differential equations that

govern this problem are the same, (1) and (2), that hold in the case of the jet into a medium at rest. In fact also in this case the axial pressure gradient is zero.

The boundary conditions are

$$u_y(x,0) = 0\,; \qquad v(x,0) = 0\,; \qquad u(x,\infty) = u_e\,. \tag{18}$$

In order to assign the intial condition at $x = 0$ we note that in this case Eq.(9) is replaced by

$$\int_{-\infty}^{\infty} u(u-u_e)dy = K_i \tag{19}$$

where K_i represents the initial momentum of the jet in this way

$$K_i = \int_{-\infty}^{\infty} u(0,y)[u(0,y)-u_e]dy\,.$$

Therefore K_i is the quantity that must be given at $x = 0$ in an integral form as initial condition.

The third equation of Eqs.(18) destroys the similarity of the solution. We assume the following expression for the stream function ψ

$$\psi = yu_e + x^{1/3} f(m,z) \tag{20}$$

where

$$f(m,z) = \sum_{i=0}^{\infty} m^i f_i(z) \tag{21}$$

and $m = 3u_e x^{1/3}$. Therefore u and v are given by

$$u = u_e + \frac{1}{3x^{1/3}} \sum_{i=0}^{\infty} m^i f_i' \tag{22}$$

$$v = \frac{1}{3x^{2/3}} \sum_{i=0}^{\infty} m^i [2z f_i - (1+i) f_i] . \tag{23}$$

The equations that determine the functions f_i are obtained by substituting Eqs.(22) and (23) into Eqs.(2), (3), (4) and (18). The function f_0 is Schlichting's solution. From Eq.(16), by assuming $C = 1/2$ (i.e. $K = 2/9$), one has

$$f_0 = Tan\frac{z}{2} . \tag{24}$$

The functions f_i, with $i > 0$, are determined by the equations

$$f_i''' + f_i'' f_0 + (2-i) f_0' f_i' + (1+i) f_i f_0'' = T_i \tag{25}$$

where

$$T_i = (i-2) f_{i-1}' - 2z f_{i-1}'' + \sum_{j=1}^{i-1} [[f_j'(j-1) - 2z f_j'']] f_{i-j}'$$

$$-[f_j(1+j) - 2zf_j'']f''_{i-j}]$$

and by the boundary conditions

$$f_i(0) = f_i''(0) = f_i'(\infty) = 0\,. \tag{26}$$

The initial conditions arising from Eq.(19) require some remarks.

Substituting Eq.(22) into Eq.(19) gives

$$\int_{-\infty}^{\infty} (\sum_{i=0}^{\infty} m^i f_i')^2 dz = 3K_i - \int_{-\infty}^{\infty} \sum_{i=0}^{\infty} m^{i+1} f_i' dz\,. \tag{27}$$

On equating the coefficients of the same power of m it results that

$$\int_{-\infty}^{\infty} f_0'^2 dz = 3K_i \tag{28}$$

$$\int_{-\infty}^{\infty} f_0' f_1' dz = -f_0(\infty) \tag{29}$$

and so on.

Only Eq.(28) must be imposed as an initial condition, the other ones are identically satisfied; in fact by integrating Eq.(25) between $-\infty$ and ∞ and taking into account Eqs.(26) one finds that Eq.(29) and all higher terms are identically satisfied.

Numerical solution of Eqs.(25) and (26) gives the values of $f_i'(0)$ that, through Eq.(22), lead to the velocity on the axis of jet. In particular the first seven values of the functions f_i' at $z = 0$ are: $f_0' = 0.5$, $f_1' = -0.4296518$, $f_2' = 0.4919479$, $f_3' = -1.142831$, $f_4' = 9.611662$, $f_5' = -162.2681$, $f_6' = 3949.968$.

The series appearing in Eq.(21) is convergent only for very small values of x. In fact its radius of convergence, calculated by means of Padé approximants in terms of the variable m, is 0.1. Therefore the series converges for $m < 0.1$, where

$$x = \left(\frac{m}{3u_e}\right)^3 .$$

The velocity field can be obtained for any values of x, through the Padé approximants P_N.

Let us consider the series $f_i'(0)$ and its approximants P_2 and P_3. Figure 2 displays the diagrams of the function $f'(0)$, defined by Eq.(21), as expressed by its MacLaurin series (5 and 7 terms) and its Padé approximants P_N ($N = 2$ and $N = 3$). In agreement with the value of the radius of convergence of the series, 0.1, the series diverges for $m > 0.1$: for $m < 0.1$ all four representations give the same results. For $m > 0.1$ the curves that refer to P_2 and P_3 nearly coincide. The numerical results of these 4 representations are listed in table 1.

4.8 Jet into a moving medium: asymptotic solution

In order to check the accuracy of the results obtained by means of the Padé approx-

imants we find the asymptotic solution which holds for high values of the abscissa x.

We put

$$u = u_e + u_{as} \tag{30}$$

where the velocity u_{as} is much smaller than u_e. The equation that determines u_{as} is obtained from Eq.(2) by neglecting terms of order of magnitude u_{as}^2 with respect to terms of order u_{as}. It results that

$$u_e \frac{\partial}{\partial x} u_{as} = \frac{\partial^2 u_{as}}{\partial y^2} . \tag{31}$$

The boundary conditions associated with this equation are obtained from Eqs. (3) and (4), namely

$$u_{as,y}(x,0) = 0 \tag{32}$$

$$u_{as}(x,\infty) = 0 \tag{33}$$

and from Eq.(19):

$$u_e \int_{-\infty}^{\infty} u_{as} dy = K_i . \tag{34}$$

The solution of the problem governed by Eqs.(31), (32) and (33), found by means of similarity solution technique, is

$$u_{as} = \frac{a}{x^{1/2}} exp(-y^2/4x) \tag{35}$$

where a is an arbitrary constant. Equation (34) gives the following value for a

$$a = \frac{K_i}{2u_e\pi^{1/2}} \ .$$

The asymptotic solution together with the initial one, as represented by P_3, is drawn in Fig.3, for $K_i = 2/9$ and $u_e = 1$. We can see that the Padé representation of the initial solution gives results that agree with those given by the asymptotic solution for m about 4. This agreement can also be checked in table 2.

Therefore the Padé representation gives practically exact values for both small and high values of m.

References to Chapter 8

[1] H. Schlichting "Laminare Strahlenausbreitung" ZAMM (1933) 13, 368-373.

[2] A. Pozzi - A. Bianchini "Linearized solutions for plane jets", ZAMM (1972), 52, 523-528.

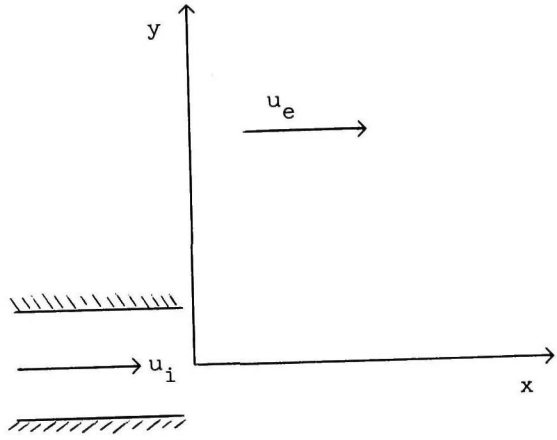

Fig.1 Scheme of the problem.

Table 1

Velocity on the axis: Comparison between the series and Padé representation.

m	Series 7 terms	Series 5 terms	Padé N=2	Padé N=3
0.25	1.248905	0.443022	0.415197	0.415015
0.5	57.513407	0.866036	0.359413	0.358710
0.75	667.516000	3.013539	0.319882	0.318573
1	3796.731027	9.031127	0.290401	0.288508
2	247751.625232	146.252432	0.222160	0.218474
3	E6 2.840846	751.326760	0.188323	0.183515
4	E7 1.601530	2394.096847	0.168111	0.162558
5	E7 6.121703	5875.085313	0.154673	0.148594

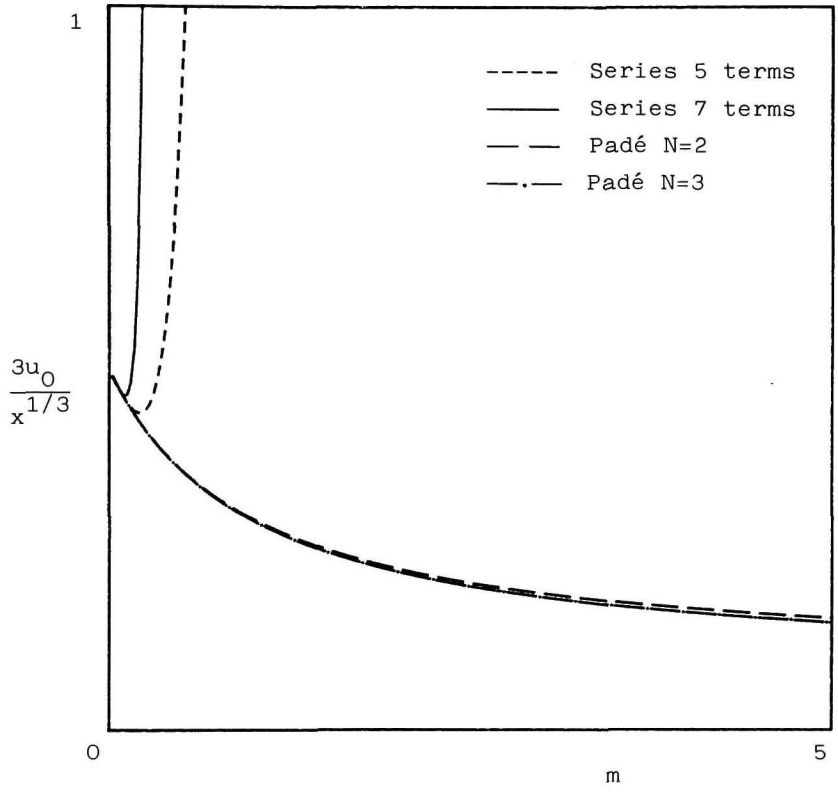

Fig.2 Velocity on the axis: comparison between the power series and Padé representation.

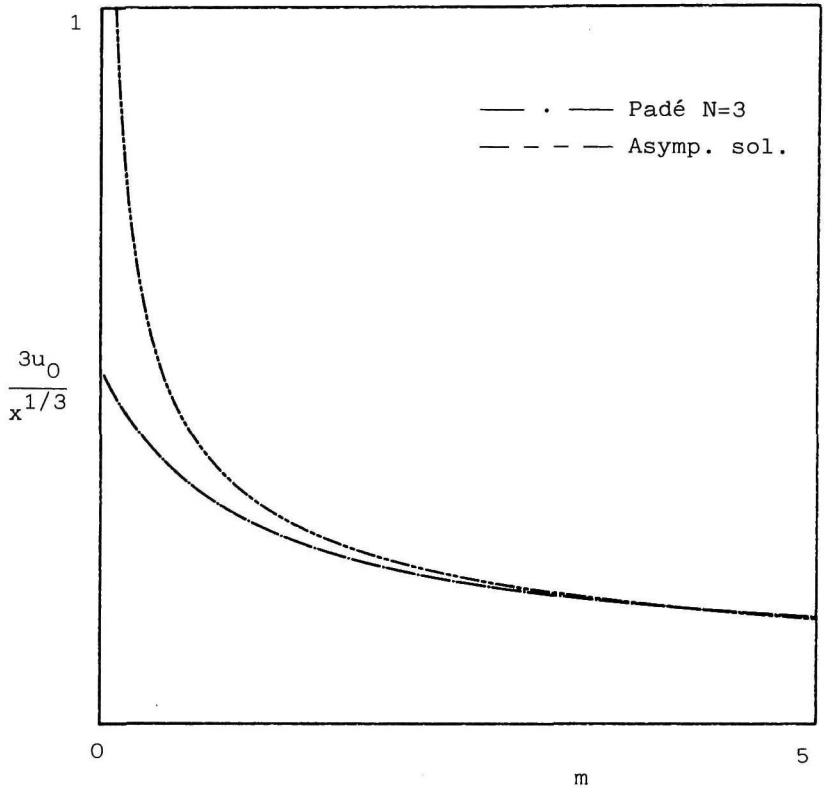

Fig.3 Velocity on the axis: comparison between the Padé representation and asymptotic solution.

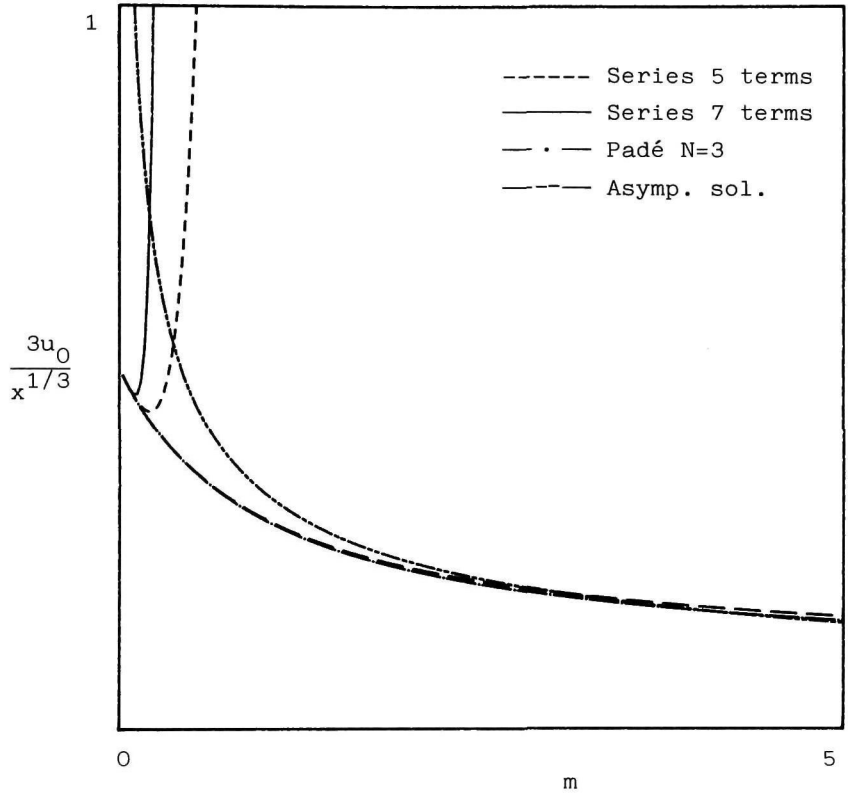

Fig.4 Velocity on the axis: comparison between the power series, Padé representation and asymptotic solution.

Table 2

Velocity on the axis: comparison between the Padé representation and the asymptotic solution.

m	Padé N=3	Asymptotic solution
0.25	0.415015	0.651482
0.5	0.358710	0.460667
0.75	0.318573	0.376133
1	0.288508	0.325741
1.25	0.265146	0.291351
1.5	0.246469	0.265966
1.75	0.231196	0.246237
2	0.218474	0.230333
2.25	0.207713	0.217160
2.5	0.198493	0.206016
2.75	0.190504	0.196429
3	0.183515	0.188066
4	0.162558	0.162860
5	0.148594	0.145675

Chapter 1

THE IMPULSIVELY STARTED FLOW AWAY FROM A PLANE STAGNATION POINT

1.1 Introduction

The plane stagnation flow, i.e. the flow that presents a point at vanishing velocity, both in the steady case and in non steady one has the property that the full Navier-Stokes equations that govern this problem are identical with the simplified boundary layers ones. Moreover it is possible to analyse this flow in terms of a function that does not depend on x.

The study of the laminar impulsively started flow around the stagnation point of a stream that impinges on a plane is simple enough. The analysis of the stagnation flow of a stream that leaves a plane is more complicate: in fact in this case the solution diverges (for instance the displacement-thickness grows exponentially with time).

The basic work for this type of research is that of Blasius [1] who, in 1908, proposed a time series expansion, obtaining two terms of the series.

Further terms of the series were calculated by Goldstein and Rosenhead [2] in 1936 and Collins and Dennis [3] in 1973.

Proudman and Johnson [4] in 1962 and Robins and Howarth [5] in 1972 studied an asymptotic expansion to model the time-dependent flow from a stagnation point and obtained a numerical solution that gives good results for finite times values.

Hommel [6] in 1983 presented a series expansion for the shear stress at the stagnation point, and then he applied series-improvement techniques in order to extrapolate this solution to large times.

In this chapter we summarize the results obtained by Hommel.

2.1 Basic equations

In order to study the impulsively started flow away from a plane stagnation point it is convenient to assume a non-dimensional system of reference x, y, t. The reference lengths for x and y are a, suitable characteristic length, and $aRe^{1/2}$, where the Reynolds number Re is given by $2V_0a/\nu$ and V_0 is the velocity at infinity. The reference time is $a/2V_0$ and the reference stream function is $a^2(2aV_0\nu)^{1/2}$.

By writing the non-dimensional stream function ψ as

$$\psi = xF(y,t) \tag{1}$$

and by substituting Eq.(1) into the Navier-Stokes equations one has the following equation for F

$$F_{yt} - F_{yyy} + FF_{yy} + 1 - F_y^2 = 0\,. \tag{2}$$

The boundary conditions associated with this equation are

$$F(0,t) = F_y(0,t) = 0 \tag{3a}$$

$$F_y(\infty,t) = 1 \tag{3b}$$

$$F_y(y,0) = 1\,. \tag{3c}$$

In order to expand F of a series of time it is convenient to introduce the variable $\eta = y/2t^{1/2}$.

Then one can write

$$F = 2t^{1/2}\sum_{i=1}^{\infty} F_i(\eta)t^i\,. \tag{4}$$

Substituting Eq.(4) into Eqs.(2) and (3) gives a series of linear, third order, ordinary differential equations. Blasius [1] solved the first two, Collins and Dennis [3] and Hommel [6] solved many others. In particular Hommel by means of a very accurate finite-difference scheme considered 44 equations.

The most representative quantity of this analysis is given by the shear stress τ, that in non-dimensional form can be written as

$$\tau = \frac{x}{2t^{1/2}}\sum_{i=1}^{\infty} F_i''(0)t^{i-1}\,. \tag{5}$$

In table 1 the first 20 values of $F_i''(0)$ are listed. (The remaining values are listed in ref.[6].)

3.1 Padé analysis of the series

Hommel first uses the Cauchy Root Test to estimate the radius of convergence of the series (4), finding a value close to 3.

Additional informations he obtains from the Padé approximants by using the diagonal sequence P_{22} and studying its poles in the complex planes (x, iy). He notes that the singularity at the angle $\beta = 3\pi/8$ dominates the series. The residue of the associated singularity is larger than the residue of any other singularities. In fact the residue magnitude are 12.1, 9.29 and 0.355 for poles at angles 67.9°, 70.5° and 90.5° respectively. All other residue magnitudes are less than 0.005.

He further notes that the Padé analysis shows that the first zero of the rear stagnation-point shear stress is at $t = 0.6438$. This result agrees very well with the values obtained in different ways by many authors. This agreement is significant because the time at which the shear stress goes to zero is very important and it is calculated with care.

References to Chapter 1

[1] H. Blasius, Grenzschincheten in Flussigkeiten mit kleiner Reibung, Z. Math. Phys. (1908) 56, 1.

[2] S. Goldstein and L. Rosenhead, Boundary layer growth, Proc. Camb. Phil. Soc. (1936) 32, 392.

[3] W.M. Collins and S.C.R. Dennis, The initial flow past an impulsively started circular cylinder, Q.J. Mech. Appl. Math. (1973) 26, 53.

[4] I. Proudman and K. Johnson, Boundary layer growth near a rear stagnation point, J. Fluid Mech. (1962) 12, 161.

[5] A.J. Robins and J.A. Howarth Boundary layer development at a two- dimensional rear stagnation point, J. Fluid Mech. (1972) 56, 161.

[6] M.J. Hommel, The laminar unsteady flow of a viscous fluid away from a plane stagnation point, J. Fluid Mech. (1983) 132, 407.

Table 1. Values of $F_i''(0)$

i	$F_i''(0)$
1	1.128379
2	-1.607278
3	-0.248092
4	0.014290
5	0.028692
6	0.006377
7	-0.001515
8	-0.001075
9	-0.97361×10^{-4}
10	0.89268×10^{-4}
11	0.30662×10^{-4}
12	-0.18844×10^{-5}
13	-0.34650×10^{-5}
14	-0.61583×10^{-6}
15	0.19425×10^{-6}
16	0.10522×10^{-6}
17	0.58123×10^{-8}
18	-0.8889×10^{-8}
19	-0.26564×10^{-8}
20	0.24906×10^{-9}

Chapter 2

THE IMPULSIVELY STARTED FLOW PAST A CIRCULAR CYLINDER

1.2 Introduction

The impulsive flow past a circular cylinder presents two types of stagnation points discussed in chap.1, i.e. that of a stream impinging on a body and that of a stream leaving a body. This flow has another important character: the fluid, initially attached to the body, separates from it and generates free shear layers.

In this case the full Navier-Stokes equations do not coincide with those of the boundary layer: the literature presents solutions of the two types of equations.

Thoman and Szewczyk [1], Son and Hanratty [2], Collins and Dennis [3] and Ta Phuoc Loc [4] are some authors that presented numerical solutions of the Navier-Stokes equations. Many authors have presented solutions of the boundary layer equations following different approaches.

Blasius [5], Goldstein and Rosenhead [6], Collins and Dennis [7], Wang [8] and Bar-Lev and Yang [9] used the series in time.

Cebeci [10] and Wang [11] used finite-difference methods.

Cowley [12] extended the series solution of Blasius to many terms and obtained

flow quantities of interest by recasting the series using rational functions. In this chapter we summarize the results obtained by Cowley.

2.2 Basic equations

The unsteady boundary layer equations describing incompressible flow past an impulsively started circular cylinder in a non-dimensional form can be written as

$$u_t + uu_x + vu_y = u_{yy} + u_e u_{ex} \tag{1}$$

$$u_x + v_y = 0 . \tag{2}$$

The cartesian coordinate x is measured along the surface of the cylinder from the first stagnation point 0 (see Fig.1) and y is measured from the cylinder surface along the local normal; u_e is the inviscid outer velocity. The variables x, y, t and u are non-dimensionalized with respect to the radius of the cylinder a, $aRe^{1/2}$, $a/2V_0$ and $2V_0$ respectively. $Re = 2V_0 a/\nu$ is the Reynolds number and ν is the kinematic viscosity. V_0 is the velocity at infinity.

The non-dimensional outer velocity u_e, i.e. the inviscid velocity along the cylinder surface obtained from the potential flow, is given by

$$u_e = sinx . \tag{3}$$

The boundary conditions associated with Eqs.(1) and (2) are

$$u(x,y,t) \;=\; 0 \quad \text{for} \quad t<0 \tag{4}$$

$$u(x,0,t) \;=\; v(x,0,t) \;=\; 0 \tag{5}$$

$$u(x,\infty,t) \;=\; u_e\,. \tag{6}$$

By introducing the stream function ψ ($\psi_y = u,\ \psi_x = -v$) Eqs.(1)-(6) give

$$\psi_{yt} \;+\; \psi_y\psi_{yx} \;-\; \psi_x\psi_{yy} \;=\; sinx\ cosx \;+\; \psi_{yyy} \tag{7}$$

$$\psi(x,y,t) \;=\; 0 \quad \text{for} \quad t<0 \tag{8}$$

$$\psi(x,0,t) \;=\; \psi_y(x,0,t) \;=\; 0 \tag{9}$$

$$\psi_y(x,\infty,t) \;=\; sinx\,. \tag{10}$$

In order to solve Eqs.(7)-(10) by numerically extending the series solution of Blasius [5] to many terms it is convenient to use his variable by writing

$$\eta = \frac{y}{2t^{1/2}} \tag{11}$$

$$\psi = 2t^{1/2} F(x, \eta, t) \tag{12}$$

$$F(x, \eta, t) = \sum_{r=0}^{\infty} F_r(x, \eta) t^r \tag{13}$$

$$F_r(x, \eta) = \sum_{p=1}^{r+1} sinpx \; f_{rp}(\eta) \; . \tag{14}$$

Substituting Eqs.(11)-(14) into Eqs.(7)-(10) gives the equations for the f_{rp}. In particular it is found that if $r+p$ is even then $f_{rp} = 0$ and that if $r+p$ is odd then

$$f'''_{rp} + 2\eta f''_{rp} - 4r f'_{rp} = 2(S_{1rp} + S_{2rp} - S_{3rp} - \delta_{1r}) \tag{15}$$

where

$$S_{1rp} = \sum_{j=0}^{r-1} \sum_{n=n_1}^{n_2} n(f'_{jn} f'_{k,p-n} - f_{jn} f''_{k,p-n})$$

$$S_{2rp} = \sum_{j=0}^{r-1-p} \sum_{n=1}^{n_3} n(f'_{jn} f'_{k,p+n} - f_{jn} f''_{k,p+n})$$

$$S_{3rp} = \sum_{j=p}^{r-1} \sum_{n=p+1}^{n_4} n(f'_{jn} f'_{k,n-p} - f_{jn} f''_{k,n-p})$$

$$n_1 = max(1, p + j - r)$$

$$n_2 = min(j + 1, p - 1)$$

$$n_3 = min(j + 1, r - j - p)$$

$$n_4 = min(j + 1, r - j + p)$$

$$k = r - 1 - j$$

$\delta_{ij} = 0$ for $i \neq j$ and 1 for $i = j$ (Kronecker symbol).

The sum S is zero if the upper bound is less than the lower bound.

The boundary conditions associated with Eqs.(15) are

$$f_{rp}(0) = f'_{rp}(0) \tag{16}$$

$$f'_{01}(\infty) = 1\,; \qquad f'_{rp}(\infty) = 0 \quad \text{for} \quad r > 0\,. \tag{17}$$

3.2 Numerical solution

Both Collins and Dennis [3] and Cowley [12] numerically solve Eqs.(15)-(17) using a scheme, described by Fox [13], that works for second- order equations involving no first derivatives. Therefore they introduced the transformations $f'_{rp} = H_{rp}(\eta)exp(-\eta^2/2)$ and $f''_{rp} = K_{rp}(\eta)exp(-\eta^2/2)$, where H_{rp} and K_{rp} are two new unknowns. This scheme is h^4 -order accurate, where h is the step of integration. In addition, two step sizes h and $2h$ were combined so that the solution is h^6 -order accurate.

The analysis of the results has been made through the shear stress τ, the displacement thickness δ and the viscous displacement velocity v_∞ at the edge of the boundary layer. In terms of the functions $f_{rp}(\eta)$ these quantities can be written as follows.

$$\tau(x,t) = u_y(x,0,t) = 4t^{1/2}\sum_{r=0}^{\infty} t^r \sum_{p=1}^{r+1} f''_{rp}(0)sinpx \tag{18}$$

$$\delta(x,t) = \int_0^\infty \left(1-\frac{u}{u_e}\right)dy = 2t^{1/2}\left[\frac{1}{\pi^{1/2}} - \sum_{r=1}^{\infty} t^r \sum_{p=1}^{r+1} f_{rp}(\infty)\frac{sinpx}{sinx}\right] \tag{19}$$

$$v_\infty(x,t) = lim(v+yu_{ex}) = 2t^{1/2}\left[\frac{cosx}{\pi^{1/2}} - \sum_{r=1}^{\infty} t^r \sum_{p=1}^{r+1} f_{rp}(\infty)pcospx\right]. \tag{20}$$

The series, occurring in these equations, are convergent in the complex- time plane for $\mid t \mid < \mid t^*(x) \mid$ where $t^*(x)$ is the location of the nearest singularity to the origin.

4.2 Analysis by means of Padé approximants

In order to find the poles of the series of Eqs.(18)-(20) and to obtain an analytic continuation of the solution in an approximate form the Padé approximant technique is used.

The presence of poles on the positive time axis is important, but not all the poles of rational functions represent singularities of the functions that they approximate: often poles and zeros of rational functions are paired so that they approximately cancel each other.

Cowley [12] analyzed the wall shear stress τ using the P_{25}^{24} Padé approximant for several values of time. The functions $\tau(x, 0.5)$, $\tau(x, 1.5)$ and $\tau(x, 2.5)$ obtained by means of P_{25}^{24} are practically coincident with those obtained by less accurate Padé approximants. The function $\tau(x, 2.7)$, for $0.62\pi < x < 0.82\pi$ is not well represented by P_{25}^{24} : for these values of t and x higher accuracy Padé approximants are necessary. With this exception the agreement between Cowley solution and those of other accurate analyses, see for instance Wang [11], is excellent.

References to Chapter 2

[1] D.C. Thoman and A.A. Szewczyk, Time dependent viscous flow over a circular

cylinder, Phys. Fluids Suppl. (19969) 12, II, 78.

[2] J.S. Son and T.J. Hanratty, Numerical solution for the flow around a cylinder, J. Fluid Mech. (1969) 35, 369.

[3] W.M. Collins and S.C.R. Dennis, Flow past an impulsively started cylinder, J. Fluid Mech. (1973) 60, 105.

[4] Ta Phuoc Loc, Numerical analysis of unsteady secondary vortices generated by an impulsively started cylinder, J. Fluid Mech. (1980) 100, 111.

[5] H. Blasius, Grenzschichten in Flussigkeiten mit kleiner Reibung, Z. Math. Phys. (1908) 56, 1.

[6] S. Goldstein and L.N. Rosenhead, Boundary layer growth, Proc. Camb. Phil. Soc. (1936) 32, 392.

[7] W.M. Collins and S.C.R. Dennis, The initial flow past an impulsively started cylinder, Q.J. Mech. Appl. Math. (1973) 26, 53.

[8] C.Y. Wang, The flow past a circular cylinder which is started impulsively from rest, J. Math. and Phys. (1967) 46, 195.

[9] M. Bar-Lev and H.T. Yang, Initial flow field over an impulsively started circular cylinder, J. Fluid Mech. (1967) 72, 625.

[10] T. Cebeci, The laminar boundary layer on a circular cylinder started impulsively from rest, J. Comp. Phys. (1979) 31, 153.

[11] K.C. Wang, On the current controversy about unsteady separation. Numerical and Physical aspects of Aerodynamic flows (Ed. T. Cebeci), Springer, (1982).

[12] S.J. Cowley, Computer extension and analytic continuation of Blasius' expansion for impulsive flow past a circular cylinder, J. Fluid Mech. (1983) 135, 389.

[13] L. Fox, The numerical solution of two-point boundary problems in ordinary

differential equations, Clarendon, (1957).

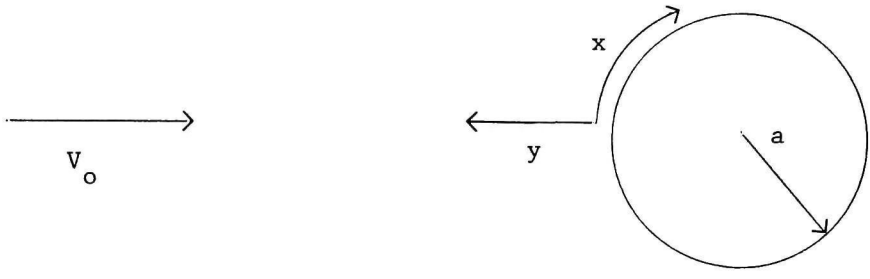

Fig.1 Schematic of flow

Subject Index

A

B

C

D

E

F

G

H

I

K

L

M

N

O

P

R

S

T

U

V

W

Author Index

A

B

C

D

E

G

H

J

K

L

M

N

This page is intentionally left blank

O

P

R

S

T